# General Disclaimer

One or more of the Following Statements may affect this Document

- This document has been reproduced from the best copy furnished by the organizational source. It is being released in the interest of making available as much information as possible.

- This document may contain data, which exceeds the sheet parameters. It was furnished in this condition by the organizational source and is the best copy available.

- This document may contain tone-on-tone or color graphs, charts and/or pictures, which have been reproduced in black and white.

- This document is paginated as submitted by the original source.

- Portions of this document are not fully legible due to the historical nature of some of the material. However, it is the best reproduction available from the original submission.

Produced by the NASA Center for Aerospace Information (CASI)
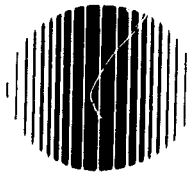
ELECTRO-OPTICAL SYSTEMS, INC.

A XEROX COMPANY

300 NORTH HALSTEAD STREET, PASADENA, CALIFORNIA 91107 · 213/681-4671, 449-1230

Final Report

ANALYSIS OF ELECTRIC PROPULSION ELECTRICAL POWER
CONDITIONING COMPONENT TECHNOLOGY

Prepared for
George C. Marshall Space Flight Center
National Aeronautics and Space Administration
Huntsville, Alabama   35812
Attention: Lawrence Garrison, Contracting Officer

Contract NAS 8-11257
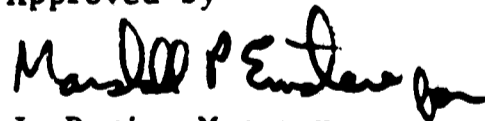
EOS Report 5400-Final   1 April 1968

Volume II: Technical Summary Report

Prepared by
L. Klynn
P. Jalichandra
R. Shattuck

Approved by

J. Davis, Manager
Plasma System Division

ELECTRO - OPTICAL SYSTEMS, INC.

A XEROX COMPANY

ABSTRACT

The 40-50 kW Mars mapper spacecraft general mission requirements are reviewed. The system consists of two solar array wings producing 50 kW with an output of 108 watts per meter^2 at a specific mass of 18 kg/kW. Sixteen cesium electron bombardment thrusters, at 2.5 kW each, are in a square matrix with one propellant tank supplying each four thruster group. The engines have an overall efficiency greater than 70 percent at a specific impulse of 3500 seconds with a power/thrust ratio of 24 kilowatts/newton.

The engine system modes of operation are described for normal operation and alternates in case of failures. As a result, a possibility of 33 percent throttling need arises. Three types of thrust programming are described, however, no conclusion can be reached until a more specific system is designed. If a computer is available to analyze thrust programming then control system and propellant masses can be minimized.

A tradeoff study is performed for the two wire transmission line between the solar panel and power conditioning. If the array produces 100 volts then the minimum system mass is achieved with an aluminum transmission line efficiency of 97 percent at a specific mass of 0.47 kg/kW.

The Mars mapper power conditioning and control system are delineated. A tradeoff between power conditioning and mass and efficiency results in a specific mass of less than 5 kg/kW for 18 kg/kW solar array.

A thermal interactions study points out numerous considerations which will be analyzed during final system design. The magnetic interaction study points out that the engine matrix magnetic fields cancel and that in specified planes a magnetometer can be used at a distance relatively close to the permanent magnets of the ion engines.

The modifications for a Mars mapper type system which are necessary for Venus orbiter or flyby missions are discussed. The problems are primarily thermal, with increasing rather than decreasing power.

The investigation of a 5 MW manned solar electric spacecraft leads to the conclusion that the launch vehicles will be severely volume-limited. It is suggested that the power be reduced to 150 kW. Brief considerations of the 150 kW manned solar-electric spacecraft yield realistic parameters using future lightweight (12 kg/kW) solar arrays.

The technical report summary is concluded by a presentation of a sample of the problems involving the utilization of large solar arrays.

CONTENTS

ILLUSTRATIONS

ILLUSTRATIONS (contd)

TABLES

SECTION 1

40-50 kW MARS MAPPER

The 1967 Mars Mapper mission will be designed for chemical launch from earth. When in space, the solar panels on the spacecraft will be unfolded and thrust will be initiated from the electric propulsion engine. A heliocentric transfer to Mars will require about 270-300 days. When approaching Mars, the chemical retro-rocket will effect capture into a Mars orbit. Cameras and other environment sensing devices will be activated while the spacecraft spirals toward the Martian surface. The 50-60 day lowering of the Mars orbit will be accomplished with the same solar electric propulsion which supplied the prime propulsion during the heliocentric transfer.

Throughout the mission a solar photovoltaic array will supply prime power although rechargeable batteries will be necessary during various phases of the mission. The ion engines will require 40 kW of power at Earth. Since additional power is required for transmission line losses, power conditioning losses, control, housekeeping and telemetry, the solar array will be assumed to produce 50 kW at Earth. The energy incident on the solar array reduces as the square of the distance from the sun. The expected solar array output as a function of the distance from the sun, taking into consideration changes in temperature, is shown in Fig. 1. The reduction in solar array temperature produces a rise in solar cell efficiency and voltage.

1.1 SPACECRAFT DESIGN

The overall spacecraft design is greatly dependent on the solar array configuration and the number of electric propulsion engines required.
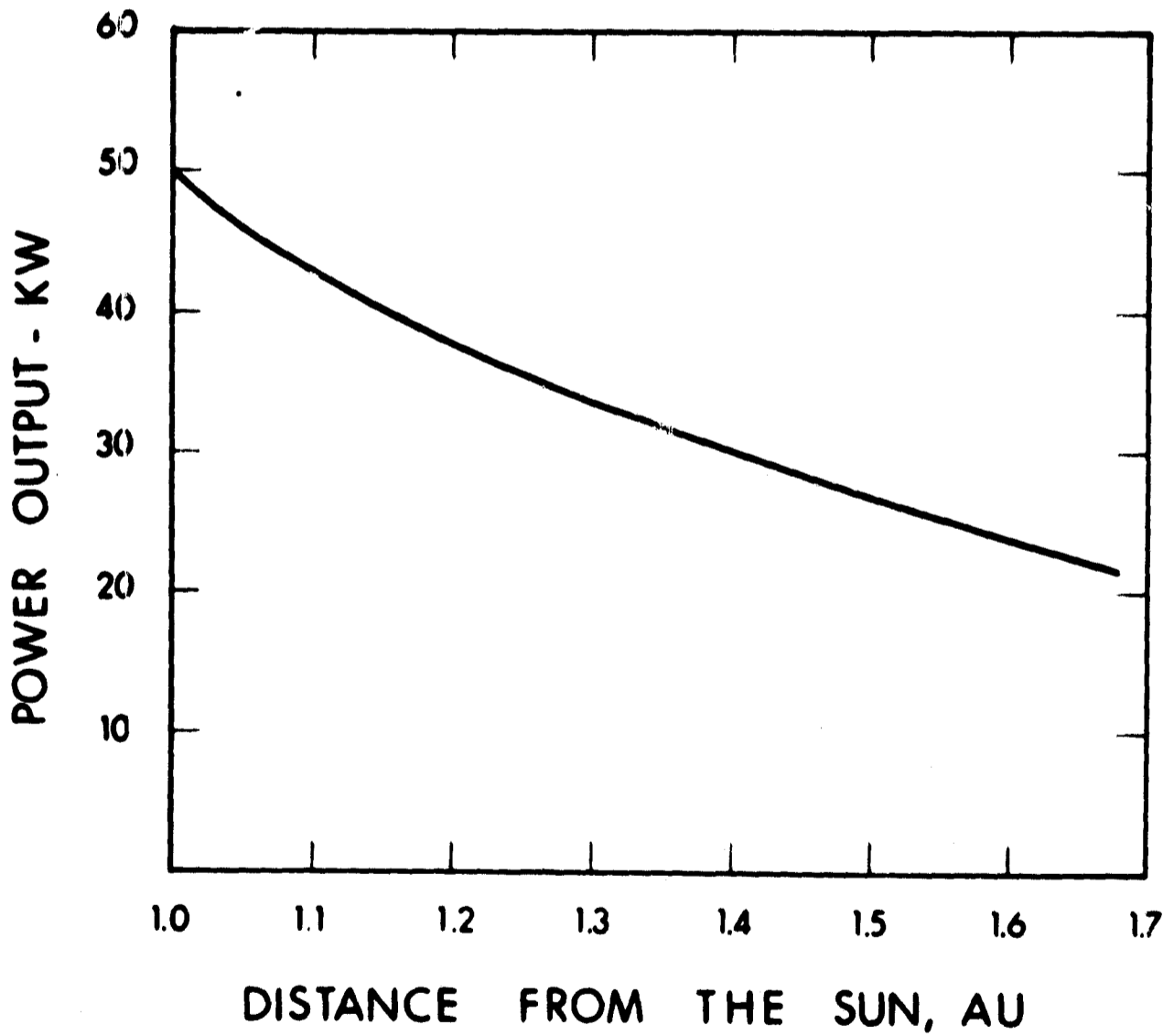
Figure 1. 50 kW Solar Array Output versus Distance from the Sun

The output of a solar array at Earth is 107 watts per square meter. This means that 470 square meters of solar array will be necessary. Two configurations for the solar array which were considered are shown in Fig. 2.

The four wing design in Fig. 2 has the advantage that the moment of inertia is low and because the power transmission distances are less than for the power two wing design. The disadvantages are that it is less stable and that the ion engines may affect at least one of the wings. The two wing design will be used for further considerations because of its stability and because it provides a clear exhaust path for the ion beam.

Consideration of the engine matrix will be based on the three leading electric propulsion thrusters. Electron bombardment engines are the first choice. Using cesium propellant, these engines have demonstrated their capability to operate in excess of the required period of time at extremely high efficiency. In addition they are very lightweight and continually display very high propellant mass utilization efficiencies. This type of engine requires a neutralizer. A cesium plasma bridge neutralizer has been developed and tested. It was found to be efficient lightweight, reliable, easily controlled, and able to operate far in excess of the required one year.

Electron bombardment engines using mercury propellant were considered because the system of which the engine is part is highly developed. However, these engines will be at least twice as heavy as comparable cesium engines. Furthermore, the mercury electron bombardment engine has not been able to demonstrate very high efficiencies while operating the required 1 year.

The third engine considered was the magnetoplasmadynamic arc jet (MPD arc jet) thruster. This engine has not demonstrated long life or high

RETRO ROCKET

SOLAR PANELS

ION ENGINE CLUSTERS

a. Spacecraft with Two-
Wing Solar Array

VEHICLE

SOLAR PANELS

b. Spacecraft with Four-
Sided Solar Array
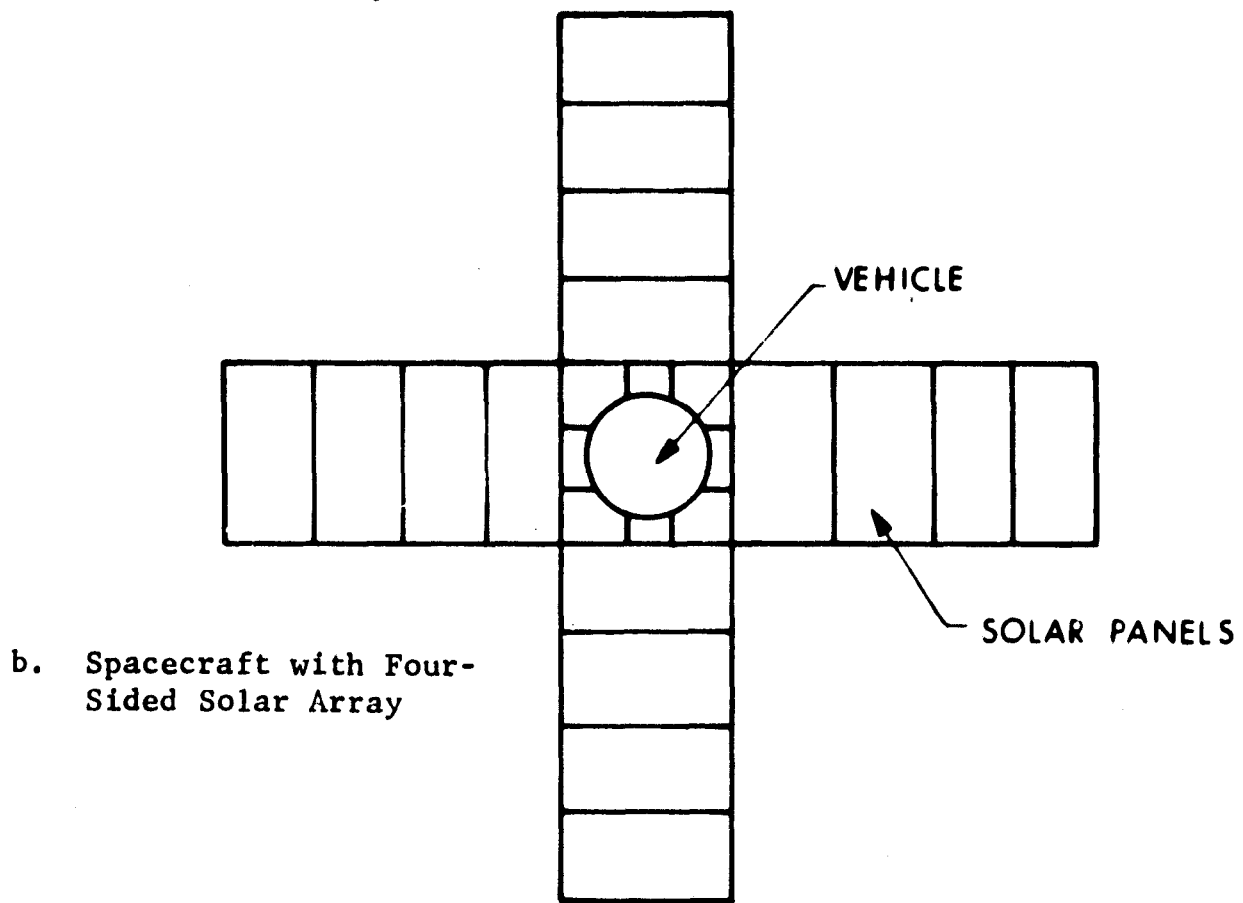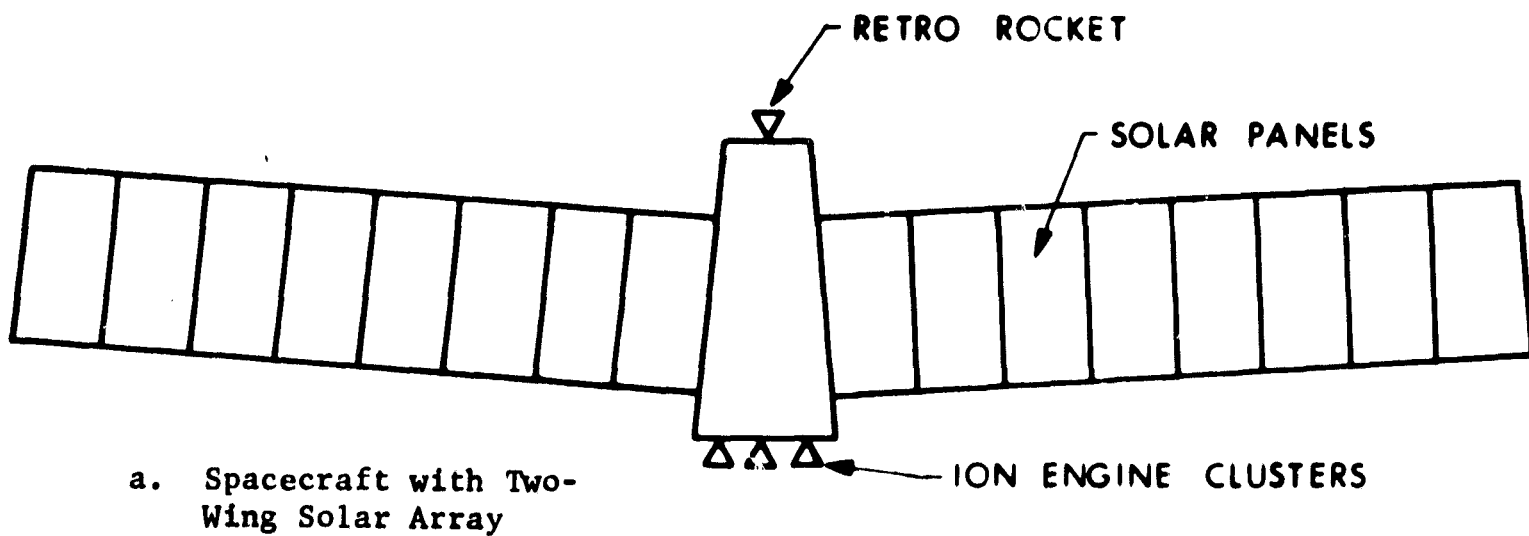
Figure 2. Solar Array Configurations

73529279

efficiency. However, its inherent ruggedness, versatility, simplicity, high thrust density and high power capabilities make it a likely candidate for missions in the next 5 to 10 years. The MPD arc jet development program is producing large gains in efficiency with specific impulses from 1500 to 4000 seconds. After the completion of life tests scheduled for the near future it will be applicable to electric propulsion missions with power levels above 25 kW.

The engine matrix investigation was based on 2.5 kW electron bombardment engines. This power level was selected since the size is convenient and because this is the largest size engine displaying high efficiency and long life. **Figures 3, 4 and 5 show a Mars mapper spacecraft with 16 cesium electron bombardment thrusters.** Four engines will operate from a common propellant tank. Two neutralizers are shown in the center on the engine matrix. The number of neutralizers that will be necessary has not been established conclusively. This configuration does not offer any redundancy in the number of available thrusters during the full power phase of the heliocentric transfer. As the power reduces with distance, pairs of thrusters will be deactivated and these deactivated thrusters will afford spare engines in the event of a failure.

Figures 6, 7, 8 and 9 incorporate two spare engines in the thruster matrix. These spares would only be useful in the event of thruster failures early in the mission. Figures 6 and 7 are arranged in a wide spaced matrix to supply maximum control torque on the spacecraft. Figures 8 and 9 are arranged in a close spaced matrix to minimize the effects of thrust vector alignment errors. Because of the low weight of the cesium bombardment thruster, the extra thrusters may well be justified. This could be particularly true if an early thruster loss should prove to abort the mission.
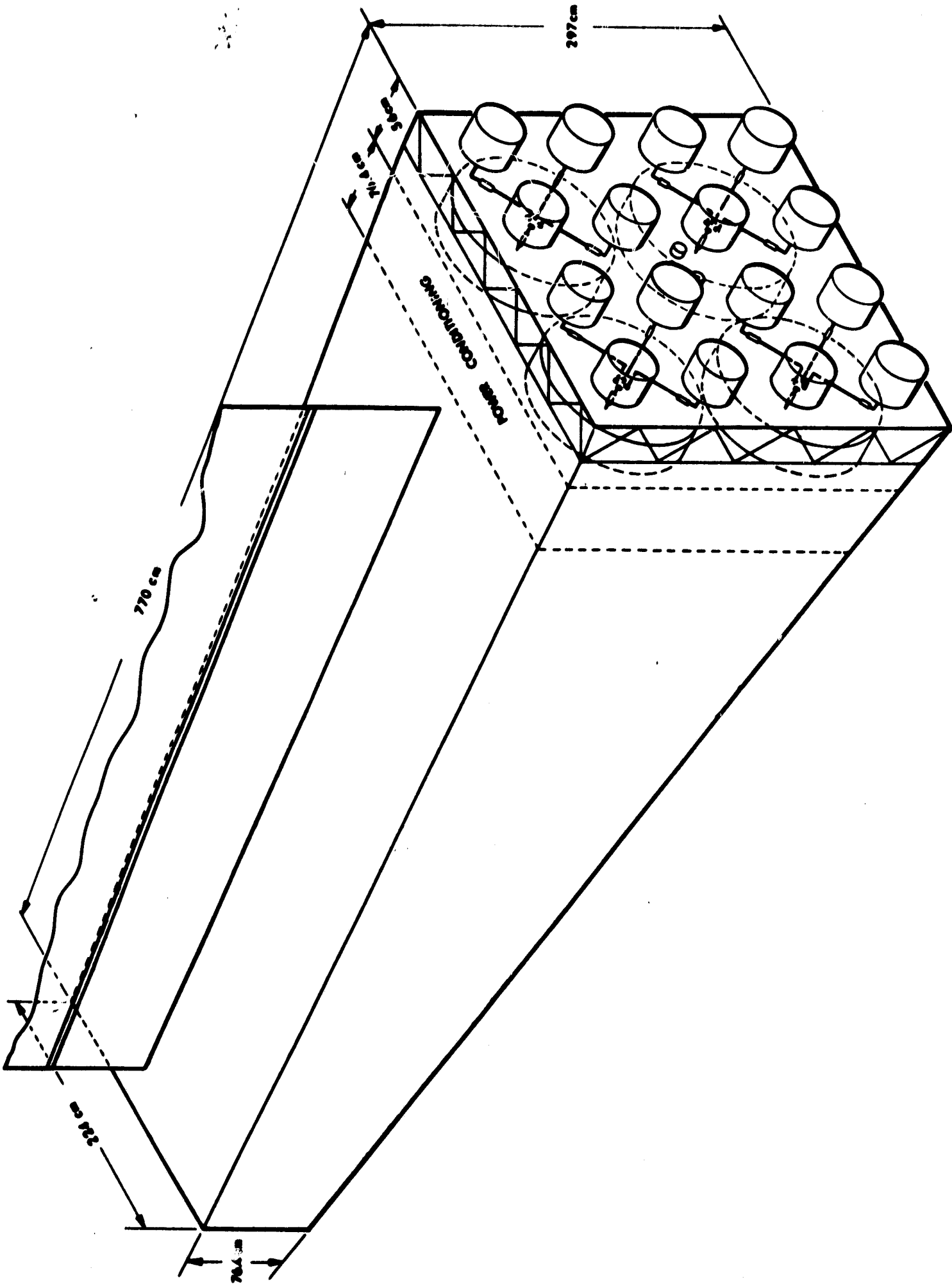
Figure 3. Mars Mapper Spacecraft with Electric Propulsion Using 16 Cesium Electron Bombardment Thrusters
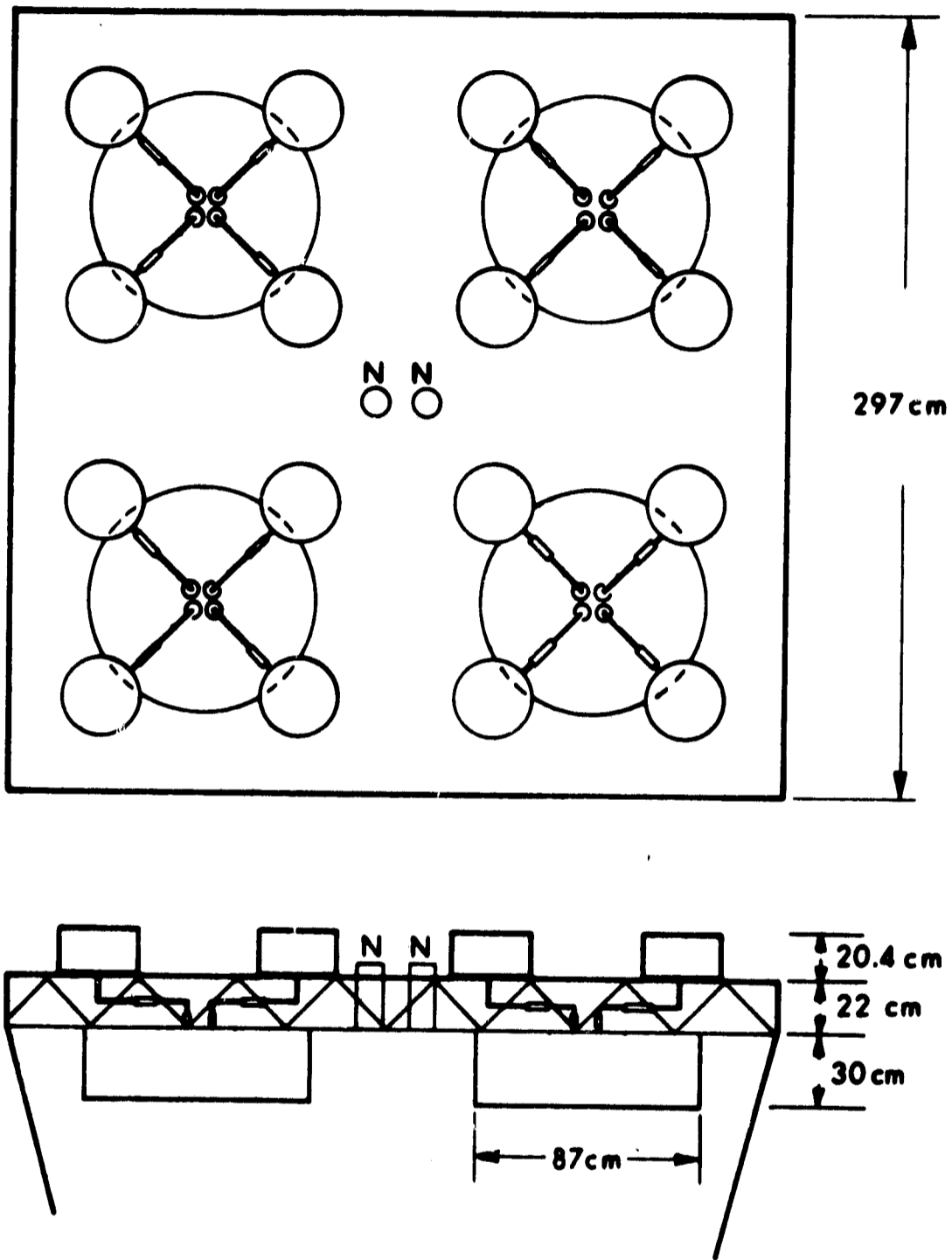
Figure 4. Mars Mapper Spacecraft with Electric Propulsion
Using 16 Cesium Electron Bombardment Thrusters
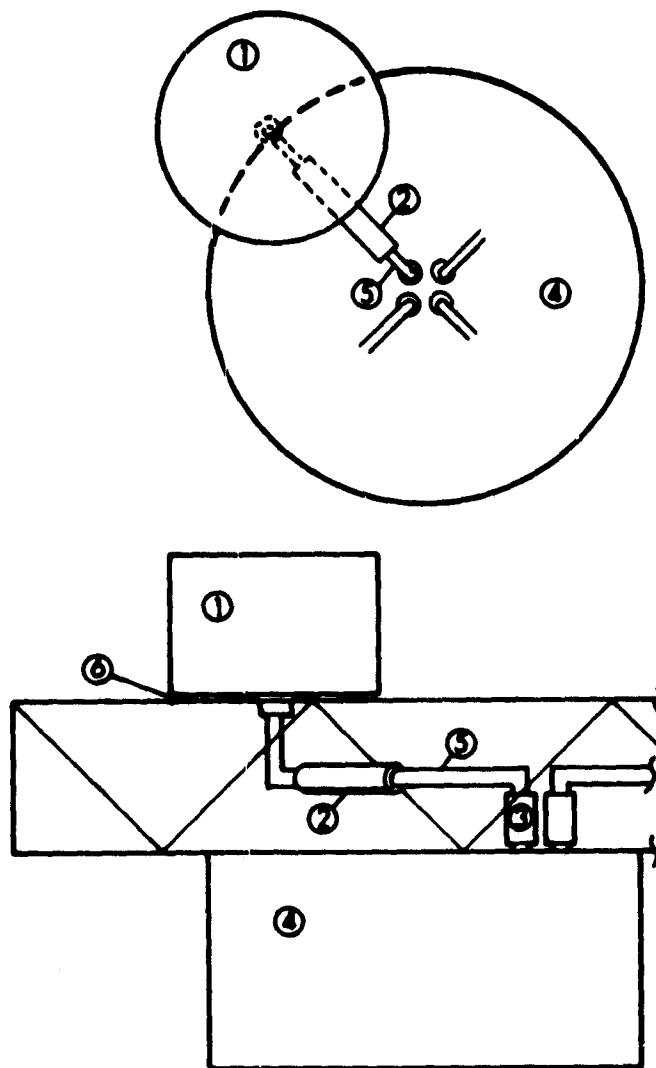
① CESIUM ELECTRON BOMBARDMENT THRUSTER
   $P_T = 2.5$ kw
   $I_{sp} = 3500$ seconds
   $T = .103$ N
   $L = 20.4$ cm.
   $D = 30$ cm
② ISOLATOR
   $V = 5$ kv
   LEAKAGE $= 1$ ma
   $L = 12$ cm
   $D = 2$ cm

③ VAPORIZER
   $P = 030$ kw
   $L = 5$ cm
   $D = 2$ cm

④ CESIUM PROPELLANT RESERVOIR
   $L = 30$ cm
   $D = 87$ cm

⑤ CESIUM VAPOR FEEDLINE
   $D = 1$ cm

⑥ INSULATORS

Figure 5.   Details of Electric Propulsion
            for a 16-Cesium Electron
            Bombardment Thruster Array

73627542
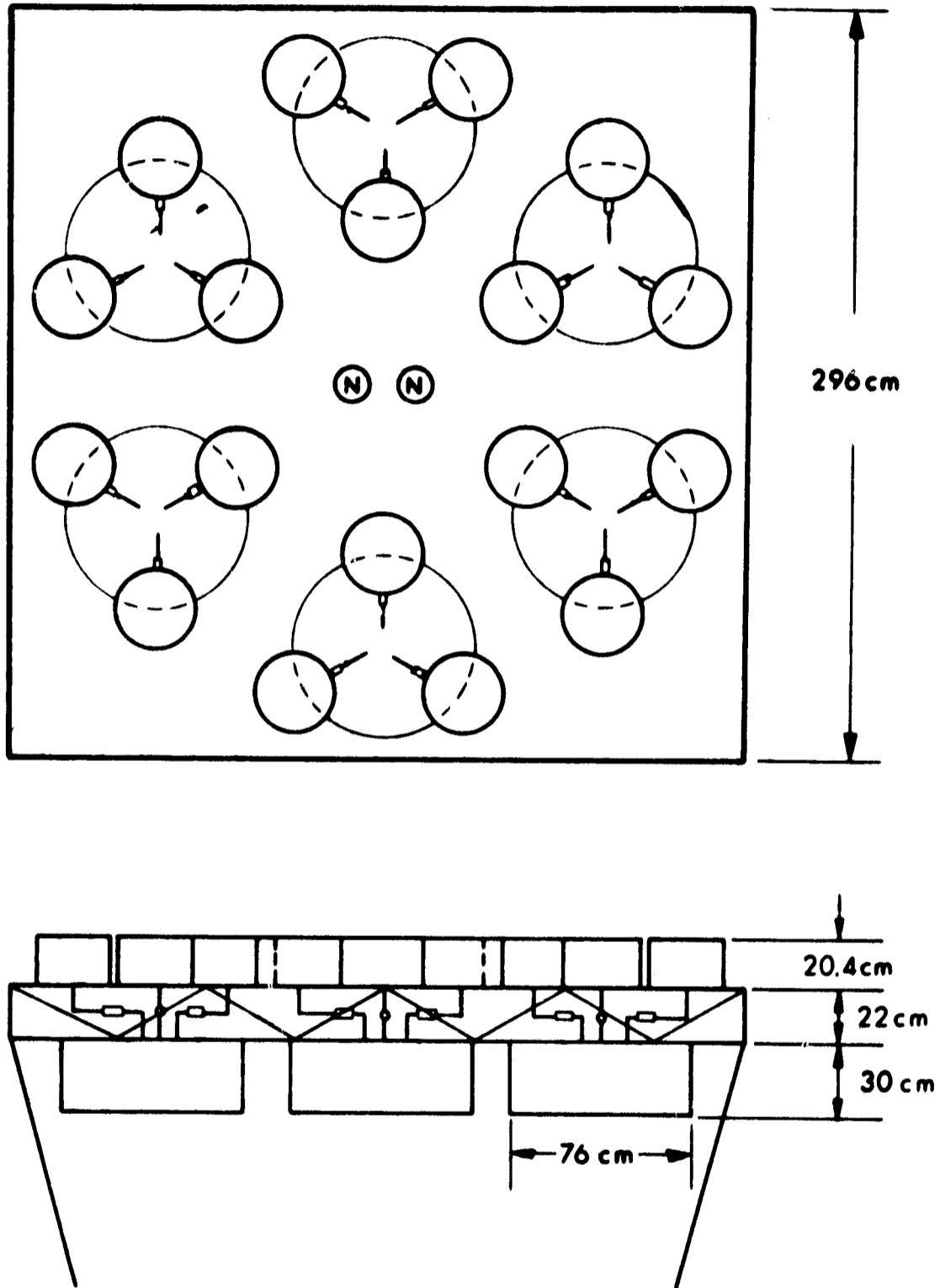
Figure 6. Mars Mapper Spacecraft with Electric Propulsion Using 18 Cesium Electron Bombardment Thrusters in a Wide-Spaced Array

73627546
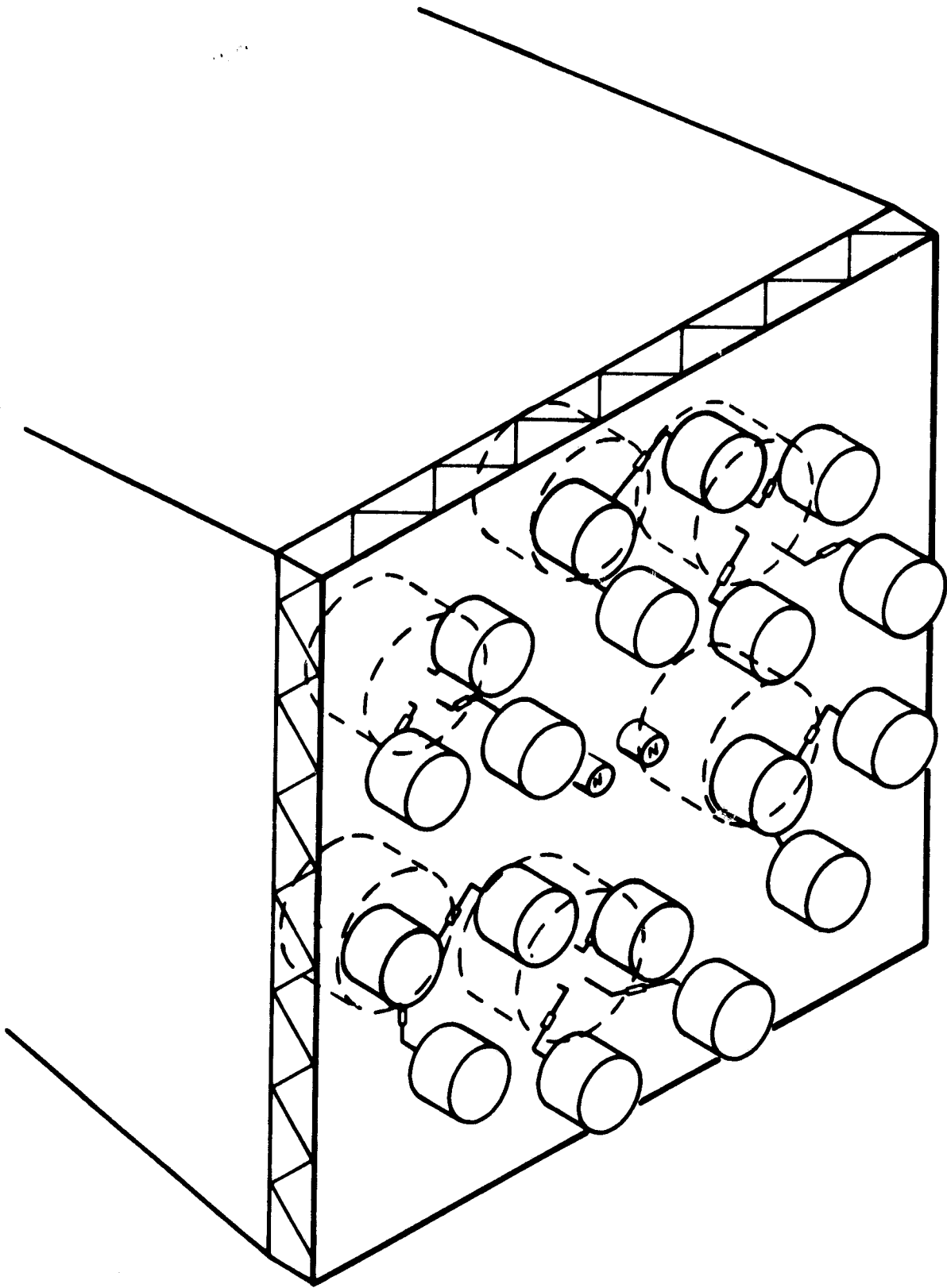
Figure 7. Mars Mapper Spacecraft with Electric Propulsion Using 18 Cesium Electron Bombardment Thrusters in a Wide-Spaced Array
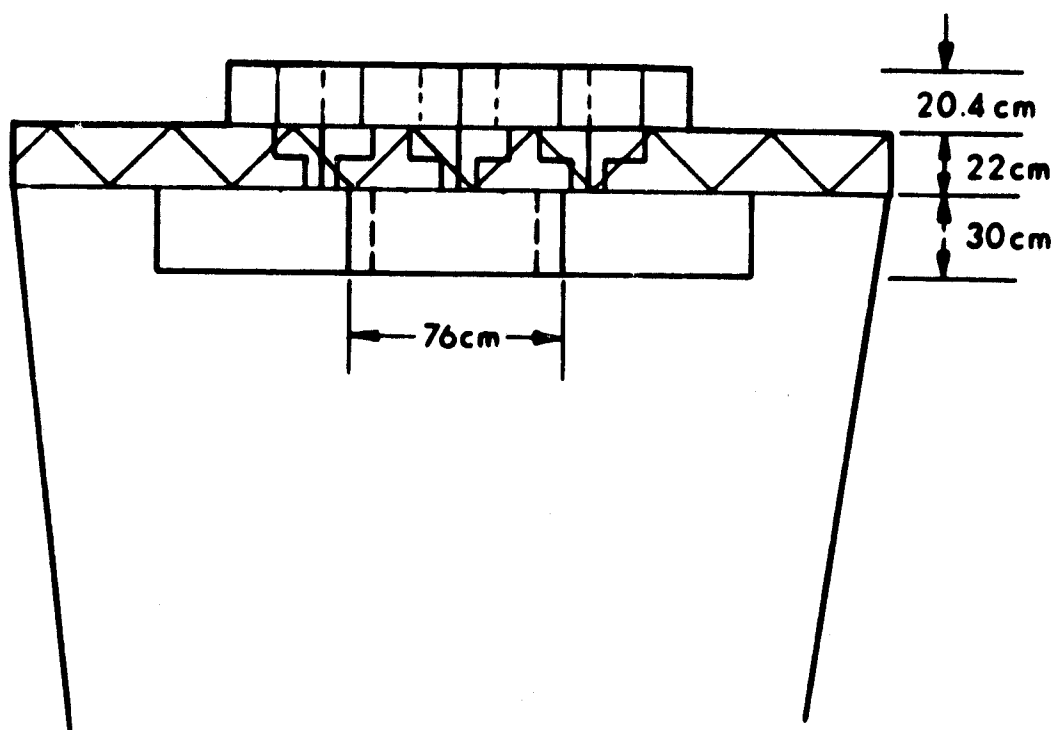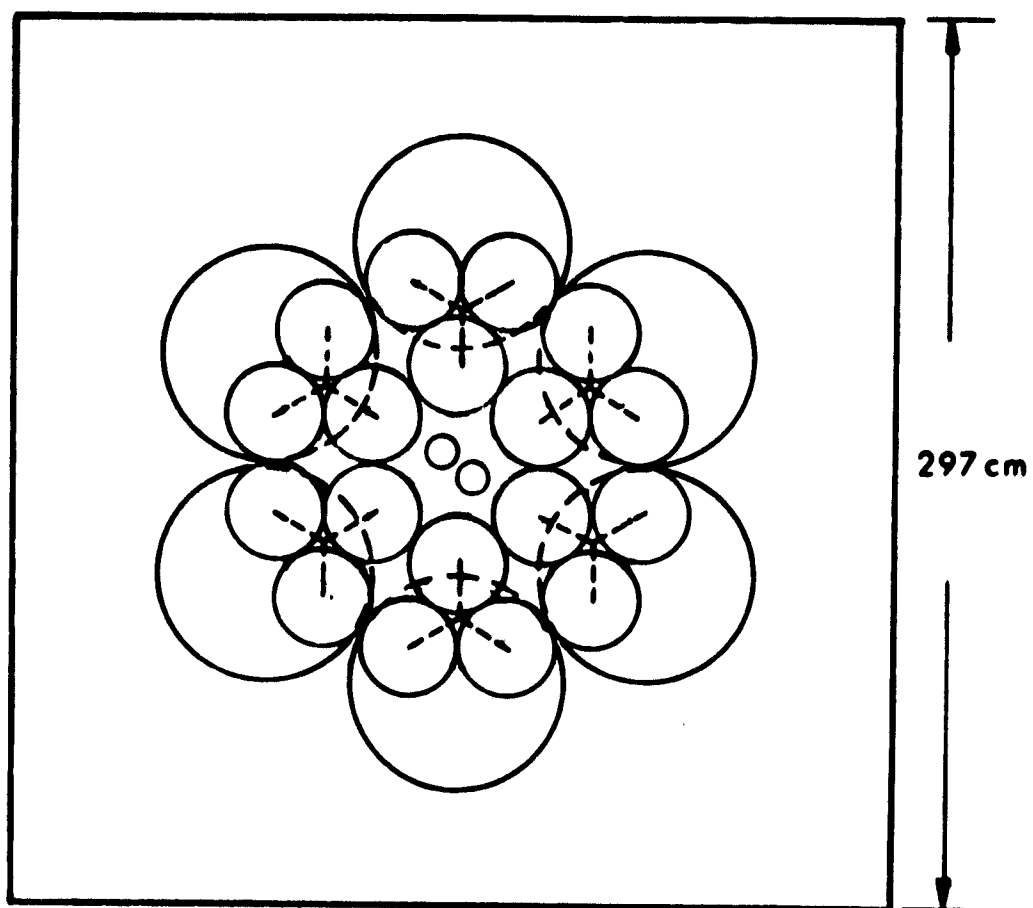
Figure 8. Mars Mapper Spacecraft with Electric Propulsion
Using 18 Cesium Electron Bombardment Thrusters
in a Close-Spaced Array

27548
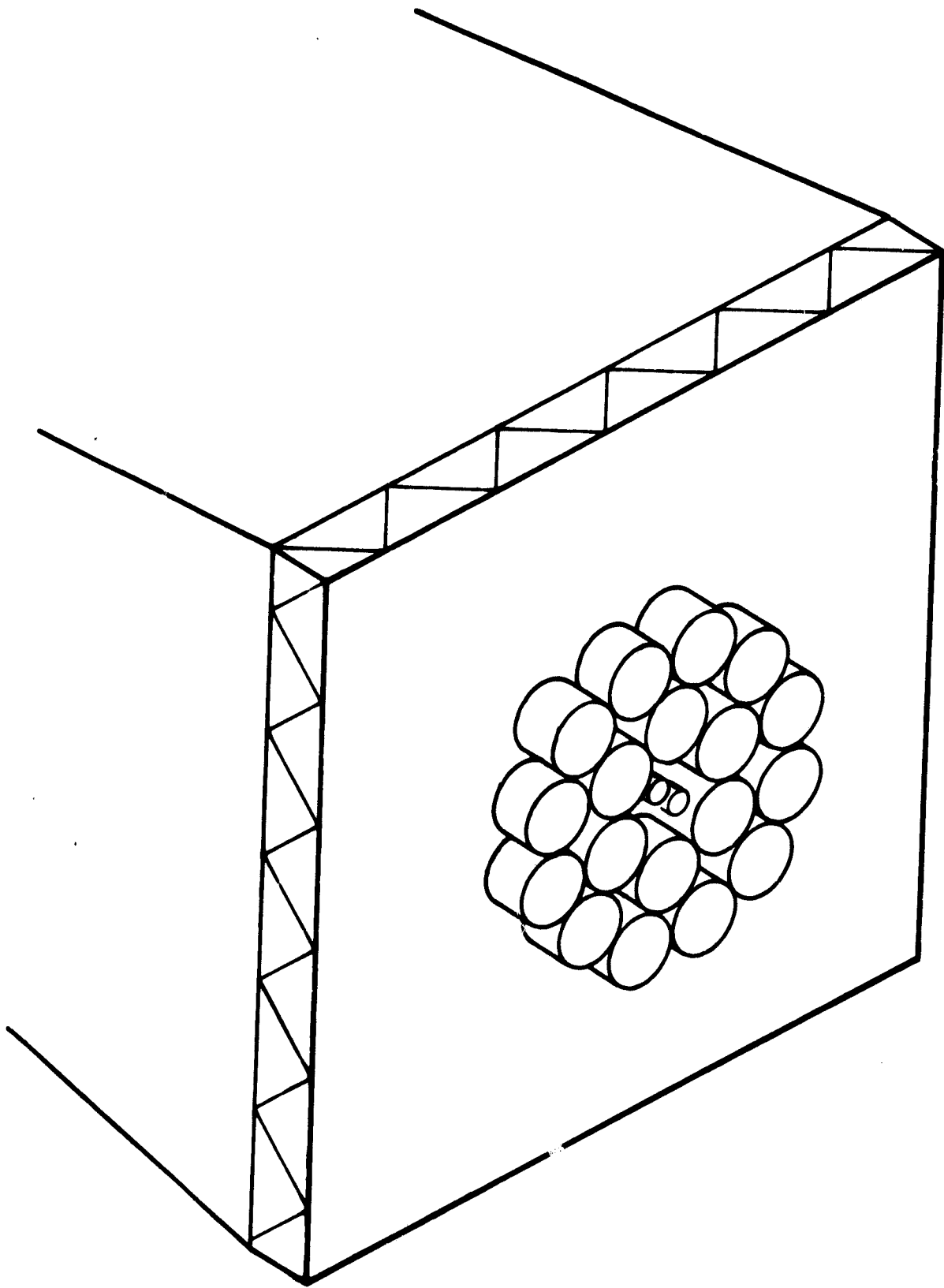
Figure 9. Mars Mapper Spacecraft with Electric Propulsion Using
18 Cesium Electron Bombardment Thrusters in a Close-
Spaced Array

In the event that MPD arc jet engines are incorporated, Figs. 10 and 11 show an engine matrix utilizing four thrusters at 10 kW each. No neutralizers are necessary. The spacecraft conceptual designs shown in Figs. 3, 4 and 5 are used for further analysis.

1.2 ENGINE SYSTEM DESCRIPTION

Preliminary mission studies have shown that the electric propulsion system will operate at a specific impulse of 3500 seconds. Further considerations on the Mars Mapper will utilize 2.5 kW cesium electron bombardment engines operating at 3500 seconds specific impulse. It will be assumed that cesium plasma bridge neutralizers are also used. The engine will have a permanent magnet shell. The arc will be run on single phase alternating current at its inverter frequency. This eliminates the need for a magnet power supply and for high current arc supply rectifiers. A summary of this engine's operating characteristics is shown in Table I. The power supply requirements for the 2.5 kW cesium electron bombardment engine operating at a specific impulse of 3500 seconds are shown in Table II. This engine should be flight ready in 1968. The efficiency of the engine is shown to be 70 percent; however, it is possible that efficiencies of 75 percent will be achieved by the time the flight ready thruster is completed.

A single propellant tank will supply four engines with cesium. The calculations for the dimensions of the propellant tankage are shown below. It was assumed that all thrusters operate during the entire 300 day mission. During a heliocentric transfer to Mars the power is decreasing, which results in some thrusters being turned off. This means more than a 25 percent decrease in the amount of propellant necessary for the transfer. The spare propellant in this calculation is assumed to be used to spiral down while in the Mars orbit. A more precise calculation will have to be based on thrust programing, duty cycle, leakage rates, etc.

297cm

12cm

18cm

13cm

45cm

275cm

① ALPHA THRUSTORS
$P_T = 10$ kW
$I_{sp} \approx 3500$ seconds
$T = .35$ N
$L = 18$ cm
$D = 12$ cm

② LITHIUM PROPELLANT RESERVIOR
$L = 45$cm
$D = 275$cm
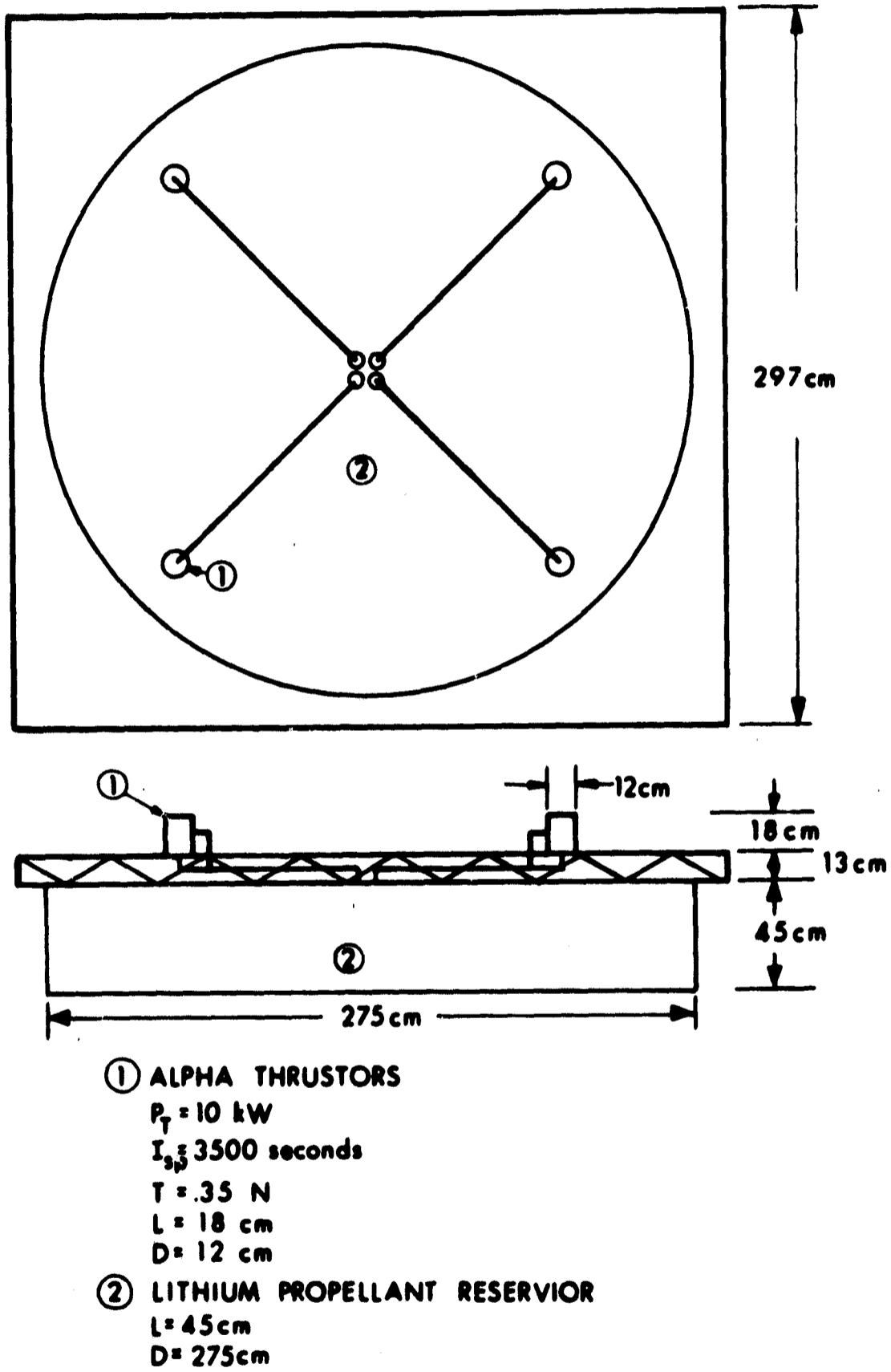
Figure 10. Mars Mapper Spacecraft with Electric Propulsion
Using Four Alkali Plasma Hall Accelerator Thrusters
with Lithium Propellant

27544
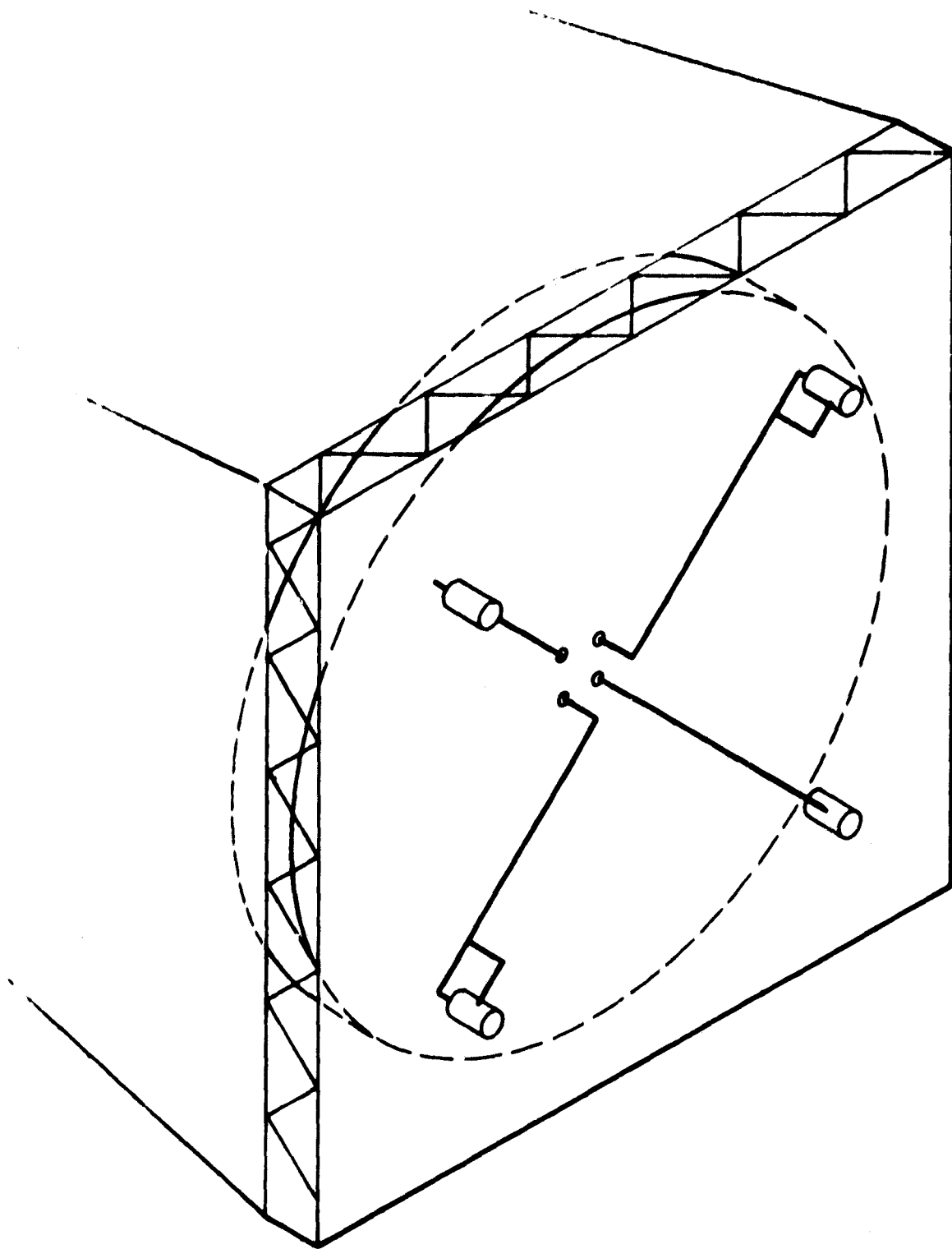
Figure 11.   Mars Mapper Spacecraft with Electric Propulsion Using
            Four Alkali Plasma Hall Accelerator Thrusters with
            Lithium Propellant

TABLE I

CESIUM ELECTRON BOMBARDMENT ENGINE (1968)

2.5 KW at I_{SP} 3500 Sec

$V+$	kV	1.0	1940 watts	D	cm.	30	
I_B	mA	1940	Beam Power	L	cm.	20	
$V-$	kV	.300	35.7 watts	W_S	lb_f	4.0	
$I-$	mA	27.5	Drain Power	M	kg	1.82	
				$\dot{m}$	gm/hr	9.7	
V_A	V	7.2	525.0 watts	PA/I_B	eV/ion	275	
I_A	A	73.0	ARC Power	$I-/I_B$	%	1.5	
				J_{B-A}	mA/cm^2	3.1	
V_M	V	0		J_{T-A}			
I_M	A	0		V_{NB}	V	0	
				I_{NB}	A	0	
V_I	V	6.0	20 watts	V_{NV}	V	4.0	6.4 watts
I_I	A	3.3	Isolator Heater	I_{NV}	A	1.6	
V_V	V	7	26.0 watts	V_{NK}	V	2.5	3.8 watts
I_V	A	3.7	Vaporizer	I_{NK}	A	1.5	
V_K *	V	10.	40.* watts				
I_K	A	4	Cathode	η_0	mA		
				η_M'			
η_0	mA			P_N	W	10.2	
η_M	%	86		P_T'	W	2502	
				η_E'	%	77.6	
P_T	W	2491.75		η_T'	%		
η_E	%	78.0					
η_{Total}	%	67.9		P'/T	KW/lb_f	109	
				P'/T	KN/N	24.3	
T	mlb_f	23.0		I'_{SP}	Sec.		
T	N	.1025					
P/T	KW/lb_f	108					
P/T	KW/N	24.2					
I_{SP}	Sec.	3360					

PRIMES INCLUDE NEUTRALIZER

* Used during start-up only

TABLE II

ELECTRON BOMBARDMENT ENGINE POWER SUPPLY REQUIREMENTS (1968)

Propellant _____ Cesium

Power _____ 2.5 kW

Specific Impulse _____ 3500 Sec

	TYPE	VOLTAGE (VOLTS)	CURRENT (AMPS)	POWER (WATTS)
Positive High Voltage	dc	1000	1.9675	1967.5
Negative High Voltage	dc	300	.0275	8.1
Arc	ac	7.2	73.0	525.0
Vaporizer Heater	ac	7	3.7	26
Isolator Heater	ac	6.0	3.3	20
Reservoir Heater	ac	7	3.7	26
Cathode Heater*	ac	10	4	40*
Cathode Keeper	--	--	--	--
Magnet	--	--	--	--
Neutralizer Vaporizer Heater	ac	4.0	1.6	6.4
Neutralizer Reservoir Heater	--	--	--	--
Neutralizer Cathode Heater	ac	2.5	1.5	3.8
Neutralizer Cathode Keeper	--	--	--	--
Neutralizer Bias				

* Startup Only

VARIABLES:

P   = Power (kilowatts)

T   = Thrust (Newton)

I_{sp} = Specific Impulse (seconds)

$\dot{m}$ = Mass Flow Rate (kilograms/second)

m   = Mass (kilograms)

V   = Volume (centimeters^3)

L   = Length (centimeters)

D   = Diameter (centimeters)

ρ = Density (grams/centimeters^3)

Cesium Electron Bombardment Thruster Tankage

P_T = 2.5 Kilowatts

T   = .103 Newtons

I_{sp} = 3500 seconds

$$\dot{m} = \frac{T}{I_{sp}\, g} = \frac{.103\ N}{3500\ sec. \times 9.8\ \frac{N}{kg}} = 3.00 \times 10^{-6}\ \frac{kg}{sec}$$

$$m = \dot{m}\, t = 3 \times 10^{-6}\ \frac{kg}{sec} \times 3600\ \frac{sec}{hr} \times 7200\ hr = 78\ kg\ \text{per Thruster}$$

$$V_1 = \frac{m}{\rho_{cs}} = \frac{7.8 \times 10^4\ g}{1.9\ \frac{g}{cm^3}} = 4.10 \times 10^4\ cm^3\ \text{per Thruster}$$

Allowing 10% additional volume for the finned array and wick, the volume of a 4 Thruster Propellant Tank is:

$$V_4 = 4 \times 4.1 \times 10^4 \times 1.10 = 1.8 \times 10^5\ cm^3\ \text{per 4 Thrusters}$$

Then the diameter for a 30 cm long Cylindrical Tank is:

$$D_4 = \sqrt{\frac{4\ V_4}{\pi\ L}} = \sqrt{\frac{4 \times 1.8 \times 10^5}{\pi \times 30}} = 87\ cm\ \text{per 4 Thrusters}$$

Allowing 10 percent additional volume for the finned array and wick, the volume of a 3 Thruster Propellant Tank is:

$$V_3 = 3 \times 4.1 \times 10^4 \times 1.10 = 1.35 \times 10^5 \ .cm^3 \text{ per 3 Thrusters}$$

The diameter for a 300 cm Long Cylindrical Tank is:

$$D_3 = \sqrt{\frac{4 \ V_3}{\pi \ L}} = \sqrt{\frac{4 \times 1.35 \times 10^5}{\pi \times 30}} = 76 \text{ cm per 3 Thrusters}$$

Isolator

As a consequence of operating a number of thrusters from a common propellant supply some means of electrically isolating each thruster from the others is necessary. Isolators have been built which consist of an insulating to segment of feed tube with a series of baffles in the insulating tube to provide a long electrical path for isolation. Such isolators have proven effective with mercury but their performance with cesium has not been as good as could be desired. Present cesium isolator performance, Fig. 12, has a leakage current of a few milli-amperes with a 5000 volt potential across them. At the 1000 volt operating level for the present system the leakage would be very much less.

In the event of a thruster to ground short circuit the failed thruster would be removed from operation and its associated vaporizer would be shut down. If at the same time the isolator were kept hot for a few minutes, all cesium remaining in it would evaporate and the leakage should drop to a negligible value. After the cleanup period, the isolator heat should not be required, but since it is presumed that an operating thruster has failed, there would be power to spare. Therefore, a better choice would probably be to leave the heater operating in case the cold vaporizer is not fully effective in stopping cesium flow.

COLUMBIUM

LUCALOX OR
AL$_2$O$_3$ WASHERS

STAINLESS STEEL
SCREEN ELECTRODES
OR

SOLID ELECTRODES
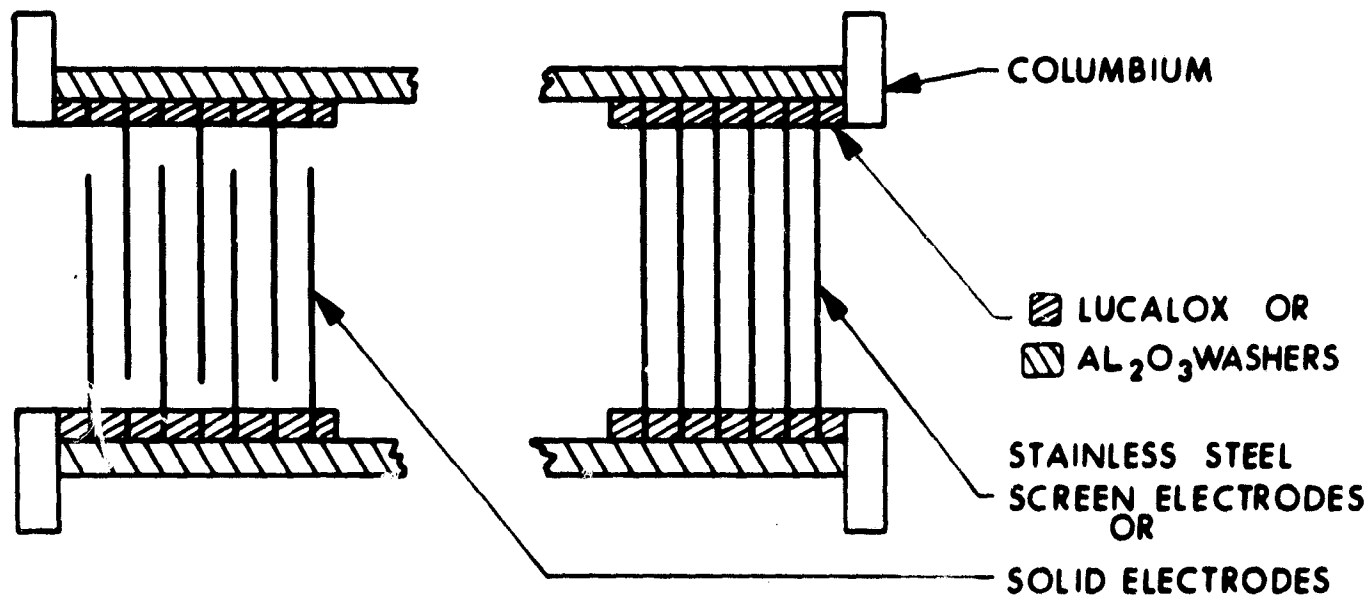
CURRENT PERFORMANCE

UP TO 5 kV AT 6-10 mA LEAKAGE
LENGTH = 6 inches
INSIDE DIAMETER = 3/4 inches
TEMPERATURE = 360 - 420°C
MASS < .275 kg

GOAL :

LEAKAGE < 1 mA
LENGTH < 5 inches
HEATER POWER < 20 watts

Figure 12.   Cesium Isolator Performance

1.3 ENGINE MATRIX MODES OF OPERATION

During the transfer from Earth to Mars, the engines which are operating in the matrix will be determined by three conditions.

    a.   Decreasing power and increasing voltage

    b.   The failure of a thruster or its complement

    c.   Changes in trajectory

        (a)   Pitch, yaw, roll maneuvers

        (b)   Error in thrust vector alignment with c.g.

        (c)   Retropropulsion

The constraints which determine the number and type of modes of engine matrix operation are as follows:

    a.   All available power will be used for engine operation. This excludes telemetry, housekeeping, etc. At Mars the power is reduced to 0.46 of that at Earth; therefore, at least one half of the engine matrix will be operating throughout the transfer.

    b.   If an engine fails, its complement in the thruster matrix must be turned off to eliminate torques on the spacecraft. Torques are, in general, undesirable since heliocentric transfer power must be used to correct for the torque.

    c.   When reducing the number of operating engines, the engines to be turned off will be those most remote from the center of the cluster. This tends to minimize the thrust vector error and resulting torques.
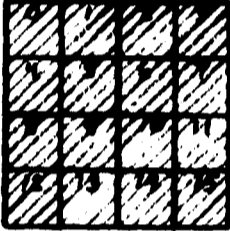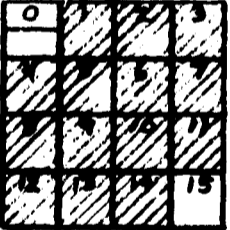
The number of possible combinations of thrusters operating in the engine cluster is $2^{16} = 65,536$ with no restrictions. With restriction a., the number of modes is cut in half to 32,768. With restriction b., the number of modes is reduced by half again to 16,384.

In order to represent these modes when describing the propulsion system requirements during the Earth-Mars transfer a binary representation will be used. This representation has the additional advantage in that it

corresponds to the output signals from the command control logic.

An operating engine = 1 =
A nonoperating engine = 0 =
A failed engine = θ =

For clarification then,

	15	14	13	12	11	10	9	8	7	6	5	4	3	2	1	0	
All operating =	1	1	1	1	1	1	1	1	1	1	1	1	1	1	1	1	=
All nonoperating =	0	0	0	0	0	0	0	0	0	0	0	0	0	0	0	0	=
Number 0 thruster failed, Number 15 complement thruster is turned off, remaining thrusters are operating.	0	1	1	1	1	1	1	1	1	1	1	1	1	1	1	θ	

The complement thrusters are
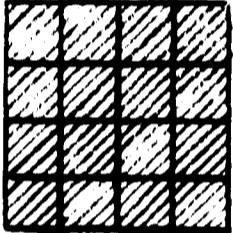
0	1	2	3	4	5	6	7
15	14	13	12	11	10	9	8
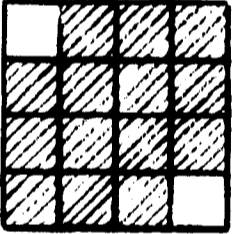
NOTE: A thruster's number and its complement number add to 15.
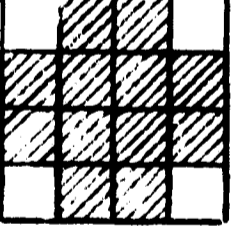
Case I - If no thrusters fail during the Earth-to-Mars transfer the following sequence of matrix operational modes should be observed. This assumes no course corrections or maneuvers.
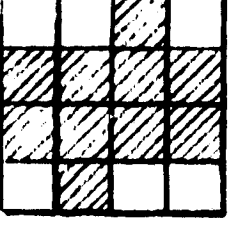
	15	14	13	12	11	10	9	8	7	6	5	4	3	2	1	0	
a. During launch	0	0	0	0	0	0	0	0	0	0	0	0	0	0	0	0	
b. Beginning transfer	1	1	1	1	1	1	1	1	1	1	1	1	1	1	1	1	
c. First power reduction	0	1	1	1	1	1	1	1	1	1	1	1	1	1	1	0	
d. Second power reduction	0	1	1	0	1	1	1	1	1	1	1	1	0	1	1	0	
e. Third power reduction	0	0	1	0	1	1	1	1	1	1	1	1	0	1	0	0	

	15	14	13	12	11	10	9	8	7	6	5	4	3	2	1	0
f. Fourth power reduction	0	0	0	0	1	1	1	1	1	1	1	1	0	0	0	0
Fourth power reduction Alternate 2	0	0	1	0	0	1	1	1	1	1	1	0	0	1	0	0
Fourth power reduction Alternate 3	1	1	0	0	1	1	0	0	0	0	1	1	0	0	1	1
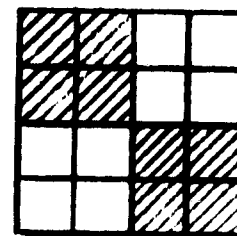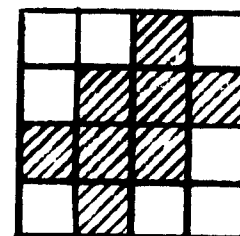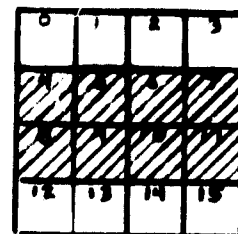
This may be a useful configuration since two reservoirs are inactive and no heater power is necessary for them.

Case II - If some thrusters fail during the Earth-to-Mars transfer
the following sequence of cluster operational modes should
be enacted. This assumes no course corrections or maneuvers.

Failed Engine Numbers	Modified Mode of Cluster Operation															
	15	14	13	12	11	10	9	8	7	6	5	4	3	2	1	0
0 or 15	θ	1	1	1	1	1	1	1	1	1	1	1	1	1	1	θ
1 or 14	1	θ	1	1	1	1	1	1	1	1	1	1	1	1	θ	1
2 or 13	1	1	θ	1	1	1	1	1	1	1	1	1	1	θ	1	1
3 or 12	1	1	1	θ	1	1	1	1	1	1	1	1	θ	1	1	1
4 or 11	1	1	1	1	θ	1	1	1	1	1	1	θ	1	1	1	1
5 or 10	1	1	1	1	1	θ	1	1	1	1	θ	1	1	1	1	1
6 or 9	1	1	1	1	1	1	θ	1	1	θ	1	1	1	1	1	1
7 or 8	1	1	1	1	1	1	1	θ	θ	1	1	1	1	1	1	1

a. If a failure occurs during launch or in the beginning transfer,
a loss of the failed thruster and its complement will be expe-
rienced during the beginning transfer.

Note that a single failure during the first power reduction
does not affect the spacecraft efficiency. It is desirable to
run at maximum efficiency during the beginning transfer; there-
fore, the thrusters should be designed to be throttled to use
up the power not being used by the failed thruster and its com-
plement. This would be a maximum increase in power per thruster of

$$\left(\frac{16}{14} - 1\right) 100 = 14\%.$$

This throttling capability is equivalent to carrying two spare
engines inactively.

b. If a single or double failure occurs during the second power reduction, there is no effect on the efficiency. The engine control system will simply turn off the complement engine or engines with no resultant torques.

If three failures occur during the second power reduction, assuming the failed engines are not complements, the complement of each thruster will be turned off and a new mode of cluster operation must be established. Again, throttling the engines will allow the efficient use of the unused power. This would be a maximum increase in power per engine of

$$\left(\frac{12}{10} - 1\right) 100 = 20\%.$$

c. If four failures occur during the third power reduction and the failed and complement engines are turned off, the maximum increase in power per thruster is

$$\left(\frac{10}{8} - 1\right) 100 = 25\%.$$

d. If five failures occur during the fourth power reduction and the failed and complement engines are turned off, the maximum increase in power per thruster is

$$\left(\frac{8}{6} - 1\right) 100 = 33\%.$$

Since the most throttling necessary is to absorb 33% extra power, this should be a design factor for the engines.

1.4 THRUST PROGRAMMING

The electric propulsion, and hence power conditioning and control operational modes, are being analyzed relative to the solar array electrical output variations resulting from Mars Mapper mission considerations.

During an Earth-to-Mars transfer the solar array output voltage increases as the available power decreases. To compensate for the decrease in power the number of thrusters in operation is reduced in complement pairs. The maximum power to any engine at any moment is 2.5 kW. Reliability considerations in the Engine Cluster Modes of Operation section add a conditional requirement of 33% more power handling capability per thruster.

The main parameters being investigated are power available, accelerating voltage, number of engines in operation, beam current, and specific impulse all as a function of the distance from the sun. The three cases considered thus far are:

Case I The accelerating voltage tracks the solar array output voltage.

Case II The accelerating voltage is held constant.

Case III The accelerating voltage is reduced on all thrusters in 100 volt increments when the tracking voltage exceeds the design voltage by 100 volts.

The control circuitry for the three cases varies from almost no control for minimum efficiency to strict control for maximum efficiency.

Case I Has engine shut down circuitry only.

Case II Has engine shut down circuitry and complex voltage regulation circuitry.

Case III Has engine shut down circuitry and incremental voltage control by the use of simple switching circuitry.

Since case II has the greatest number of parts and the most complexity, it would be expected to have the least reliable power conditioning and control. Case I, being the simplest, should be the most reliable. Case III should be almost as reliable as Case I since it has only small increases in number of parts and complexity over Case I.

The calculations of parameters for Cases I, II, and III are as follows:

a. Power found by power reduction estimate from graph. Assuming p = 40 kW to the engines at 1 AU

b. Voltage found by voltage increase estimate in the Design Data Bank. Assuming V = 1000 volts at 1 AU

c. Number of engines is found by turning off 2 engines at a time at 2.5 kW reduction in power available per engine. Starting with 16 engines.

d. Specific impulse was found by the equation:

η_m = mass efficiency (percent)

$\frac{q}{m}$ = charge-to-mass ratio (C/kg)

V+ = net accelerating voltage (volts)

I_{SP} = specific impulse (seconds)

$$I_{SP} = 1.445 \times 10^{-3} \, \eta_m \left[(V+) \, \frac{q}{m} \right]^{1/2}$$

For a 2.5 kW cesium electron bombardment thruster with a primary specific impulse of 3500 seconds:

η_m = 90%

$$\frac{q}{m} = 7.255 \times 10^5 \, \frac{C}{kg}$$

$$I_{SP} = 111.0 \, (V+)^{1/2}$$

e. The thrust is found by the equation:

η_e = electrical efficiency (percent)

P = power (kilowatts)

I_{SP} = specific impulse (seconds)

T = thrust (Newtons)

$$T = 2.04 \, \frac{\eta_e \, P}{I_{SP}}$$

For a 2.5 kW cesium electron bombardment thruster with a primary specific impulse of 3500 seconds

$$\eta_e = 70\%$$

$$T = 139.0 \frac{P}{I_{SP}}$$

The total thrust for the input power to the entire engine cluster was found at one time, the efficiency is assumed constant but actually will tend to rise with increased I_{SP}:

f. The total beam current for all thrusters operating in the engine cluster is:

T = thrust   (Newtons)

$\frac{q}{m}$ = charge-to-mass ratio (C/kg)

$V+$ = net accelerating voltage (volts)

I_{BC} = cluster beam current (amps)

$$I_B = \frac{T \frac{q}{m}}{1.42 \quad V+}$$

For a 2.5 kW cesium electron bombardment thruster with a primary specific impulse of 3500 seconds $\frac{q}{m} = 7.255 \times 10^5$ C/kg

$$I_B = 588 \frac{T}{\sqrt{V+}}$$

g. The individual thruster beam currents are then found by dividing the total beam current by the number of engines operating.

The results from these calculations listed in Tables III, IV and V and plotted as a function of distance from the sun in Figures 13, 14 and 15.

NOTE: These calculations are based on constant efficiencies which were found to be a reasonable assumption due to relatively small variations in the operating point parameters.

TABLE III

CASE I — THE ACCELERATING VOLTAGE TRACKS THE SOLAR ARRAY OUTPUT
VOLTAGE. THE NUMBER OF ENGINES TRACKS THE SOLAR ARRAY
POWER.

POWER (kW)	V+ (VOLTS)	NUMBER OF ENGINES	CLUSTER THRUST N	I_{SP} (sec.)	TOTAL I_B	I_B (AMPS)	DISTANCE (A.U.)
40.0	1000	16	1.63	3500	30.2	1.89	1.00
37.0	1060	16	1.42	3610	26.3	1.65	1.06
35.0	1090	16	1.32	3660	24.1	1.51	1.11
35.0	1090	14	1.32	3660	24.1	1.72	1.11
33.5	1110	14	1.26	3690	22.8	1.63	1.13
33.5	1110	14	1.26	3690	22.8	1.63	1.13
31.7	1130	14	1.18	3730	21.1	1.51	1.18
30.0	1160	14	1.11	3770	19.5	1.39	1.23
30.0	1160	12	1.11	3770	19.5	1.63	1.23
26.6	1180	12	.972	3810	17.0	1.42	1.32
25.0	1200	12	.905	3840	15.7	1.31	1.38
25.0	1200	10	.905	3840	15.7	1.57	1.38
23.2	1220	10	.833	3870	14.3	1.43	1.44
21.25	1230	10	.761	3885	13.1	1.31	1.51
21.25	1230	10	.761	3885	13.1	1.31	1.51
20.7	1240	10	.734	3910	12.5	1.25	1.54
20.0	1250	10	.707	3920	12.1	1.21	1.58
20.0	1250	8	.707	3920	12.1	1.51	1.58
18.3	1260	8	.650	3930	11.1	1.39	1.70

TABLE IV

CASE II — THE ACCELERATING VOLTAGE IS HELD CONSTANT. THE
NUMBER OF ENGINES TRACKS THE SOLAR ARRAY POWER.

POWER (kW)	V+ (VOLTS)	NUMBER OF ENGINES	CLUSTER THRUST N	I_{SP} (sec.)	TOTAL I_B	I_B (AMPS)	DISTANCE (A.U.)
40.0	1000	16	1.63	3500	30.2	1.89	1.00
37.0	1000	16	1.47	3500	27.9	1.75	1.06
35.0	1000	16	1.39	3500	26.4	1.65	1.11
35.0	1000	14	1.39	3500	26.4	1.89	1.11
33.5	1000	14	1.33	3500	25.3	1.81	1.13
33.5	1000	14	1.33	3500	25.3	1.81	1.13
31.7	1000	14	1.25	3500	23.8	1.70	1.18
30.0	1000	14	1.19	3500	22.7	1.62	1.23
30.0	1000	12	1.19	3500	22.7	1.89	1.23
26.6	1000	12	1.05	3500	20.0	1.67	1.32
25.0	1000	12	.995	3500	18.9	1.58	1.38
25.0	1000	10	.995	3500	18.9	1.89	1.38
23.2	1000	10	.916	3500	17.4	1.74	1.44
21.25	1000	10	.842	3500	16.0	1.60	1.51
21.25	1000	10	.842	3500	16.0	1.60	1.51
20.7	1000	10	.819	3500	15.6	1.56	1.54
20.0	1000	10	.793	3500	15.1	1.51	1.58
20.0	1000	8	.793	3500	15.1	1.89	1.58
18.3	1000	8	.726	3500	13.8	1.73	1.70

TABLE V

CASE III — THE ACCELERATING VOLTAGE IS REDUCED ON ALL THRUSTERS IN 100 VOLT INCREMENTS WHEN THE TRACKING VOLTAGE EXCEEDS THE DESIGN VOLTAGE BY 100 VOLTS. THE NUMBER OF ENGINES TRACKS THE SOLAR ARRAY POWER.

POWER (kW)	V+ (VOLTS)	NUMBER OF ENGINES	CLUSTER THRUST N	I_{SP} (sec.)	TOTAL I_B	I_B (AMPS)	DISTANCE (A.U.)
40.0	1000	16	1.63	3500	30.1	1.88	1.00
37.0	1060	16	1.42	3610	26.3	1.65	1.06
35.0	1090	16	1.32	3660	24.2	1.51	1.11
35.0	1090	14	1.32	3660	24.2	1.73	1.11
33.5	1110	14	1.26	3690	22.8	1.63	1.13
33.5	1000	14	1.33	3500	25.3	1.80	1.13
31.7	1025	14	1.23	3550	23.8	1.70	1.18
30.0	1042	14	1.17	3580	21.75	1.55	1.23
30.0	1042	12	1.17	3580	21.75	1.81	1.23
26.6	1078	12	1.01	3640	18.6	1.55	1.32
25.0	1090	12	.943	3670	17.2	1.43	1.38
25.0	1090	10	.943	3670	17.2	1.72	1.38
23.2	1108	10	.873	3690	15.8	1.55	1.44
21.25	1120	10	.797	3710	14.4	1.44	1.51
21.25	1000	10	.842	3500	16.00	1.61	1.51
20.7	1010	10	.814	3520	15.5	1.55	1.54
20.0	1020	10	.783	3540	14.8	1.48	1.55
20.0	1020	8	.783	3540	14.8	1.85	1.58
18.3	1030	8	.716	3560	13.5	1.69	1.70
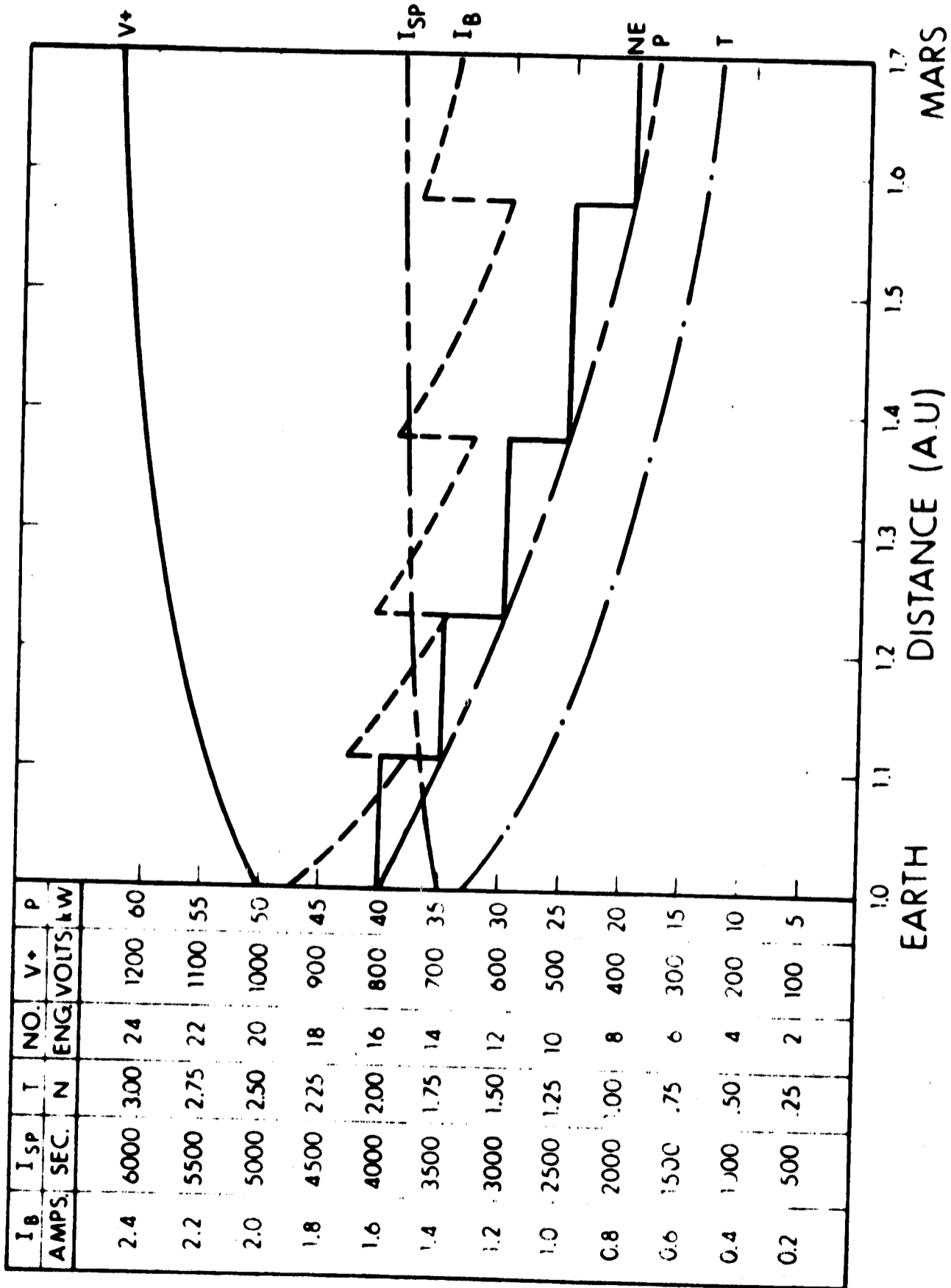
Figure 13. CASE I The Accelerating Voltage Tracks the Solar Array Output Voltage.
The Number of Engines Tracks the Solar Array Power

73628148
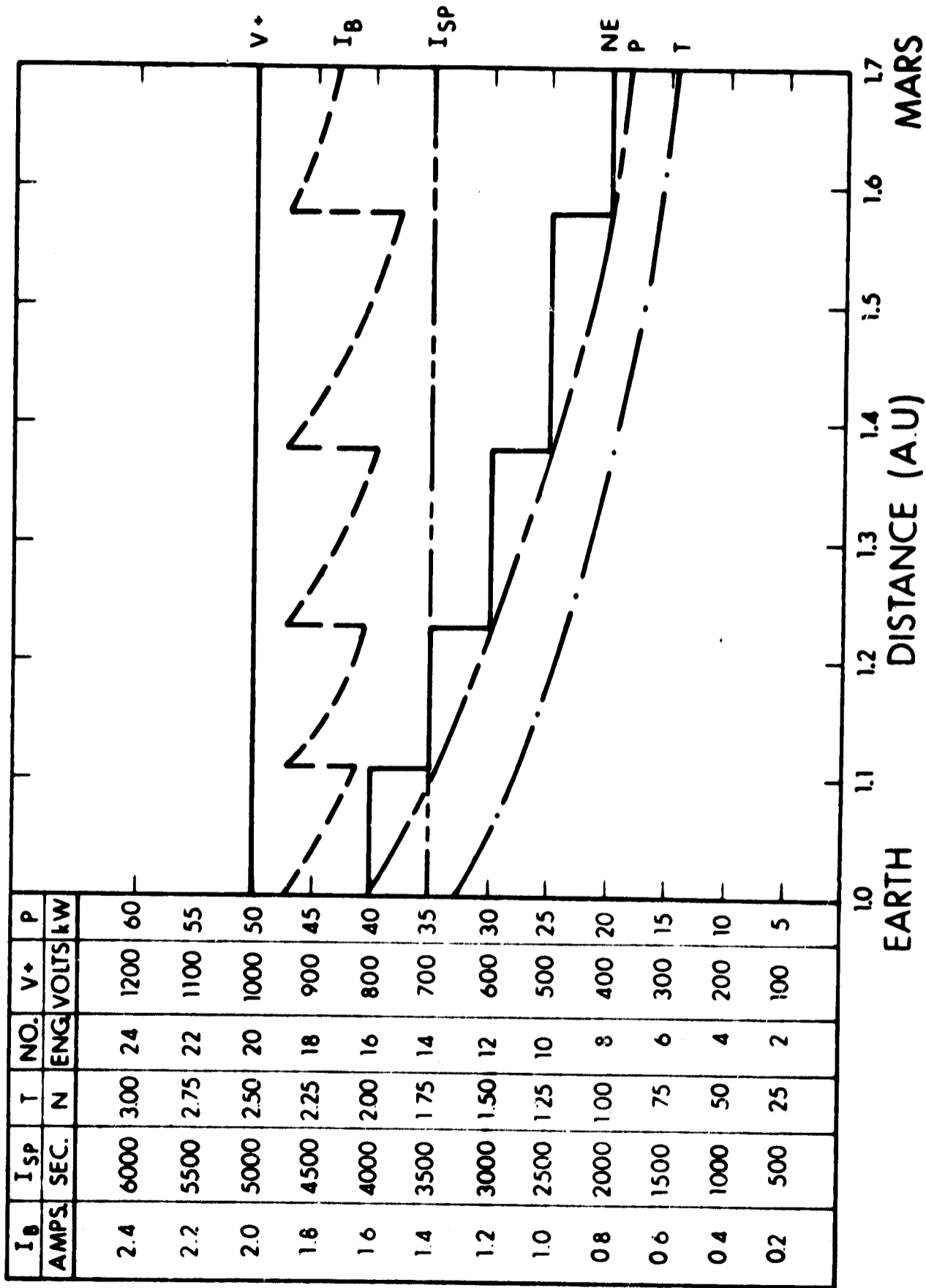
Figure 14. CASE II The Accelerating Voltage is Held Constant. The Number of Engines Tracks the Solar Array Power

73628147

I_B AMPS.	I_{SP} SEC.	T N	NO. ENG	V+ VOLTS	P kW
2.4	6000	3.00	24	1200	60
2.2	5500	2.75	22	1100	55
2.0	5000	2.50	20	1000	50
1.8	4500	2.25	18	900	45
1.6	4000	2.00	16	800	40
1.4	3500	1.75	14	700	35
1.2	3000	1.50	12	600	30
1.0	2500	1.25	10	500	25
0.8	2000	1.00	8	400	20
0.6	1500	.75	6	300	15
0.4	1000	.50	4	200	10
0.2	500	.25	2	100	5

Figure 15.   CASE III   The Accelerating Voltage is Reduced on All Thrusters in 100 Volt Increments When the Tracking Voltage Exceeds the Design Voltage by 100 Volts.   The Number of Engines Tracks the Solar Array Power

The three cases of thrust vs distance from the sun are compared in
Figure 16. This very rough comparison is made since mission time is
not compuable. When integrating the area under the curves an
approximation of the work done is the result.

$$W_I \quad = \quad .693 \quad N\text{-}AU.$$

$$W_{II} \quad = \quad .745 \quad N\text{-}AU.$$

$$W_{III} \quad = \quad .724 \quad N\text{-}AU.$$

If the work approximation of case II, which is the optimum case, is
100% than a measure of tue relative value of the three cases is
obtained.

Case I   = 92.9%
Case II   = 100.0%
Case III = 97.2%

On first glance, it looks like the Case I work can increase by only 7.1%.
When evaluating these results it should be kept in mind that for a
true comparison of these three power conditioning and control cases
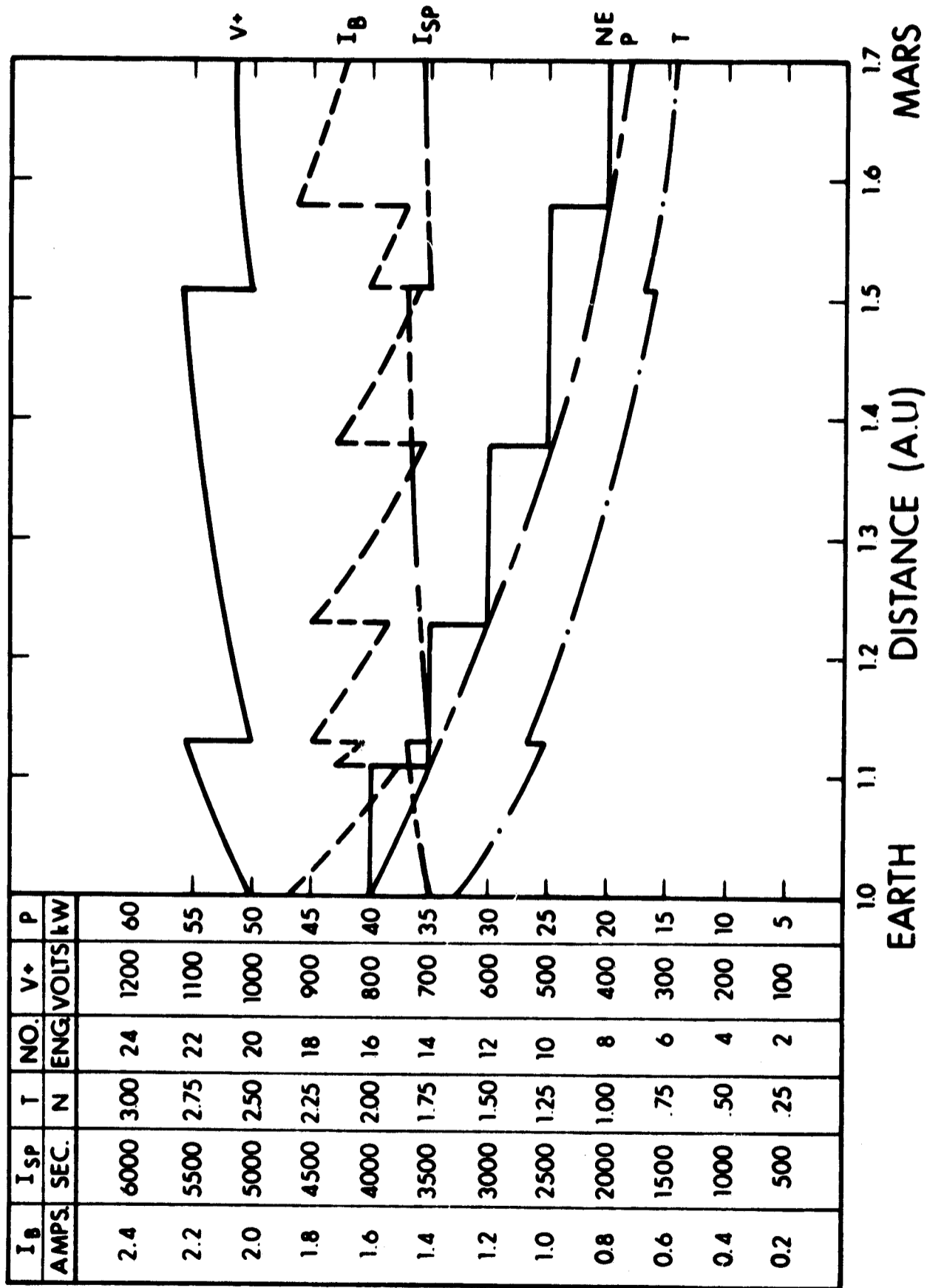it is necessary to do a mission time and trajectory analysis for
each.

These three cases lead to the extrapolation to other forms of control.
If the engine cluster is mounted on a gimbaled platform, the engines
could track the available solar array power more accurately. The
misalignment of the total thrust vector with the spacecraft center of
mass would be corrected by the gimbaling system. The value of such a
system would depend on the increase in power conditioning efficiency,
the mass increase due to the gimbaling on the platform, the power needs
of the gimbled platform drive and control system, and the accuracy and
sensitivity of the thrust misalignment detector. If the spacecraft is
allowed to rotate before the thrust misalignment is detected then
penalties must be included for correcting the rotation.
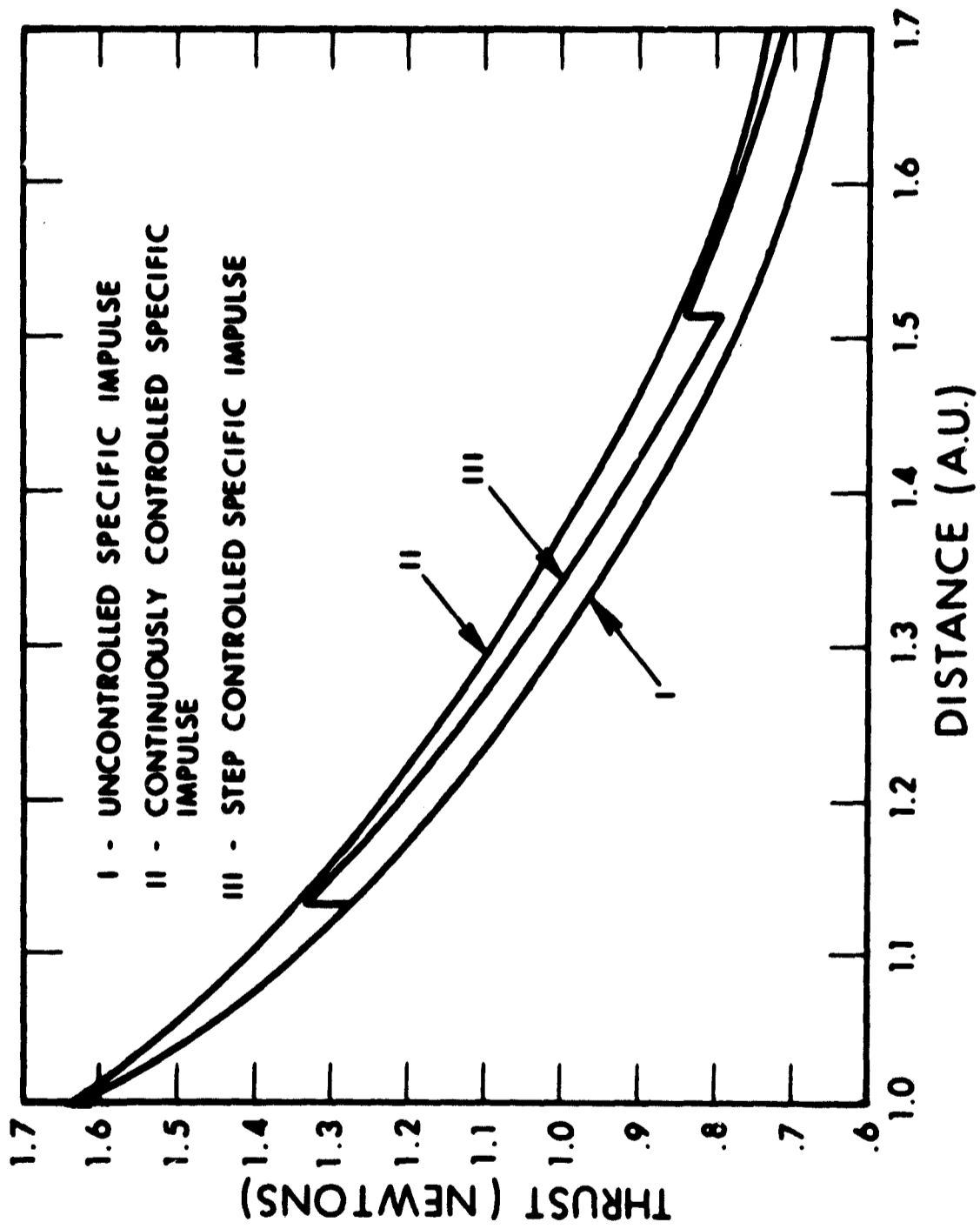
Figure 16. Thrust versus Distance From Sun for Cases I, II, and III

Another approach might be smaller steps in the high voltage supply.
This yields a closer stepwise approximation of the power conditioning
and control of Case II without the complex control circuitry of Case II.
Unfortunately the number of inverter modules increases as the voltage
steps decrease. This approach is not attractive because an increase
in the number of modules seriously affects the reliability.

All cases evaluated thus far assume that the same voltage is applied
to all engines. The application of nonuniform voltage to the engines
will cause each thruster to operate at a different specific impulse.
Thru the use of simple switching circuitry it is possible to control
high voltage steps to each engine to produce a constant specific
impulse for the engine cluster. The control system for this scheme
would be considerably more complex than the Case III control system
but could have reliability and efficiency advantages over the Case II
control system.

1.5 TRANSMISSION LINE PERFORMANCE EQUATIONS

For the purpose of the trade-off study, the mass of the transmission
lines will be expressed as a function of conductor properties, trans-
mission efficiency, transmitted power, operating voltage, and trans-
mission distance. In normal circumstances, the power level and the line
length are specified. The operating voltage should be high, consistent
with other system contraints. Since the transmission line weight de-
creases with decreasing transmission efficiency, it is traded off against
the mass penalty of the power source. In the following section, the
derivation will be given for the case of a single and multiple power
sources. The treatment will be limited to a 2-wire, dc transmission
line since most space power systems, such as solar arrays, thermoelec-
tric, and thermionic, are direct current power sources.

1.5.1 SINGLE POWER SOURCE
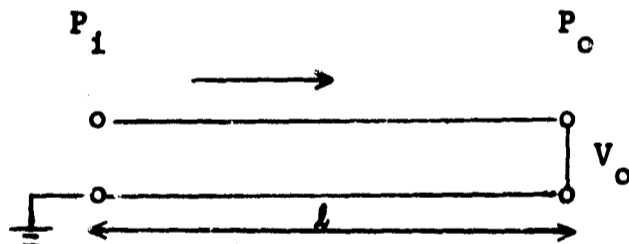
For a given input power P_i and output power P_o, the line loss P_1 is
simply

$$P_1 \quad = \quad P_i - P_o \qquad (1)$$

Defining the transmission efficiency as:

$$\eta \quad = \quad \frac{P_o}{P_i} \qquad (2)$$

then

$$P_1 \quad = \quad \frac{1 - \eta}{\eta} P_o \qquad (3)$$

The transmission power loss can also be expressed as:

$$P_1 = \left(\frac{P_o}{V_o} \right)^2 \left(\frac{2\rho\ell}{A} \right) \tag{4}$$

where
ρ = resistivity of the conductor

ℓ = line length

A = cross-section area

The weight of the transmission line is related to the material density (d) and its volume (1A) by:

$$M_1 = 2\, d\, \ell\, A \tag{5}$$

Combining equations (3), (4), and (5), we have:

$$M_1 = (4\, d\, \rho) \frac{\eta}{1 - \eta} \frac{P_o}{V_o^2} \ell^2 \tag{6}$$

Equation (6) relates the conductor weight as a function of line efficiency, power level, operating voltage, and transmission distance. The weight computed from equation (6) should be increased approximately 25% to account for connectors, insulation, etc. It shall also be borne in mind that the computed weight will be minimal since it has been assumed that the conductor cross section can be made consistent with all other specified parameters. In practice, conductor sizes are available in discrete steps such as 1/0, 2/0, 4/0, etc. Such refinement must be taken into consideration when a detail conceptual design is made. But, for the parametric study, this refinement will be neglected.

In the determination of the material properties, the density should be evaluated at room temperature, and the resistivity at operating temperature. The temperature of the transmission line is a function of the

line loss, conductor geometry and the means of heat rejection. For this study, it will be assumed that the operating temperature is 100°C.

Aluminum and copper are promising candidates for the conductor material. The material constants will be the following:

Aluminum:
$$4\,d\rho = 4(0.098\underline{\text{lb}}/\text{in}^3)\,(1.5 \times 10^{-6}\ \text{ohm} - \text{in})$$

$$= 5.9 \times 10^{-7}\ \frac{\Omega\text{-lb}}{\text{in}^2} = 4.1 \times 10^{-8}\ \frac{\Omega\text{-kg}}{\text{cm}^2}$$

Copper:
$$4\,d\rho = 4(0.324\underline{\text{lb}}/\text{in}^3)\,(1 \times 10^{-6}\ \text{ohm} - \text{in})$$

$$= 1.26 \times 10^{-6}\ \frac{\Omega\text{-lb}}{\text{in}^2} = 8.8 \times 10^{-8}\ \frac{\Omega\text{-kg}}{\text{cm}^2}$$

Thus, an aluminum conductor will be used since for the same efficiency a copper transmission line will have twice the mass, everything else being equal.

1.5.2   MULTIPLE POWER SOURCES

The single source transmission line discussed previously is applicable to power systems such as nuclear thermionic or small solar arrays. For a large array required for the electric propulsion, it will be advantageous to divide the entire array into several panels connected in parallel. This arrangement will not only increase the system reliability, but also reduce the voltage and power losses.

The solar array "wing" consists of several small panels connected in parallel. For example, a 50 kW system which has a configuration similar to Fig. 2(a) can be made from 8 panels per wing. Each panel produces 3.13 kW at 100 volts. If the panel size is 3.8 x 7.6 meters, the total transmission distance will be 30.5 meters.

The block diagram of the electrical connection and its equivalent circuit are shown in Fig. 17. In the derivation of the transmission line performance equation we shall make the following assumptions:

a. All panels are of equal size and therefore produce approximately the same amount of power.

b. To a first approximateion, the current output of each panel is equal. In effect, we assume that the output voltage of each panel will vary only slightly from the value corresponding to maximum power point of the P-V curve. This assumption is justified only for the case of high transmission efficiency (greater than 95%).

c. For practical reasons, the transmission line has a uniform cross section throughout the entire length.

Referring to the equivalent circuit shown in Fig. 17, the power loss in the line for m panels is:

$$P_1 = R [I^2 + (2I)^2 + \text{--------} (m - 1)^2 I^2]$$

Since mI is equal to P_o/V_o, we have:

$$P_1 = \frac{P_o^2}{V_o^2} \frac{R}{m^2} [1 = 2^2 + \text{-----} (m - 1)^2] \quad (7)$$

For this case,

$$R = \frac{2 \rho}{A} \frac{1}{m} \quad (8)$$

As in the case of the single source the line power loss and mass are given by the equations

$$P_1 = \frac{1 - \eta}{\eta} P_o \quad (9)$$
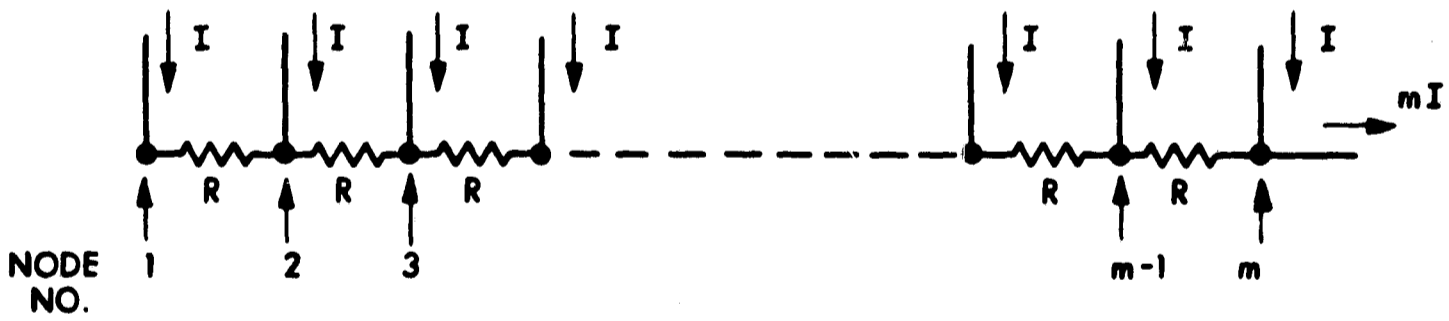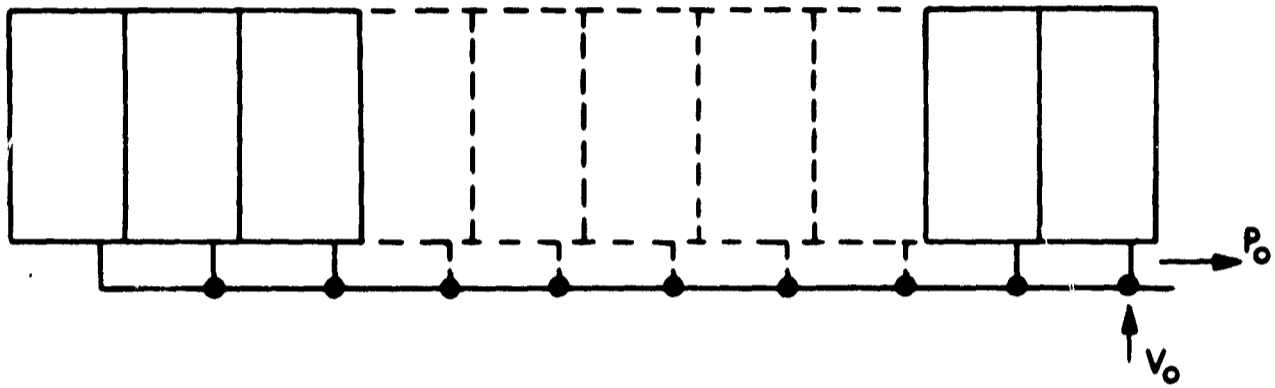
$$M_1 = 2 d A \ell \quad (10)$$

Figure 17.   Block and Circuit Diagrams for "m" Solar Panels
             Connected in Parallel

73629283

Combining equations (7), (8), (9), and (10), we have:

$$M_1 = K_m \, (4 \, d_0) \, \frac{\eta}{1 - \eta} \, \frac{P_o}{V_o^2} \, \ell^2 \qquad (11)$$

where

$$K_m = \begin{array}{ll} \dfrac{m-1}{m^3} \, m^2 & \\[2mm] \dfrac{1}{m^3} & m = 1 \end{array}$$

It can be seen that equation (11) is similar to (6) with exception of the K_m factor which is less than unity. In effect, the transmission line for a multiple source power system will have less mass for the same efficiency and distance.

The mass factor K_m is plotted against the number of solar panels connected in parallel (Fig. 18). Mathematically, K_m tends to approach 1/3 when m is large. In using the K_m factor a word of caution is in order.

In the formulation of the problem, it is presupposed that each panel has sufficient internal wiring so that the panel output voltage is stiff. For a given total power output, the panel size increases as the number of panels is decreased. With smaller number of panels, the transmission line mass will decrease (as seen by the decreasing K_m), but the mass of the internal bussing will increase. The variation in the internal bus mass with the panel size can not be assessed without making a detailed layout of the panel wiring. Suffice it to say that the K_m factor corresponding to m less than 4 should not be used without assessing the mass penalty in internal wiring. Fortunately, the packaging requirements will, in most circumstances, dictate that the number of panels be large.
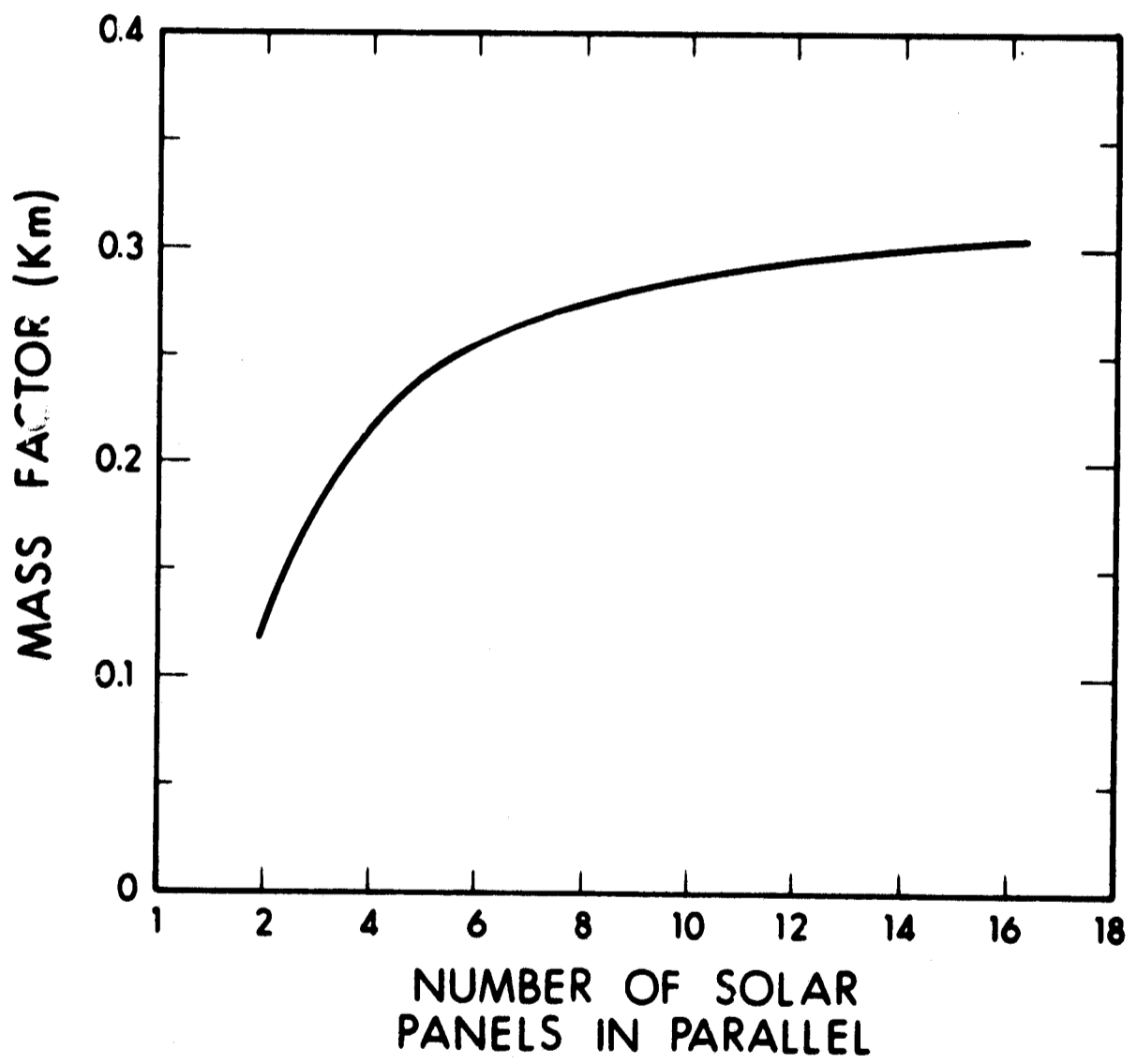
Figure 18. Weight Factor K_m

73629284

1.6 MARS MAPPER POWER CONDITIONING AND CONTROL SYSTEM

The power conditioning and control system for the Mars Mapper mission
is described in this section. The system design is based on the follow-
ing assumptions:

a. All thruster turn-on and turn-off will be by a command external
to the thruster system. This includes power programming, failed
thruster exchanges, and thrust vector correction commands.

b. Sixteen thrusters will be provided with no redundancy initially.

c. Power conditioning will use the small high frequency modules
concept.

Figure 19 is a block diagram of the entire thruster system for the Mars
Mapper. Shown are the interconnections from the spacecraft to the
electric propulsion system controller; from the system controller to
the sixteen (16) thruster controllers and the connections from the six-
teen (16) power conditioning units to the electric thrusters. Also
shown are the reservoir and neutralizer circuit in the system.

The system controller will provide the main control functions, providing
control for all of the sixteen (16) subsystems. The thruster controller
in turn, provides individual control of each thruster subsystem; com-
pletely independent of each other.

1.6.1 SYSTEM CONTROLLER

A block diagram of the system controller is shown in Fig. 20. The
system controller can be broken down into four (4) main subsystems.
These subsystems are:

a. Thruster power on-off section

b. Initiate thrust control section

c. Terminate thrust control section
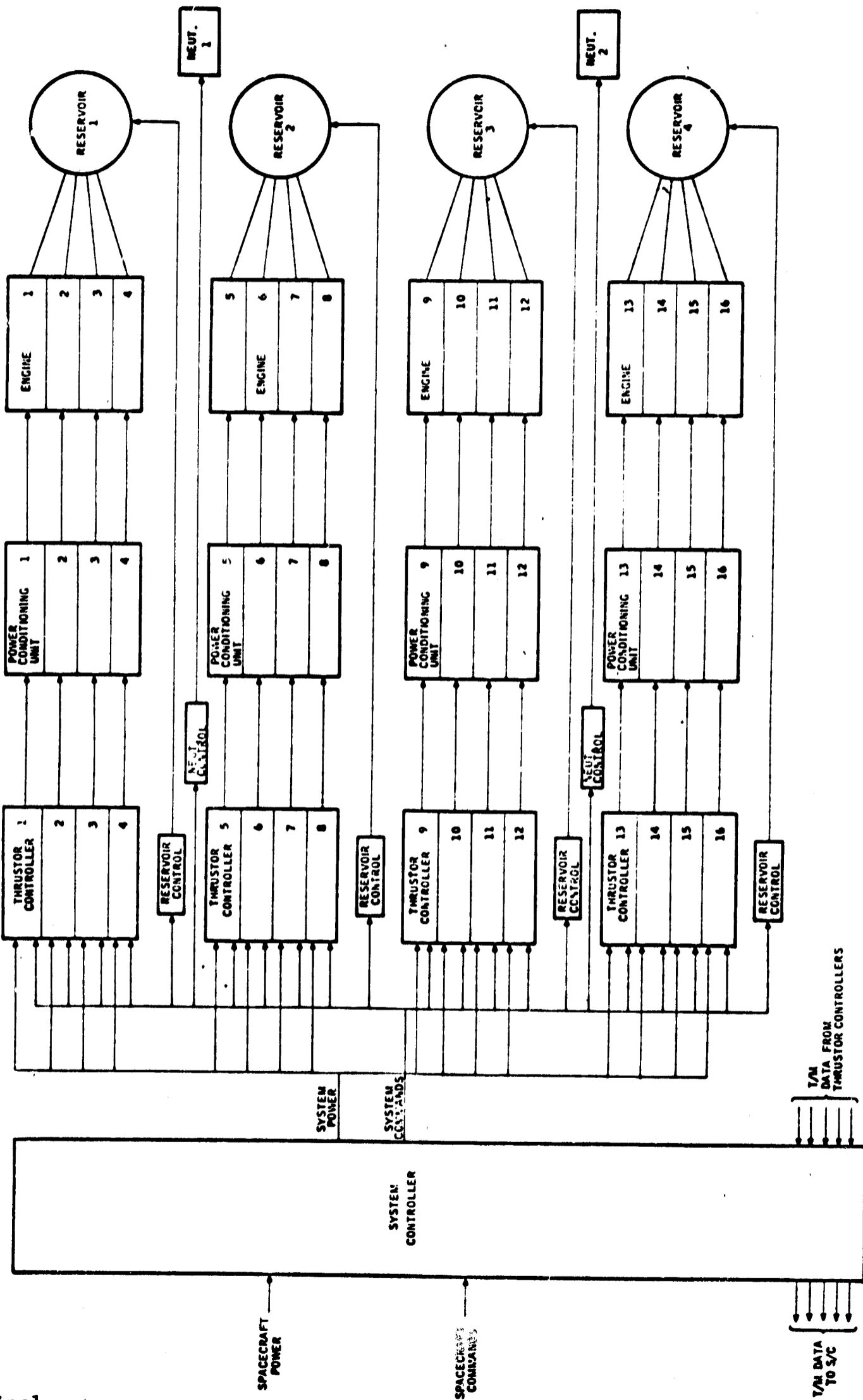
d. System T/M conditioning section
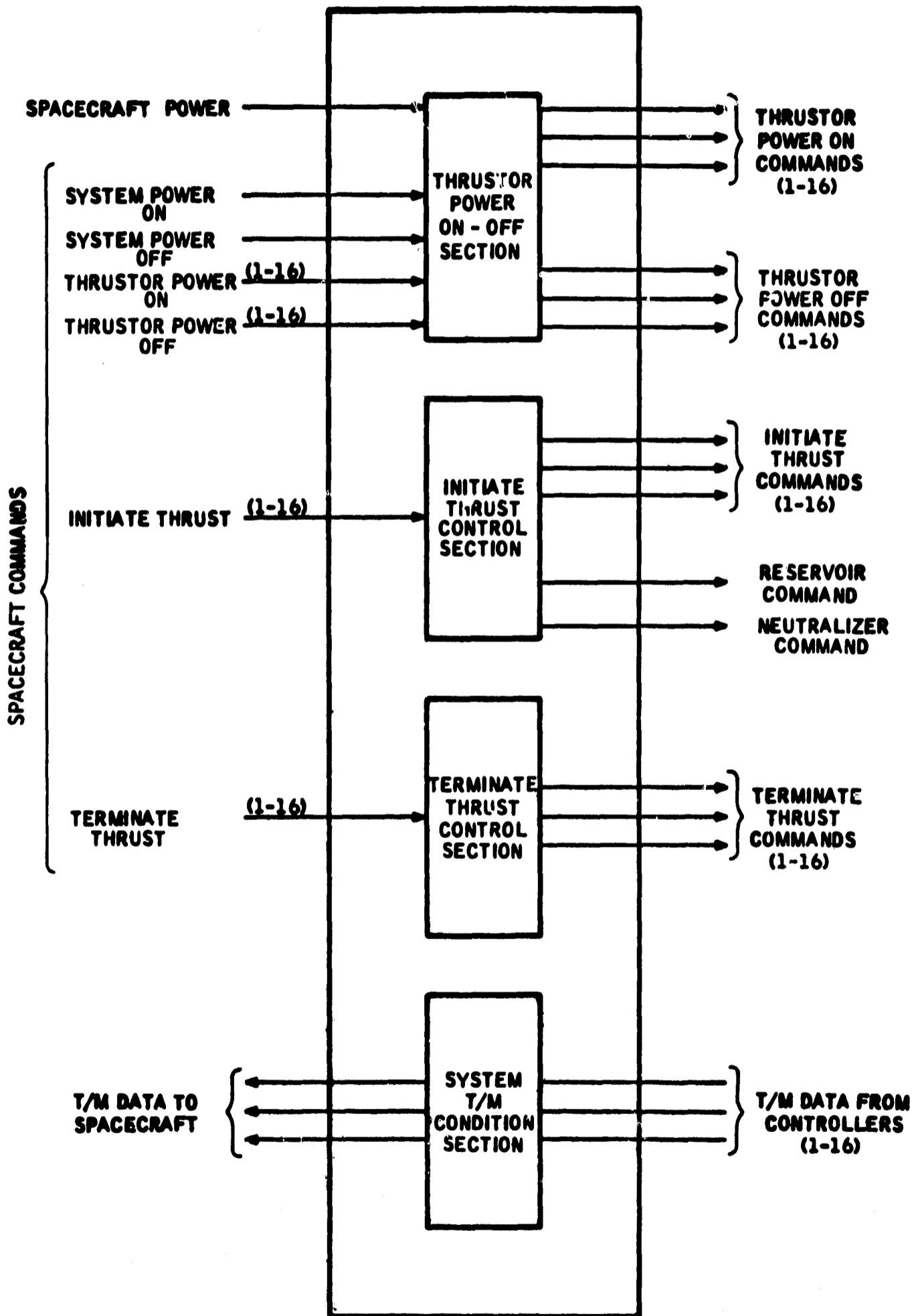
Figure 19. Mars Mapper System Block Diagram

Figure 20.   System Controller Block Diagram

1.6.1.1 Thruster Power On-Off Section

This section receives the system power on-off commands, which makes space-craft power available to the entire electric propulsion system. It also receives the thruster "power on" and "power off" commands from the spacecraft. Upon receiving these commands, it decodes the information and either turns on or turns off system power to the desired thruster controllers. Power can be provided to any number of the sixteen thruster controllers at any given time.

1.6.1.2 Indicate Thrust Control Section

This section receives the "initiate thrust" commands from the spacecraft. When the information is received, it is decoded and the proper "initiate thrust" commands are sent to the appropriate thruster controllers in the system. An additional function of this section is to provide turn on commands for the system reservoir and neutralizer.

1.6.1.3 Terminate Thrust Control Section

This section receives the "terminate thrust" commands from the spacecraft. Upon receipt, the information is decoded and the appropriate thruster subsystems are turned off. All commands are completely independent.

1.6.1.4 System T/M Conditioning Section

All telemetry information from each of the thruster controllers is channeled to this section of the system controller. This section will properly condition the T/M information to provide the proper voltage and impedance levels for the spacecraft system.

1.6.2 THRUSTER CONTROLLER

The thruster controller is the heart of each of the electric propulsion systems.

Figure 21 shows a block diagram of the thruster controller. There are sixteen (16) controllers in the system, as shown in Fig. 19. Each controller is independent of the others and only dependent on the system controller.

The system controller "power on" command is received and decoded by the thruster sequencer section of the thruster controller. This command makes spacecraft power available to a specific thruster subsystem.

The "initiate thrust" command to the thruster sequencer will automatically begin the turn on cycle for the subsystem. The turn on cycle or sequence is shown in Table VI.

The system controller turns on the appropriate reservoir and neutralizer supplies.

The appropriate cathode supply is turned on by the thruster sequencer upon receiving the "initiate thrust" command. When the reservoir and cathode supplies have reached 50° and 350^oC temperature, respectively, feedback information is provided to the thruster controller. Thermally-sensitive switches will be used on the various parts of the engine for this purpose. When the feedback information is received by the sequencer, the vaporizer supply will be automatically commanded on by the sequencer. When the reservoir housing reaches 50^oC, feedback information will be provided to the system controller to turn-off the power supply.

When the ion chamber housing reaches a temperature of 150^oC, feedback information will be provided to the thruster sequencer to turn on the arc,
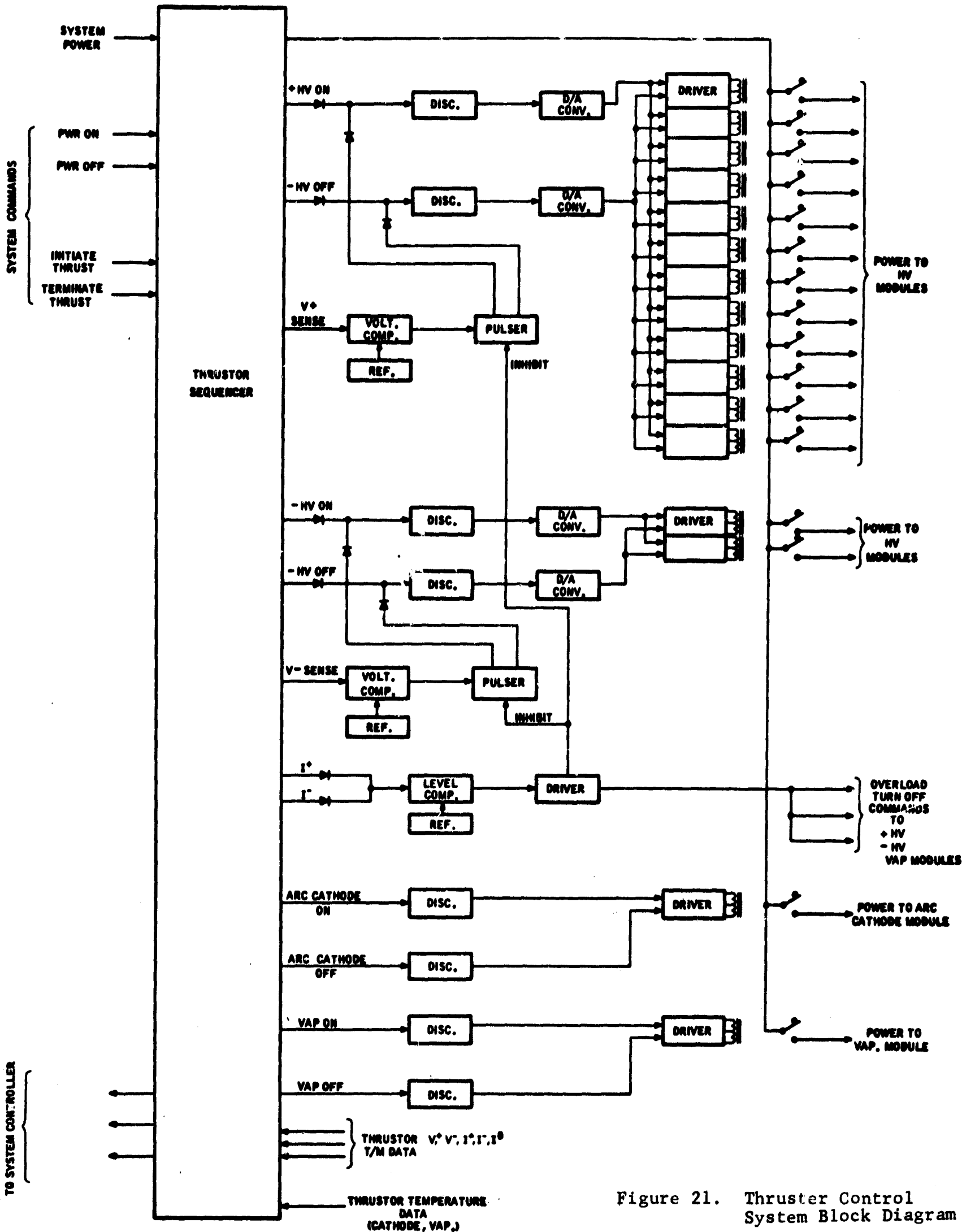
Figure 21. Thruster Control System Block Diagram

TABLE VI

START SEQUENCE

1. Energize reservoir, neutralizer, and cathode supplies.

2. After the reservoir and cathode housing temperatures have reached 50°C and 350°C respectively energize vaporizer supply.

3. When reservoir housing reaches 50°C, de-energize reservoir supply.

4. After the ion chamber housing has reached 150°C turn on arc, V^{+}, and V^{-} supplies.

5. When the arc begins, turn off cathode power.

V^+ and V^- supplies. The cathode supply will automatically be turned off when the arc starts. All power supplies necessary for steady state operation are now energized.

The thruster sequencer has up to this point turned on, sequentially, all of the power supplies as a function of temperatures (feedback). The unit is now in steady state operation.

It has been mentioned in the preceding paragraphs that the various power supplies have been commanded on by the thruster control system. The following is an explanation of how the commands are generated and sent.

The vaporizer and the arc-cathode modules are energized by a pulse command generated in the thruster sequencer section. The command pulse is processed thru a discrimination circuit which rejects pulse information below a prescribed level. This will prevent stray or transient noise from affecting the circuitry. Once the pulse in processed thru the discriminator, it is coupled to a relay driver circuit, where it is amplified and used to drive a latching relay.

The V^+ modules are turned on in a slightly different manner. When it is time to bring on the V^+ modules, the thruster sequencer will generate a proper number of pulses. For the V^+ supply, ten pulses are necessary to turn on ten modules. The pulses are generated in the sequencer then processed in the discriminator circuit before being coupled to a digital-to-analog converter. The output of the D/A converter is then coupled to relay driver where the signal is amplified in order to energize the latching relays that turn-on the V^+ modules.

The V^- modules are turned on in a similar manner as the V^+ modules, except only two modules are used.

Voltage regulation to the engine is provided by two methods. A variable output voltage module is provided for the V^+ and V^- section. Should the V^+ or V^- change at the output terminals, a feedback signal to the drive circuitry of the variable module will provide the appropriate a compensation. In the event that a module should fail, the output voltage would drop and the V^+ and V^- voltages would be compared in a voltage-comparator circuit. The error signal would inform the pulser circuit, shown in Fig. 22 to sequence the next module on.

The power conditioning subsystem is also provided with over load and short circuit protection. They would operate as follows: I^+ and I^- current sensors are provided in the P.C. system. An analog voltage of the I^+ and I^- currents are provided to the thruster control system. These analog voltages are compared in a level comparator circuit. When preset values of I^+ and I^- currents are exceeded, an error signal amplified in a driver circuit provides turn-off power to all the V^+, V^- and the vaporizer modules. At the same time an inhibit signal is sent to the V^+ and V^- pulser circuits to prevent more modules from being turned on when the high voltages are turned off by the overload circuit.

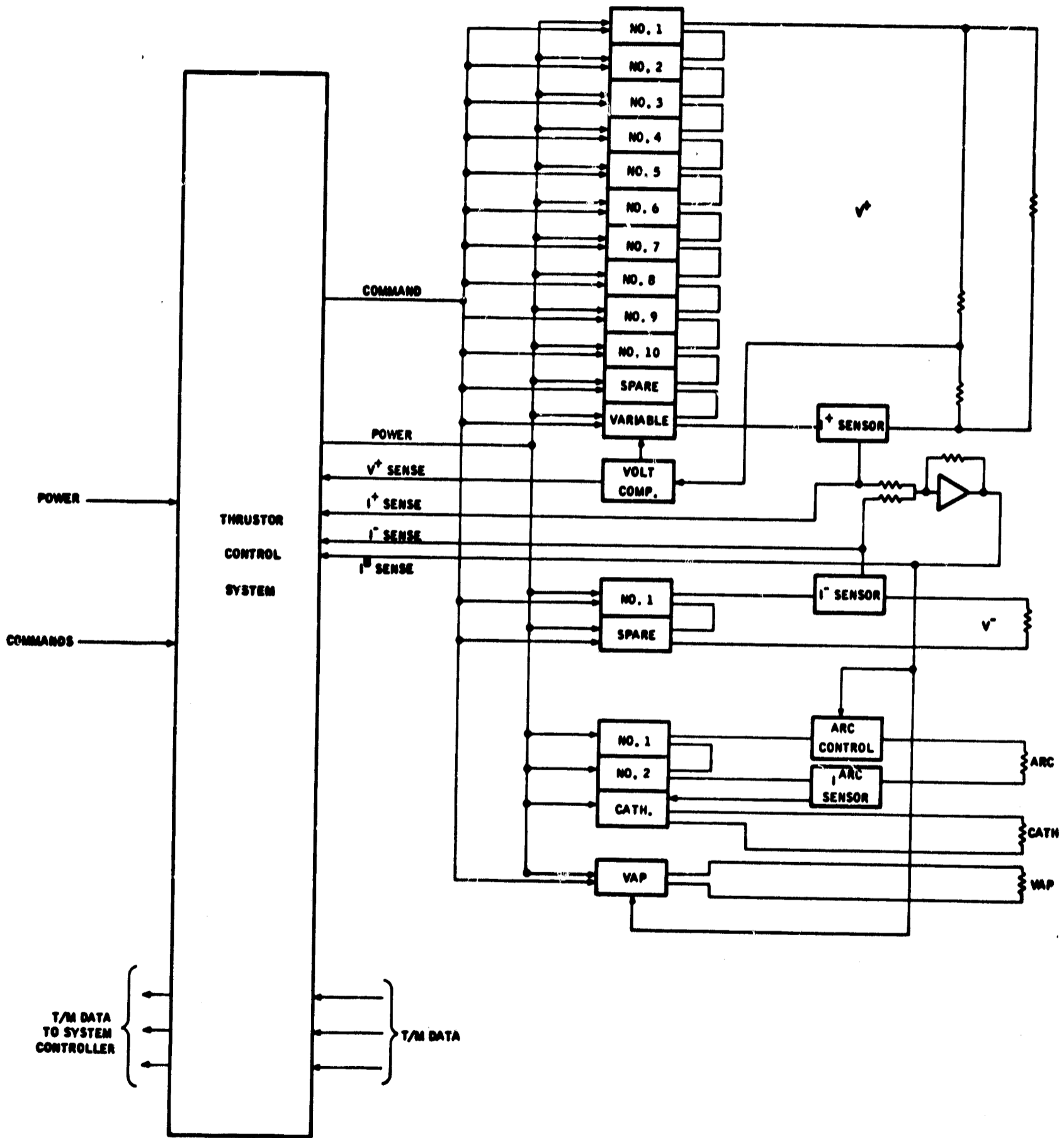Telemetry information is provided to the system controller by the thruster controller.

Figure 22. 2.5 kW Unit Schematic Pulser Circuit

1.7 POWER CONDITIONING TRADEOFF STUDY FOR A 50 kW SOLAR-ELECTRIC PROPELLED SPACECRAFT

The following study was completed early in this program. The methods and general conclusions are valid but the specific conclusions should be adjusted to reflect the results obtained during the later phase of the program. Specifically, it now appears that the solar array should be limited to about 56 volts because well documented transistors to operate with 100 volt line voltages are not forthcoming. This change penalizes the mass by about 1 kg/kW.

A more current solar array specific mass would be 18 kg/kW, instead of the 25 kg/kW used in this study. The solar array transmission line mass could be reduced considerably by using a tapered line instead of the constant size used in the study.

One of the heaviest items in any power conditioning system is the power transformer. An optimum design for the transformer involves a tradeoff among a staggering number of variables. A computer program for such a tradeoff study is available at EOS. This program accepts input and output voltage and current, frequency, flux density, core properties and several other inputs. It then makes wire size selection, insulation buildup, core size decisions and computes the mass and efficiency of the transformer, and presents the results in a graph. It prints out the complete description of the transformer design information.

Transformers were designed for three frequencies, three input voltages, three power levels and several other selected variables. Several thousand transformers were designed and the maximum efficiency point for each mass was plotted.[*] This study showed that lighter and more efficient

---

[*] These transformers are to indicate design trend only. More stringent values of permeability and coupling must be applied to design realistic transformers.

transformers can be built than were used in the earlier study. As a result, the power conditioning system mass should be less than 500 pounds instead of the 700 to 1000 pounds found in the earlier study.

The more recent studies also reveal that the optimum operating frequency may well be closer to 20 kHz than 10 kHz and the optimum module size closer to 400 watts than 100 watts.

All of these considerations were developed too close to the end of the program to permit a complete updating of the previous work. However, estimates of the effects of this work are included here.

The methodology leading to the revised results was to generate universal curves for the mass and losses of transistors, transformers, controls and miscellaneous components. From these new estimates of power penalties were computed and the results compared in a series of curves. The revised results are presented in a series of curves in Figs. 23 through 26. The final system was based on a 18 kg/kW solar array and a 56 volt line voltage.

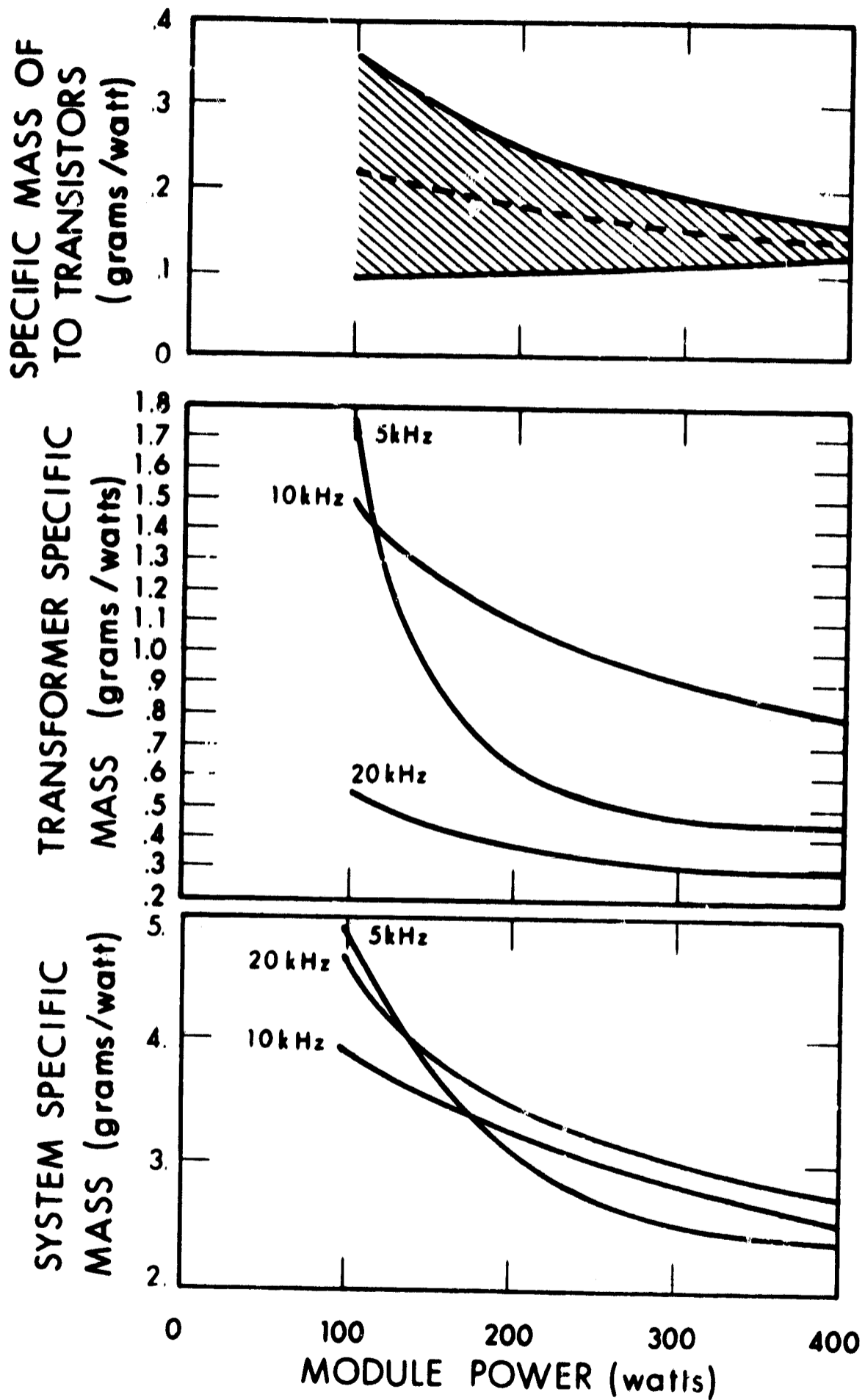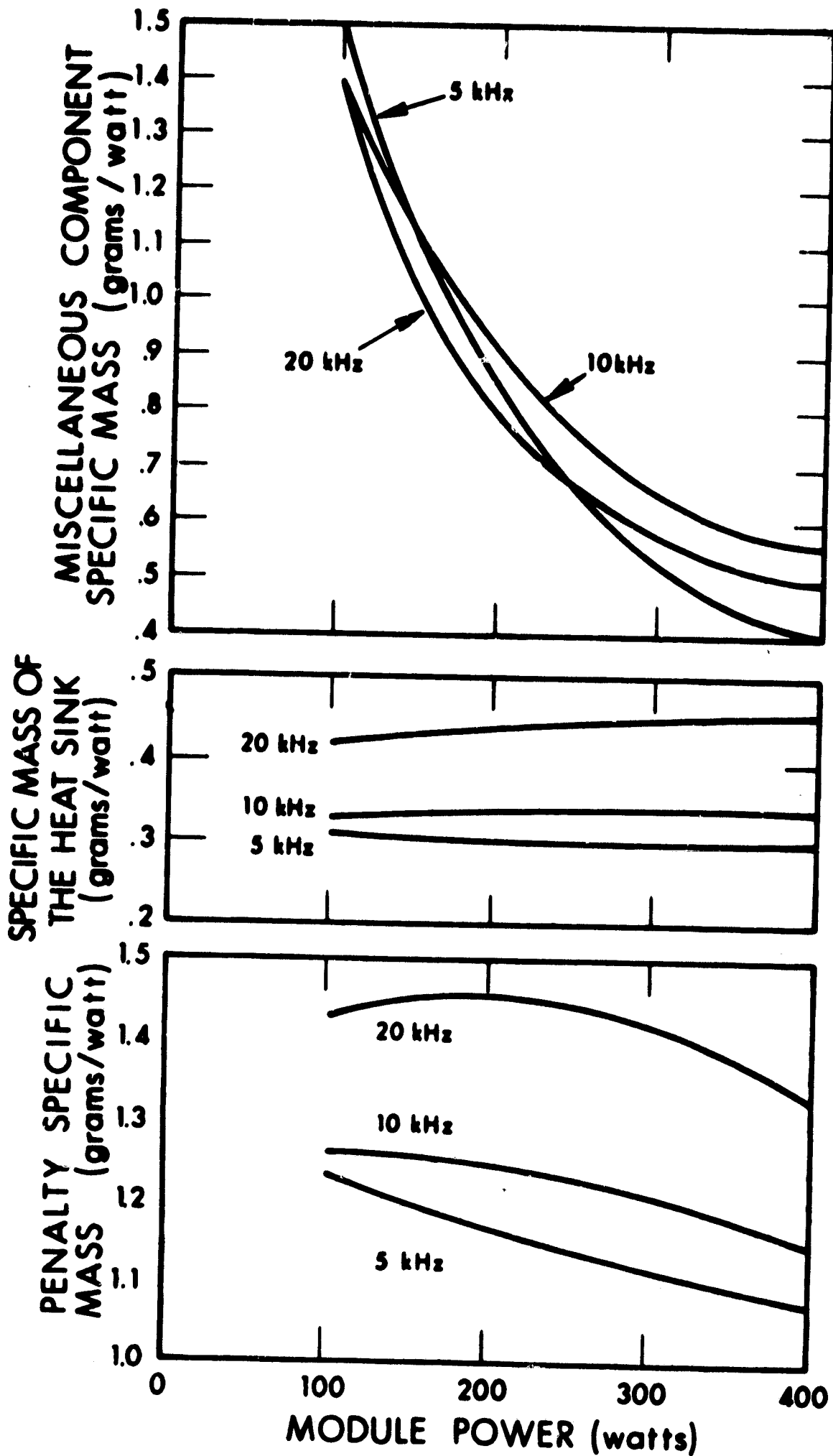Figure 23. Converter Losses for Two Switching Transistors

73629166

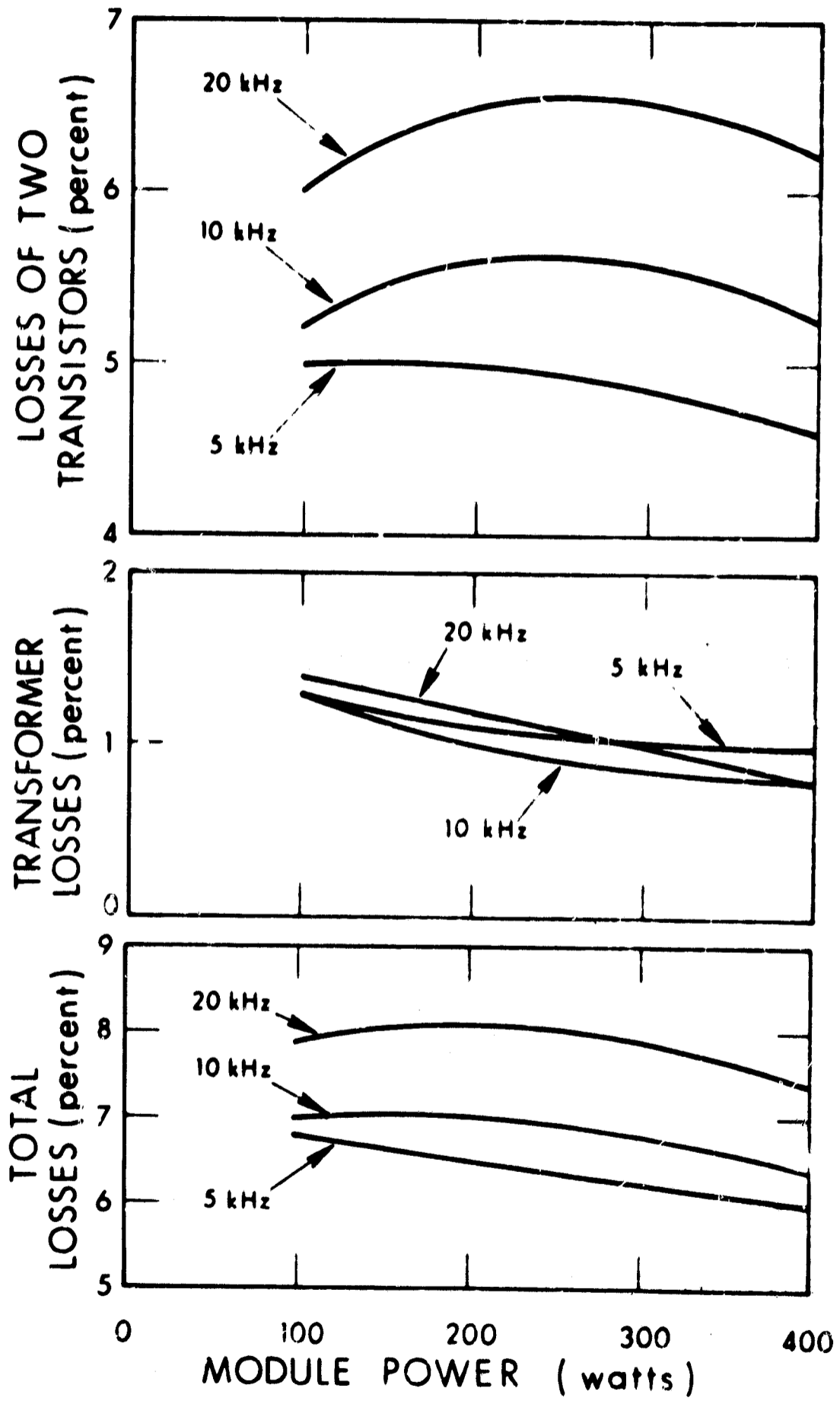Figure 24. Converter Component and Power Conditioning System Losses

73629165
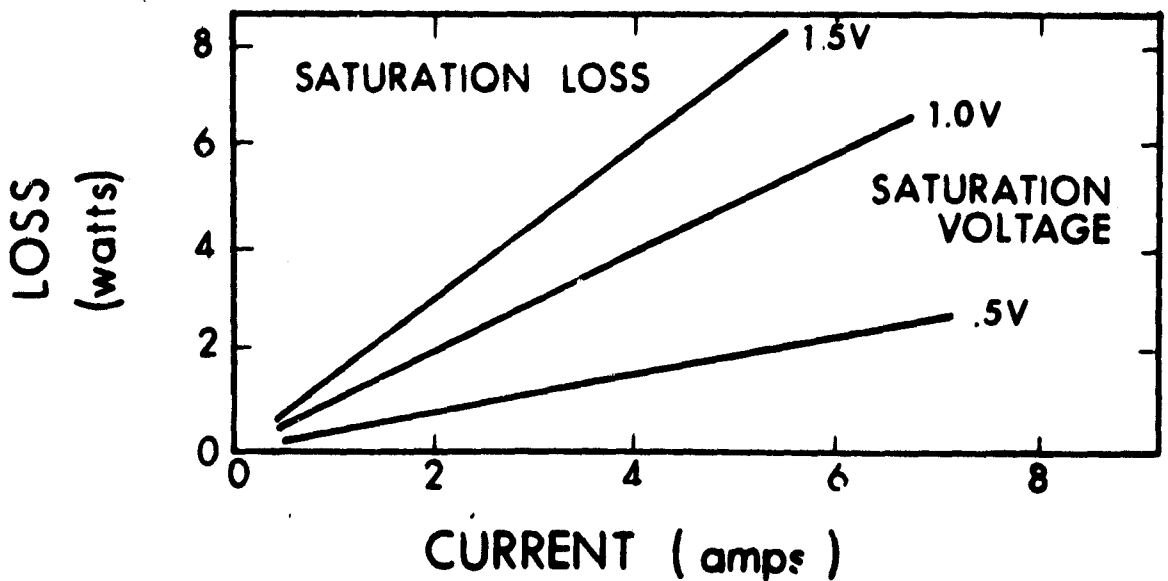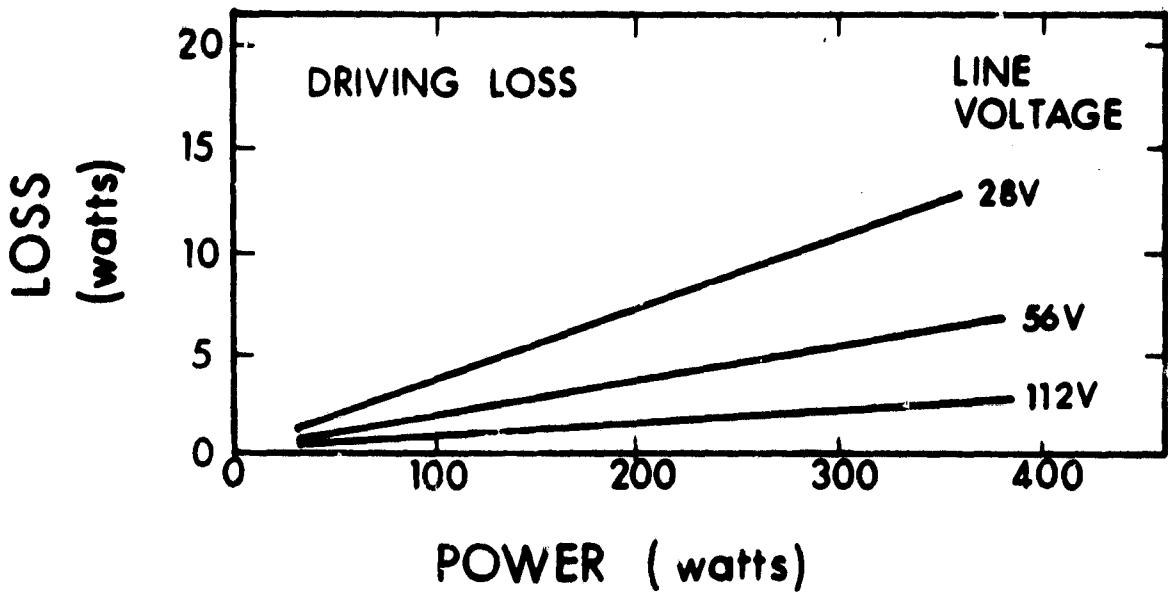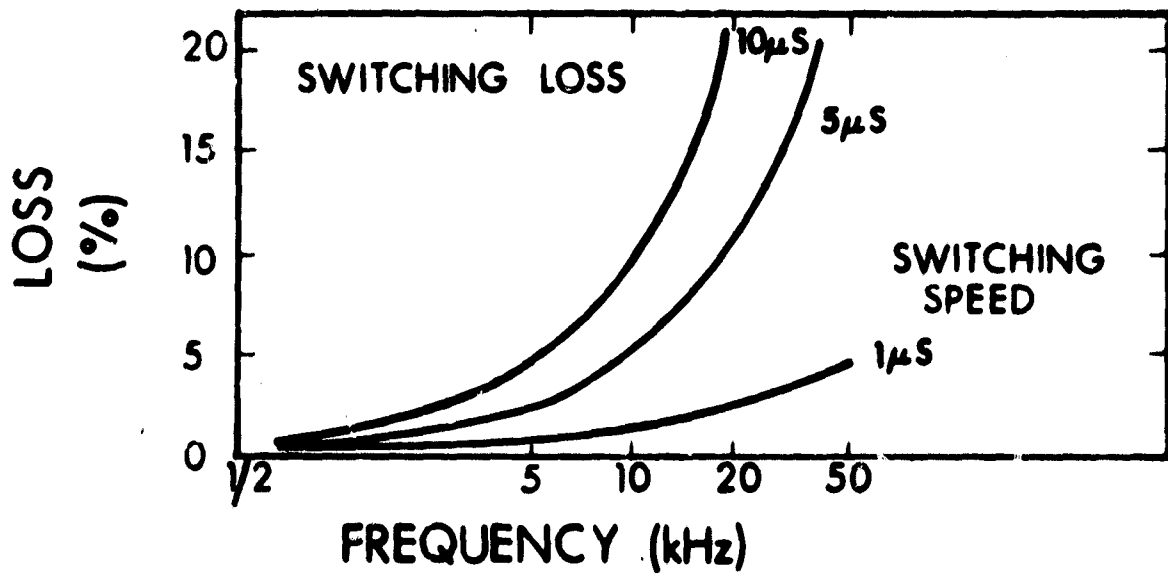
Figure 25.   Converter Component Specific Masses

Figure 26. Converter Component and Power Conditioning
System Specific Masses

1.8 PROPULSION SYSTEM THERMAL ANALYSIS

This propulsion system thermal analysis is based on a 40-50 kW
Mars Mapper spacecraft shown in Fig. 3. The propulsion system consists
of 16 2.5 kW cesium electron bombardment engines. Four engines will
use propellant from a common reservoir as shown in Figs. 4 and 5. During
a voyage to Mars, as the power from the solar panels is reduced the
number of engines in operation is reduced which creates a thermal
unbalance.

The thermal analysis was performed to determine design requirements
consistent with the temperature profile of the thruster and cesium
feed system assembly required for operation. The thermal requirements
of the system include stable temperature control, minimum power and
weight requirements and satisfactory transient response at start up
and shut down.

1.8.1 THRUSTER

It appears that an average case temperature of less than 400°C will
result with radiation from the face of the thruster alone. In view
of this, it may be advisable to shield the cylindrical sides of the
thruster with a combination thermal-electrical screen or with a
low absorptivity coating, such as gold to minimize the effects of
solar radiation under side illumination. The gold can be applied
either directly to the outer case, or a thin shield can so that
the required effective emissivity for 400°C is given by

$$\epsilon = \left(\frac{P}{\sigma AT^4}\right)^{1/4} = \left(\frac{500}{5.67 \times 700 \times .673^4}\right)^{1/4} = .89.$$

It is doubtful that the effective emissivity is quite that high in practice. However, with a gold coating on the cylindrical sides of the thruster 50 to 100 watts will be radiated from the sides reducing the power which must be rejected from the end of the thruster.

It will be advisable to shield the entire thruster array around the sides with a radiation shield. A lightweight skirt of Kapton with gold on the interior surface would reduce the unsymmetric effects of solar illumination on the thrusters and the amount of solar radiation absorbed by the reservoir radiators under side illumination. This would also serve to establish a ground potential plane.

1.8.2 CESIUM VAPOR FEEDLINE

The heat transfer properties of a bare cesium vapor feedline consist of rather poor conduction down the thin walled tube combined with radiation from the surface. If convection with the cesium vapor is neglected the equilibrium temperature distribution is governed by:

$$\frac{d^2 T}{dx^2} = \frac{\sigma \epsilon P T^4}{KA} \quad \text{where}$$

T is the absolute temperature,

x is the distance down the tube,

σ is the Stephan-Boltzman constant

ϵ is the emissivity of the outer tube surface,

P is the circumference of the tube,

A is the cross sectional area of the tube metal, and

K is the thermal conductivity of the metal.

The boundary conditions are established by the temperatures of the vaporizer and isolator respectively at the ends of the tube. This equation can be solved numerically for two finite boundry conditions. An approximate solution can be achieved by linearizing the equation in the following manner:

Let $T = T_o + \underline{\overline{X}}(x)$,

Then if $\dfrac{\underline{\overline{X}}}{T_o} \ll 1$

$$T^4 \cong T_o{}^4 + 4T_o{}^3 \underline{\overline{X}}$$

and

$$\frac{d^2 T}{dx^2} = \frac{d^2 \underline{\overline{X}}}{dx^2} \cong \frac{\sigma \epsilon P 4 T_o{}^3}{KA} (\underline{\overline{X}} + \frac{T_o}{4})$$

which has a solution of the form

$$\underline{\overline{X}} = Ae^{mx} + Be^{-mx} - T_o/4$$

where $m = 2T_o \sqrt{\dfrac{\sigma \epsilon P T_o}{KA}}$

It is convenient to let T_o be the vaporizer temperature. For a 20 cm stainless steel tube, 1 cm in diameter and 0.05 cm wall, boundary temperatures of 270°C and 375°C, and an emissivity of 0.05 (gold), the solution shows that 0.9 watts is conducted away from the isolator, 0.4 watts is conducted from the vaporizer and a minimum temperature of 210°C occurs 8 cm away from the vaporizer. To avoid the possibility of condensing cesium in the tube it may prove advisable to wrap the tube with multi-layer insulation. This would eliminate the occurance of a minimum temperature and also reduce the amount of heat conducted from the end units by curtailing radiation.

1.8.3 ISOLATOR

The amount of power required to maintain the interior temperature of the isolator near 375°C is dependent primarily on the radiation from the exterior surface of the isolator itself. This radiation can be reduced by the addition of multi-layer insulation. Empirical results indicate that the isolator heater power can be held below 20 watts for the system under consideration. Analytical calculations indicate that this power might be cut in half with multi-layer insulation on both the isolator and feed tubes, and with gold coated exterior surfaces.

1.8.4 VAPORIZER AND POROUS WICK

The cesium vaporizer uses a relatively small percentage of its heater power to actually vaporize the cesium. With a flowrate of 11 gms/hr the latent heat of vaporization and the specific heat capacity require 1.9 watts to warm the cesium from reservoir temperature and vaporize it. With a gold plated exterior surface another 0.6 watts will radiate from the vaporizer. The remaining heat is conducted to the cesium reservoir and is subsequently used to maintain the reservoir temperature.

The knowledge that approximately 27 watts will be conducted down the porous nickel wick to the reservoir with a desired temperature difference of 170°C establishes a design limitation on the geometry

of wick and tube connecting the two units. That is, the thermal conductance must be

$$K = \frac{q}{\Delta T} = \frac{27}{170} = .16 \text{ watt}/^{0}C.$$

For a 1 cm wick consisting of 40% nickel, 60% cesium, and surrounded by a stainless tube the required length is

$$L \approx \frac{\Sigma kA}{K} = \frac{.30}{.16} = 1.9 \text{ cm.}$$

One problem associated with turning off a thruster involves the length of time required for the vaporizer to cool sufficiently to stop the cesium vapor flow after the heater power is turned off. An approximate solution can be obtained by considering the vaporizer to be a thermal capacitor discharging through a thermal resistance to the reservoir. Since the reservoir heat capacity greatly exceeds that of the vaporizer, the temperature of the reservoir end will remain relatively constant during the vaporizer cooling.

Conservation of energy requires that

$$C\frac{dT}{d\tau} = -K \quad (T - T_R) - q$$

where C is the heat capacitance of the vaporizer

    K is the conductance
    T is the vaporizer temperature
    T_R is the reservoir temperature
    τ is the time from heater shut off
    q is the heat lost through radiation vaporization, etc.

In fact, q would be time dependent decreasing from an initial value of
approximately 3 watts to less than a watt below $120^{\circ}C$. In an approximate
solution it has been considered constant at 2.5 watts for the design
under consideration. The solution becomes:

$$\frac{T - T_4 + q/K}{T_3 - T_4 + q/K} = e^{\frac{-CJ}{K}}$$

Where T_3 is the initial vaporizer temperature. A typical result is
shown in Fig. 27. It shows that the vaporizer temperature would drop
to $120^{\circ}C$ in 5-6 minutes for the design under consideration.

1.8.5 RESERVOIR

The reservoir temperature during steady state operation is maintained by
the heat conducted from the vaporizers and subsequently radiated from
sized radiating surfaces on the face of the reservoir. For this passive
thermal control system to be effective it is important to isolate the
reservoir from the rest of the spacecraft with low conductance structural
supports and multi-layer insulation on the back, sides and much of the
top of the tank. Assuming that this isolation is effective the
radiator area required to maintain an equilibrium temperature of $100^{\circ}C$
is given by

$$A = \frac{q}{\sigma e T^4} = \frac{108}{5.67 \times .9 \times (.373)^4} = 1100 \text{ cm}^2.$$

This is the area of the top reservoir surface which should be painted
with white paint, to limit solar radiation absorption, and view deep
space. If this radiating surface was faced directly towards the sun
in Earth space for a prolonged period of time (hours) the temperature
would rise to $140^{\circ}C$. Ten watts of conduction between the reservoir
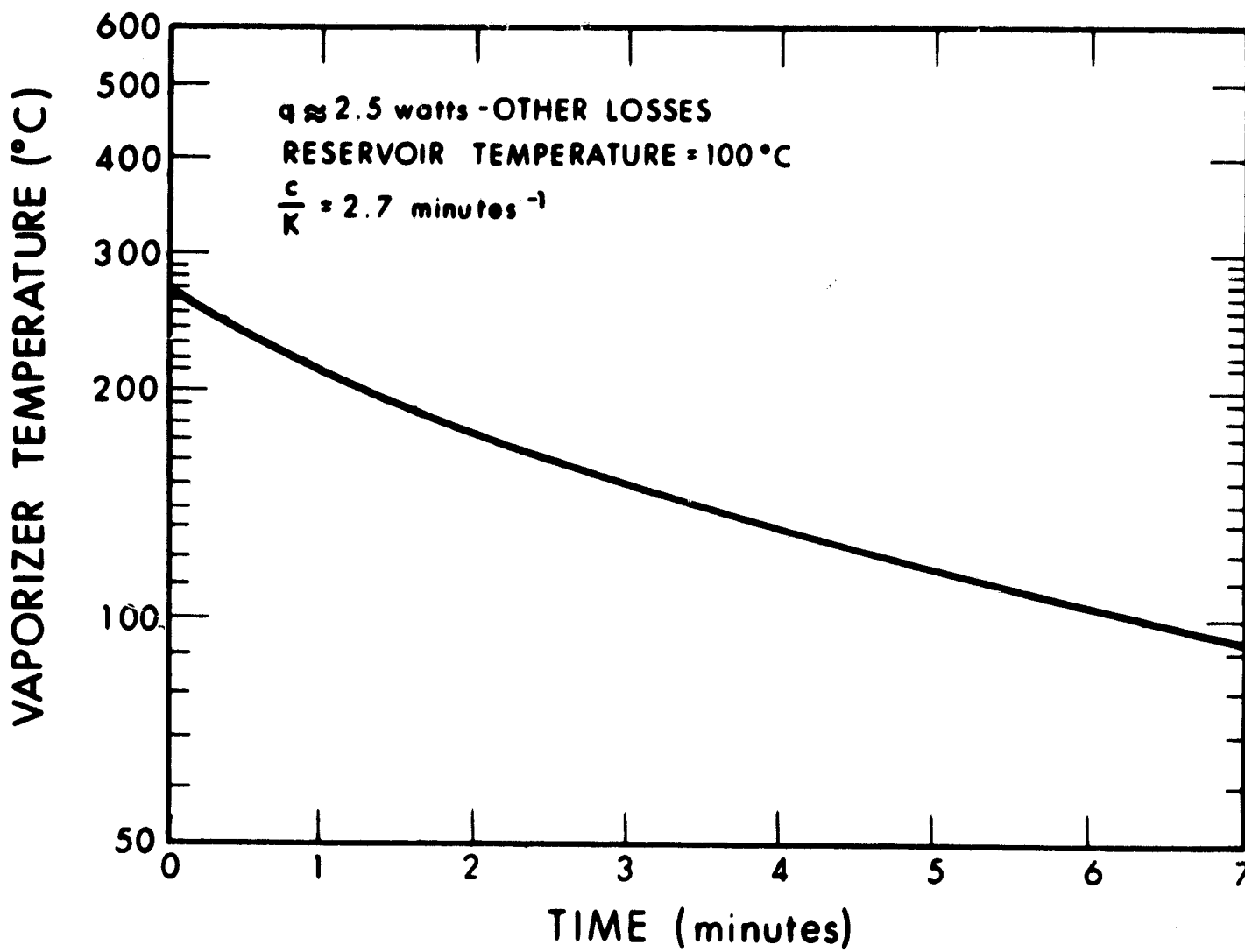and spacecraft would change the temperature by $8^{\circ}C$.

Figure 27. Vaporizer Temperature Decay After Power is Turned Off

The transient temperature change in the reservoir is controlled by the following energy balance:

$$q = C\frac{dT}{dJ} + \epsilon\sigma AT^4$$

where

q = is the total power, vaporizer plus reservoir heaters if they are on,

C = is the heat capacity of the reservoir,

T = is the temperature of the reservoir,

A = is the radiator area described above,

ϵ = is the thermal emissivity of the radiator, and

J = is the time.

A typical warm-up case is shown in Fig. 28. The assumed initial temperature was 50°C and the warm-up response is shown with and without a 200 watt reservoir heater to supplement the 108 watts from four vaporizers.

As the Mars Mapper power reduces the engines being turned off reduces the power to the reservoir. Table VII shows the temperature as a function of the number of vaporizers turned on if no additional reservoir heater is used. The temperatures in Table VII indicate that to maintain the reservoir temperature it will be necessary to supply power to the reservoir heater when the number of operating vaporizers is reduced from four. This can be accomplished by simply diverting the power from the off vaporizer to the reservoir heater.
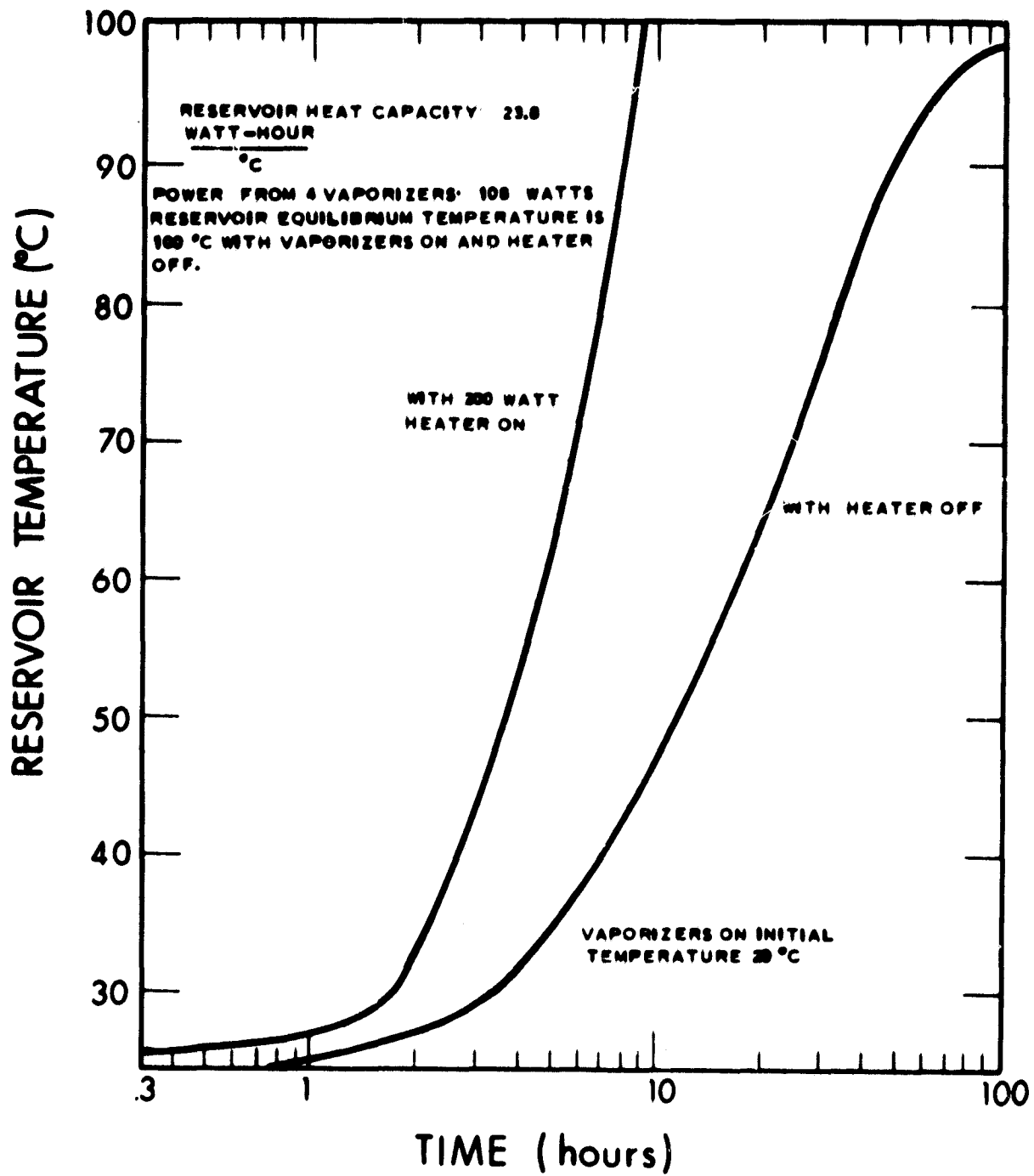
Figure 28.   Reservoir Heat-Up Time, With and Without a 200 Watt
Reservoir Heater

TABLE VII

NUMBER OF VAPORIZERS PER RESERVOIR VERSUS RESERVOIR
TEMPERATURE ASSUMING ALL RESERVOIR HEAT COMES FROM THE VAPORIZERS

| Number of Vaporizers	Reservoir Temperature
4	$100^{o}C$
3	$75^{o}C$
2	$40^{o}C$
1	$-10^{o}C$

1.9 MAGNETIC INTERACTIONS STUDY

On a Mars Mapper spacecraft it is likely that some of the instrumentation will be sensitive to magnetic fields generated within the spacecraft. The primary sources of magnetic flux in the spacecraft are the electron bombardment engines, the power conditioning and control, and the transmission lines. The magnetic field external to the power conditioning will be minimized by the incorporation of toroid transformers. The control circuitry could contain latching relays which could give transient magnetic flux. Transmission lines will require further analysis based on aluminum conductors, possibly tubular, in a tapered configuration. Transmission lines leading to the power conditioning and returning to the solar panels will be in close proximity thus reducing the resulting magnetic field.

The primary source of magnetic flux will be the electron bombardment engine cluster. The following are calculations of magnet size for cesium thrustors and an analysis of the field resulting from a single engine and the engine cluster for the Mars Mapper spacecraft.

   a.   Electron Bombardment Thrustor Magnets
        Electrons emitted from the cathode are attracted to the anode. If the electrons are allowed to travel the direct route there is little interaction with the propellant to create positive ions. An axial magnetic field produces Lorentz $\bar{j} \times \bar{B}$ forces which cause electrons to spiral. The long helical path results in sufficient interaction between electrons and propellant to produce positive ions.
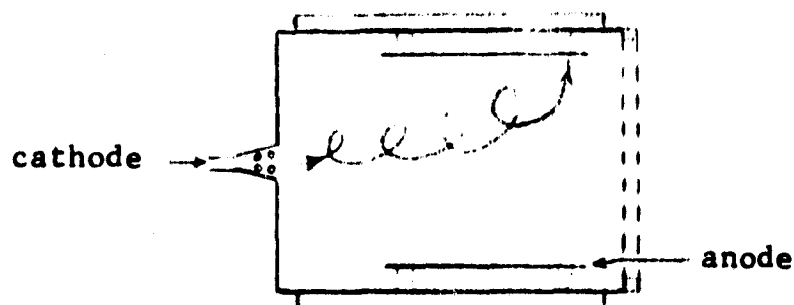
Electrons spiral due to magnetic field in an electron bombardment engine.

Equating the forces on the electrons:

$$\frac{mv^2}{r} = ev \times B = evB \quad 1PF \ v \perp B$$

$$B = \frac{mv}{er}$$

B = flux density

m = mass electron

e = charge electron

r = radius of path $\approx \dfrac{engine\ diameter}{4}$

v = linear velocity of electron
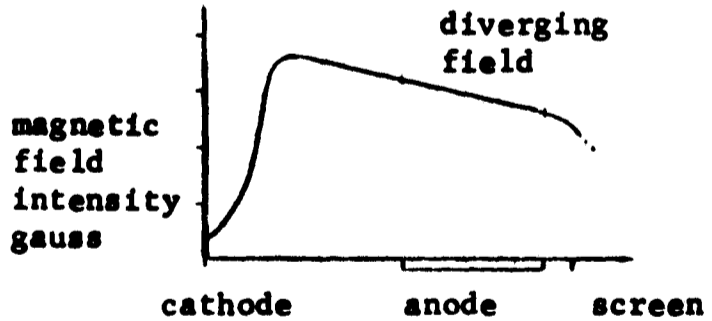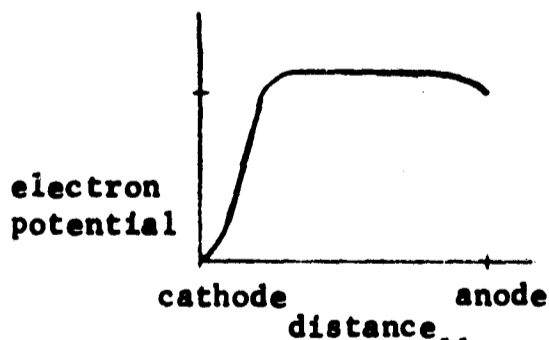
V = potential difference between cathode and anode

Equating the kinetic energy of the electrons:

$$eV = \frac{mv^2}{2}$$

$$v = \left[\frac{2ev}{m}\right]^{\frac{1}{2}}$$

combining:

$$B = \frac{m}{er}\left[\frac{2ev}{m}\right]^{\frac{1}{2}} \qquad B = \frac{1}{r}\left[\frac{2mV}{e}\right]^{\frac{1}{2}}$$

electron potential

cathode   anode
          distance

magnetic field intensity gauss

diverging field

cathode   anode   screen

$$\frac{e}{m} = 1.7589 \times 10^{11}\ \frac{coul}{kg}\ \text{for electrons}$$

V = 7 volts

$$B = \frac{1}{r}\sqrt{\frac{2mV}{e}} = \frac{8.9 \times 10^{-6}}{r}\ \frac{Webers}{meter^2}$$

The actual maximum magnetic flux density is higher than the
theoretical magnetic flux density because the cathode to
anode potential measurement is not accurate and because the
magnetic flux lines diverge as they cross the anode. Additional
error may be introduced by the spacing between the magnet and
anode and the energy lost due to interaction between ions. A
more accurate determination of magnet strength can be made by
multiplying the calculated magnetic flux density by a factor of
4.0 to get the actual maximum magnetic flux density.

Thrustor Diameter	- inches	1	2	5	8	12
Radius Path	- inches	.25	.50	1.25	2.00	3.00
Radius Path	- meters	.00636	.01274	.0318	.0508	.0763
Flux Density	- $\dfrac{W}{m^2}$	1.4×10^{-3}	6.98×10^{-4}	2.8×10^{-4}	1.75×10^{-4}	1.17×10^{-4}
Flux Density	- gauss	14	7	2.8	1.75	1.17
4x(Flux Density)	- gauss	56	28	11	7	4.8

5400-Final
Volume II
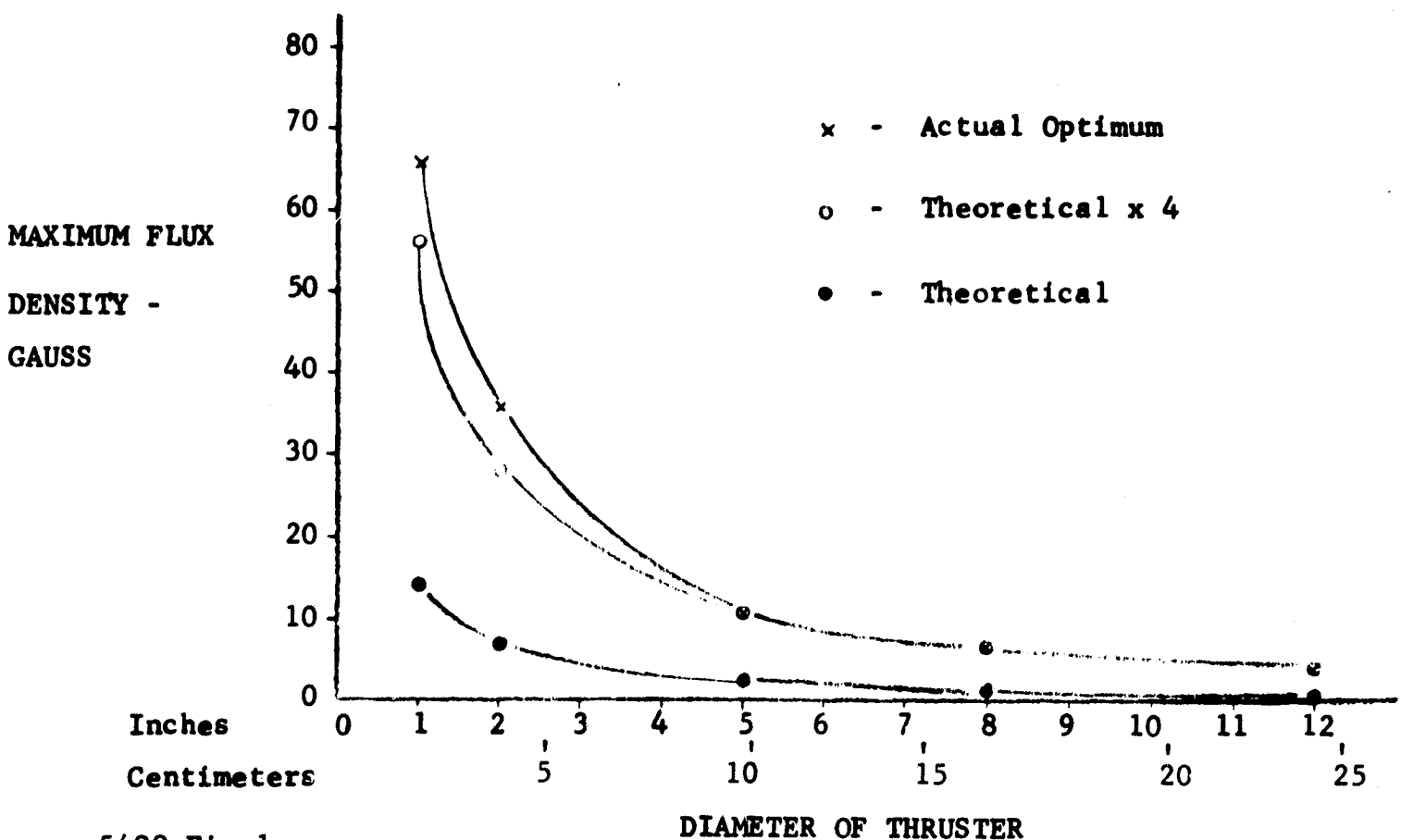
b. **Magnetic Field External to a 2.5 kW Cesium Electron Bombardment Thrustor**

$$B_r = \frac{\mu_o M}{2\pi} \frac{\cos\theta}{r^3}$$

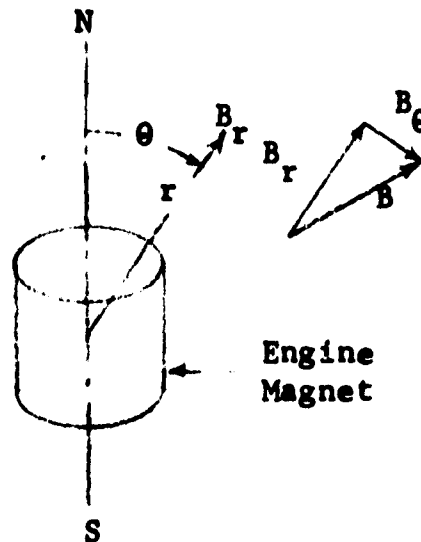$$B_\theta = \frac{\mu_o M}{4\pi} \frac{\sin\theta}{r^3}$$

$$B_\phi = 0$$

$\mu_o = 4\pi \times 10^{-7}$

M in ampere-meters^2

r in meters

B in webers/meter^2

$$\frac{4\pi\, B_\theta r^3}{\mu_o \sin\theta}$$

$\theta = 90° \therefore \sin\theta = 1$

$B = 4.8$ gauss $\approx 5 \times 10^{-4} \frac{W}{m2}$

$\mu_o = 4\pi \times 10^{-7}$

$r = \frac{11 \text{ inches}}{2} = 5.5$ inches $= .15$ meters

$$M = \frac{4\pi \times (5 \times 10^{-4})(.14)^3}{4\pi \times 10^{-7} \times 1} = 13.8 \text{ ampere-meters}^2 \text{ for a 2.5 kW thruster}$$

2.5 kW cesium Electron Bombardment Thrustor

outside diameter	=	12 inches	=	.305 meters
anode diameter	=	11 inches	=	.28 meters
peak magnetic flux	=	4.8 gauss	

For a single 2.5 kW thruster the external magnetic field may be calculated.

$$\theta = 0° \quad B = B_r = \frac{\mu_o M}{2\pi} \frac{\cos\theta}{r^3} = (2.76 \times 10^{-6})/r^3 \quad \frac{\text{webers}}{\text{meters}^2}$$

$$\theta = 45° \quad B_r = \frac{\mu_o M}{2\pi} \frac{\cos\theta}{r^3} = \frac{4\pi \times 10^{-7} \times 13.8 \times \cos 45°}{2\pi} \frac{1}{r^3} = \frac{19.5 \times 10^{-7}}{r^3} \quad \frac{\text{webers}}{\text{meters}^2}$$
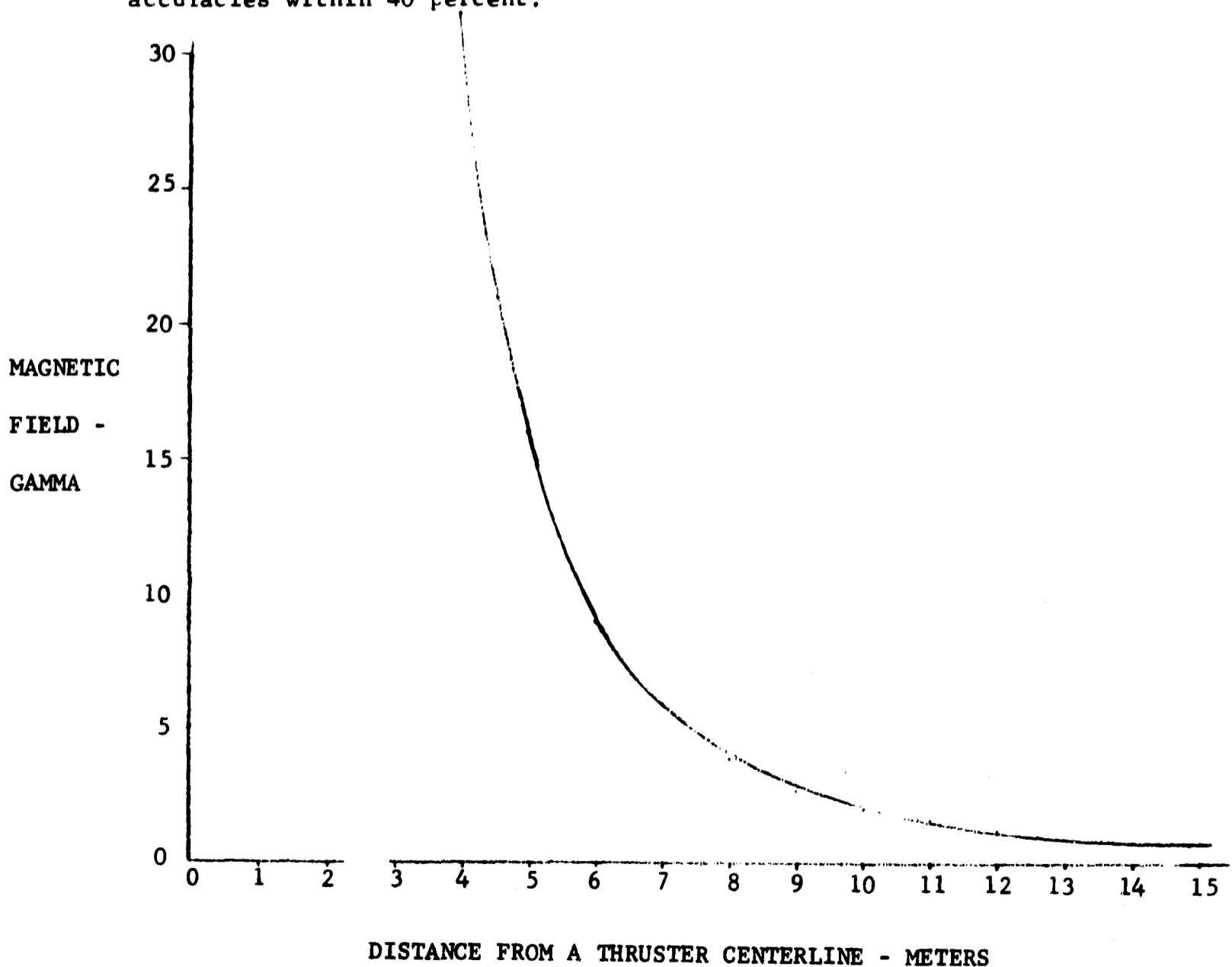
$$B_\theta = \frac{\mu_o M \sin\theta}{4\pi \ r^3} = \frac{4\pi\times10^{-7}\times13.8\times\ \sin 45^o}{4\pi \quad r^3} = \frac{9.75\times10^{-7}}{r^3}$$

$$B = (B_r^2 + B_\theta^2)^{1/2} = (2.18\times10^{-6})/r^3 \quad \frac{webers}{meter^2}$$

$$\theta = 90^o \quad B_r = \frac{\mu_o M \cos\theta}{2\pi \ r^3} = \frac{4\pi\times10^{-7}\times13.8\times\ \cos 90^o}{2\pi \quad r^3} = 0$$

$$B = B_\theta = \frac{\mu_o M \sin\theta}{4\pi \ r^3} = \frac{4\pi\times10^{-7}\times13.9\times\ \sin 90^o}{4\pi \quad r^3} = (1.39\times10^{-6})/r^3 \quad \frac{webers}{meter^2}$$

Rather than calculate the field for all values of θ, an average value may be used for any given radial distance for absolute field strength accuracies within 40 percent.

DISTANCE FROM A THRUSTER CENTERLINE - METERS

c. **Magnetic Effects for an Engine Cluster**

When organizing the format for a cluster of cesium electron bombardment engines it is possible to alternate the direction of the magnetic fields of adjacent thrusters in an axial symmetric cluster. This layout causes the external field, due to both engines, to cancel in plane equal distances from the center of both engines.

In a four engine symmetrical cluster two planes of zero magnetic field exist. For a six engine axial symmetric cluster there are three planes of zero magnetic field.

Two Engine Cluster

Four Engine Cluster

Six Engine Cluster

Sixteen Engine Cluster
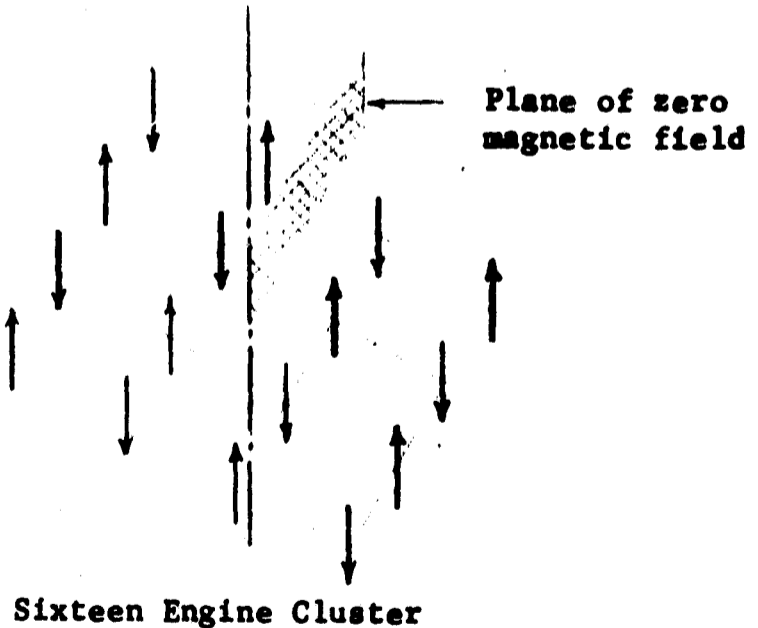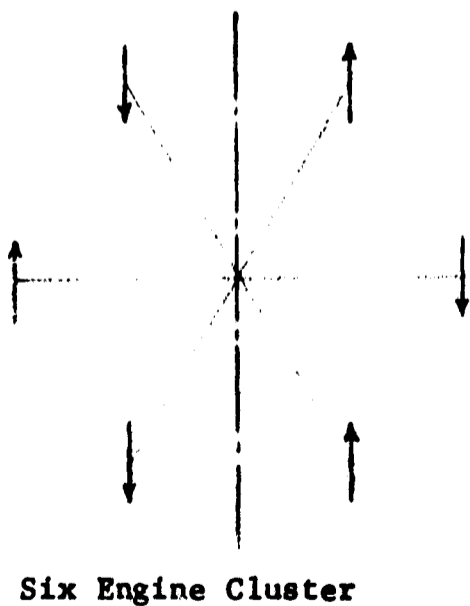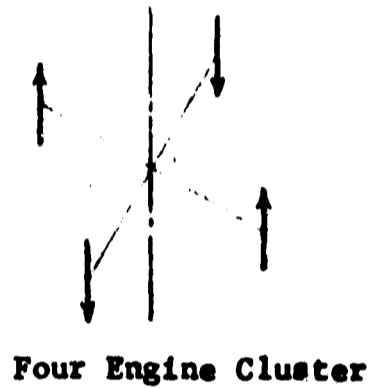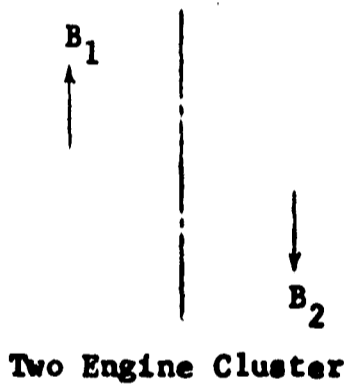
A final position of interest should be mentioned. This is the point on a cluster axis at $\theta = 54.7°$ with respect to all thrusters. At this point the field component from a single thruster is perpendicular to the cluster axis. Failure of a single engine magnet in a cluster would not create an axial (N-S) component at this location.

54.7°

Components of field lines are
perpendicular to the cluster
axis at $\theta = 54.7$ degrees.

B_1

B_2

Magnetic lines of flux
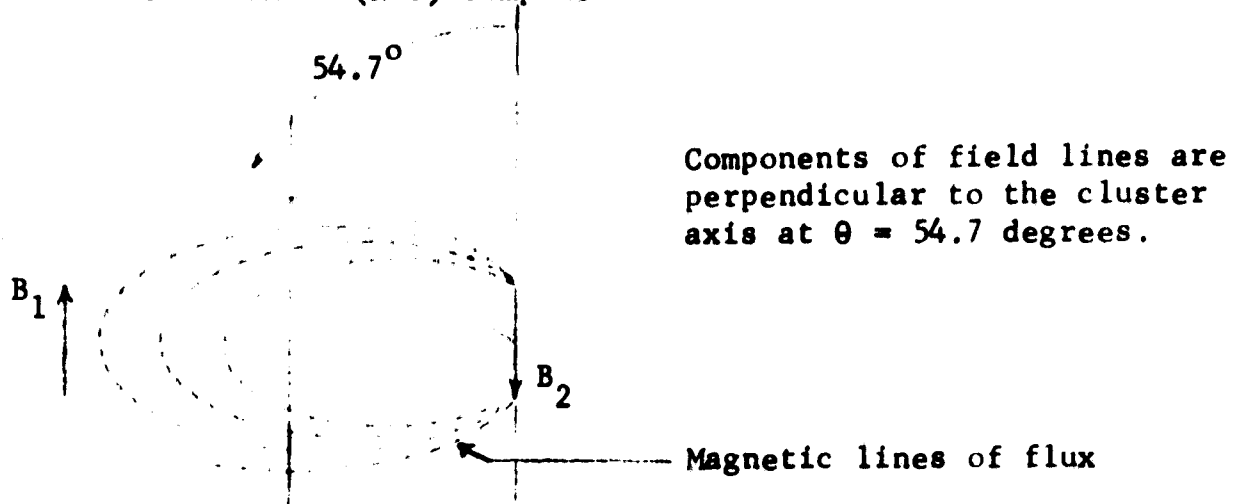
It is possible to position an instrument sensitive to magnetic flux, such that the net magnetic flux from the engine cluster is zero. This is accomplished by locating the instrument in a plane passing thru the axis of symmetry of the engine cluster at equal distances from equal and opposite magnetic poles.

The magnetic flux sensing instrument may, in addition, be located in a angular plane where some single engine magnetic flux components are perpendicular to the cluster axis of symmetry. This would mean a zero vector magnetic flux parallel to the cluster axis of symmetry of the angular plane.

SECTION 2

VENUS ORBITER AND FLYBY MISSIONS

The basic spacecraft used for the Mars Mapper mission would require several modifications to enable it to fly by Venus on the way to Mars or to spiral in on a Venus orbit.

The most important factor to be considered is that during the heliocentric transfer to Venus the solar radiation is increasing as the square of the distance to the sun is decreasing. The increase in solar radiation results in increasing temperature and available power. This may be seen in Fig. 29, which shows the solar array temperature versus solar radiation, and in Fig. 30, which shows solar array power versus distance from the sun.

Considerations for increasing temperature must include:

a. Tilting the solar panel to avoid extensive solar array temperatures.

b. Enlarging all heat radiating capabilities.

c. Investigation of the tradeoff between active and passive heat rejection systems. Heat pipes must also be considered, particularly for sensors, instruments, telemetry and power conditioning.

d. Investigate the thermal transient of the spacecraft passing into the shadow of Venus.

The temperature rise of the solar array tends to reduce the output efficiency and therefore the transmission line voltage. Considerations for the increasing power and decreasing voltage include:
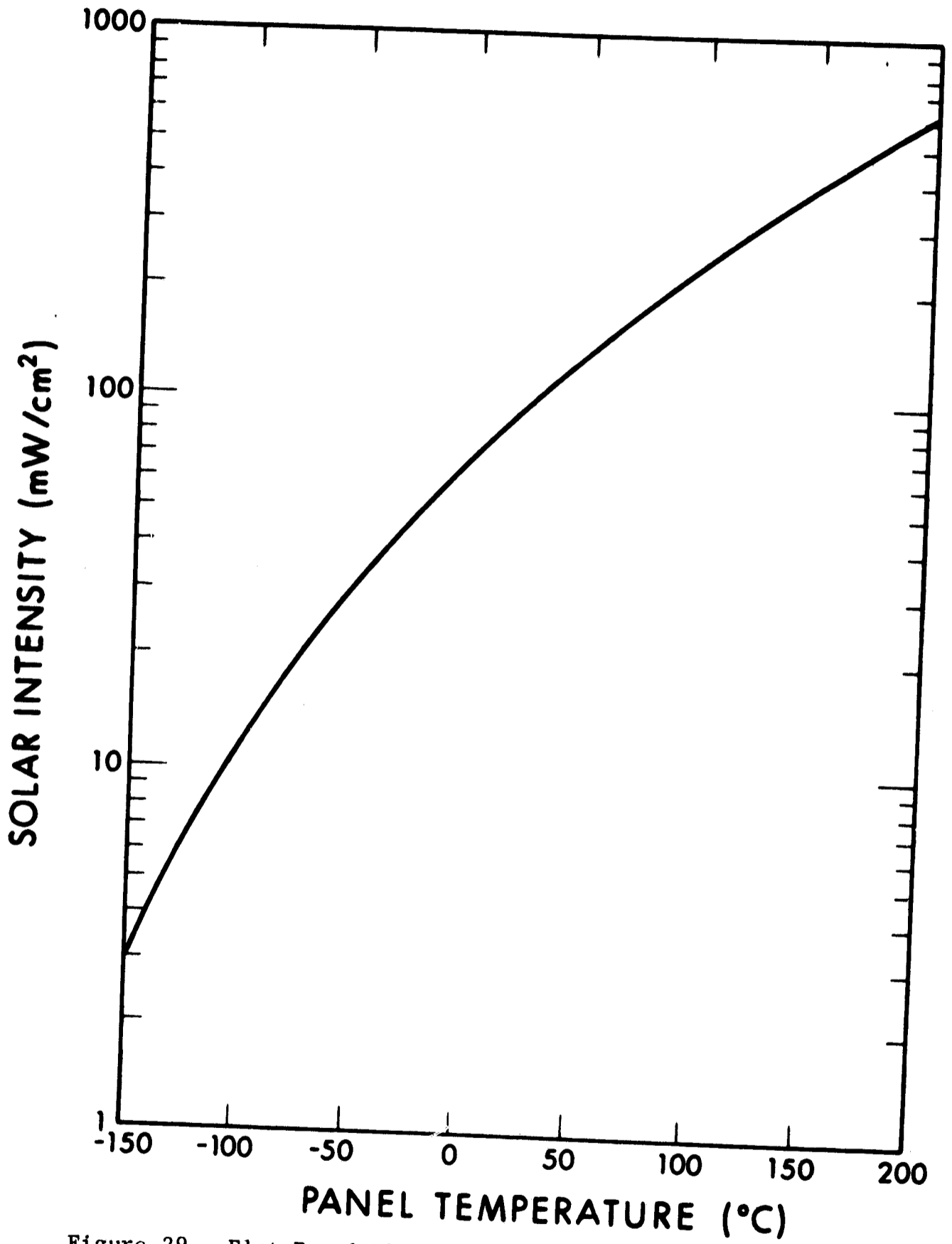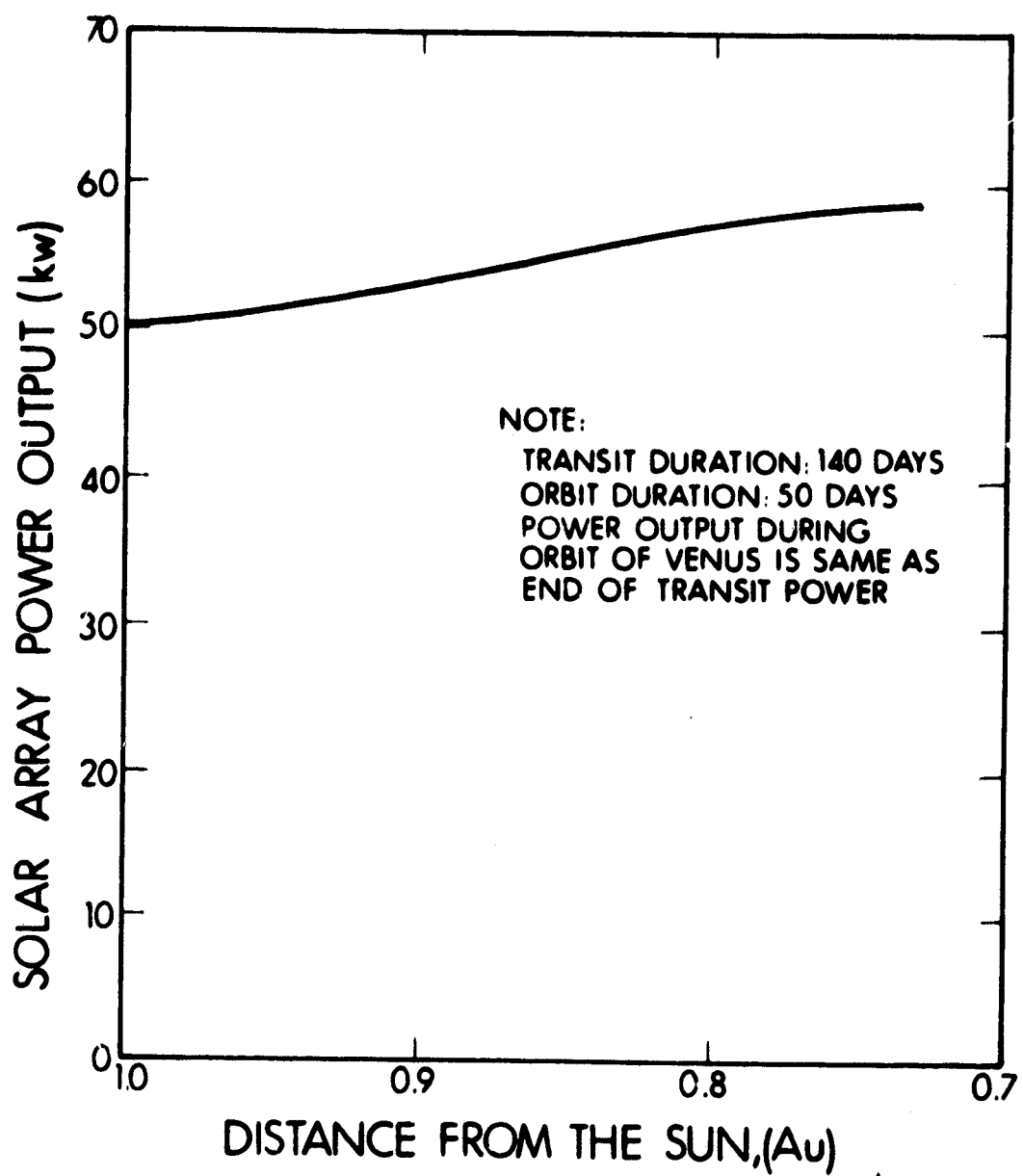
Figure 29. Flat Panel Thermal Equilibrium Temperature

Figure 30.   Solar Array Power Output versus Distance from
the Sun for a Venus Probe and Orbiter

a. Providing power conditioning and engines to utilize the increasing power. This might be accomplished by over-designing earth orbit type power conditioning and raising the specific impulse of the engines by changing a reference voltage in the power conditioning.

b. Modifying the power conditioning to accept a wide variation in transmission line voltage. This is particularly important for a Venus flyby to Mars.

c. Investigation of batteries which are charged at high temperature and discharged at low temperature for a Venus orbit.

The gravity of Venus, being more than double that of Mars, will necessitate a higher altitude capture orbit. The capture deceleration must be studied in conjunction with solar panel g loading and the need for avoiding excessive solar panel temperatures.

The Venusian atmosphere will necessitate employing a nonphotographic means to provide information on surface characteristics. Sensors must also be incorporated which are applicable to the Venusian environment.

SECTION 3

5 MW MANNED SOLAR ELECTRIC SPACECRAFT

The purpose of this study is to investigate a solar electric propulsion
for a manned spacecraft. The time for interplanetary missions is long
even with chemical rockets which cannot carry nearly the payload of an
ion rocket. The electric propulsion effective payload capabilities
are enhanced by the need for large amounts of electric power when the
destination is reached.

A spacecraft arriving at a Mars orbit would be divided into two units.
The major part would remain in orbit to serve as a relay station,
repeater for TV and radio, computer, observation station, and return
spacecraft. Some power would also be needed for housekeeping, life
support, orientation, and orbit maintenance.

The Mars lander would carry men, equipment and a return-to-orbit
vehicle to the Martian surface. On the surface of Mars power might
be necessary for the following:

    a. TV communications

    b. Radio communications

    c. Light

    d. Heat

    e. Computer Relay

    f. Melting water

    g. Hydrolysis of water to get O_2

    h. Other life support

    i. Housekeeping

    j. Experiments

    k. Transportation

The amount of solar panel which is detached from the spacecraft in orbit and landed is a function of the Mars lander requirements and the requirements for returning to Earth. The solar panel which is landed on Mars will remain on Mars. Only the landing party, essential gear, and a return rocket will leave Mars. Some of the remaining gear should continue to transmit data to Earth. On returning to Earth some of the solar panel might remain on a Mars orbit to act as a repeater and to photograph Mars.

The electric thrusters will be electron bombardment engines or lithi Hall arcjets. Looking into the future, say 1980, Hall arcjets should display efficiencies similar to electron bombardment engines, but, the Hall arcjets should show a wider range of throttleability, higher reliability, and greater thrust density.

The optimistic performance for either engine should be:

Specific Impulse (seconds)	3500	5000	7000
Efficiency (percent)	73	86	90
Thrust-5MW (Newtons)	214	174	131
Specific Mass (kg/kW)	.5	.5	.5

The starting point 5 MW mass allocations for a 1000 day mission are:

Specific Impulse (seconds)	3500	5000	7000
Mass Solar Array (12 kg/kW)	60,000 kg	60,000 kg	60,000 kg
Mass Engines (0.5 kg/kW)	2,500	2,500	2,500
Mass Propellant (700 days)	487,000	243,000	121,000
Mass Tankage (10% propellant)	48,700	24,300	12,100
Mass Power Conditioning (4 kg/kW)	20,000	20,000	20,000
Mass Electric Propulsion System	618,200 kg	349,800 kg	215,000 kg

NOTE: This mass is for the electric propulsion system only.

The approach to designing the spacecraft is to construct a large number of units containing solar panel, power conditioning, power control, electric engines, and propellant. The control logic will be remotely located. The size of each module will be determined by the launch vehicle's payload mass and shroud dimensions.

The Saturn V is a likely candidate for the launch vehicle. The payload for a 500 kilometer orbit is 110,000 kg or 45,400 kg to escape velocity. The useable shroud space will probably be a cylinder 6.1 meters in diameter with a height of 15.2 meters.

Due to the low packing density of solar panels, the shroud dimensions will be the limiting factor rather than the payload mass. This mission may require the incorporation of a more functional shroud on the Saturn V.

The maximum strength of the solar array is achieved when the moment of inertia is minimized. The shape for the minimum moment of inertia is a circle. The structural design and assembly problem is then to break down a solar array, whose shape approximates a circle, into elements which fit in the Saturn V shroud and can be easily assembled in space. Assembly may be done by an assembly crew, an automatically unfolding array or both.

A typical solar panel would have a frame with its longest dimension (diagonal or diameter) equal to 20 ft. The thickness of the support frame on the edge of the panel would correspond to the length of the engine as in Figure 31. Many other configurations for propulsion units are possible. These include offset engine designs and plug-in engine designs for better packing density. This basic design uses propulsion unit thickness of 8 inches.
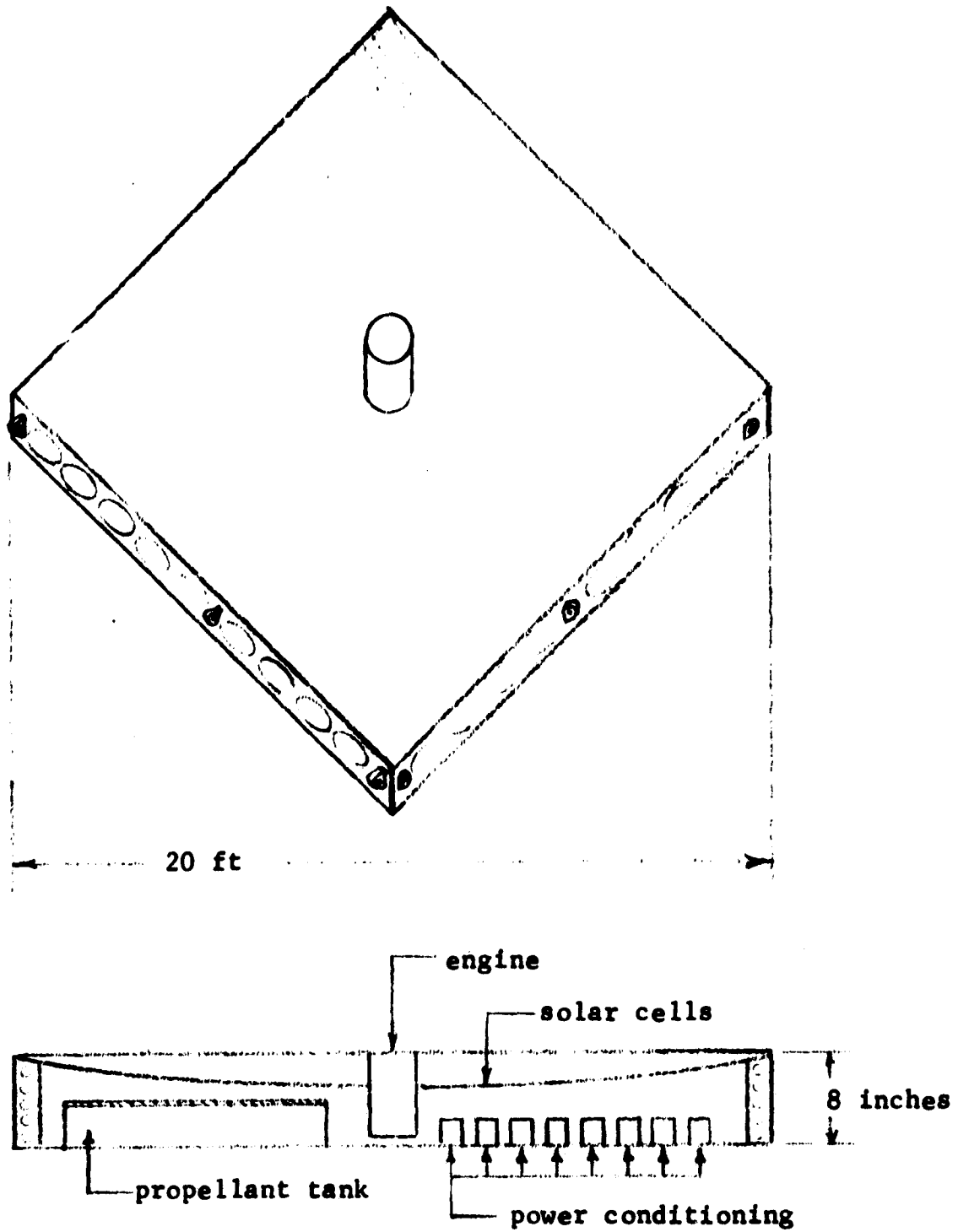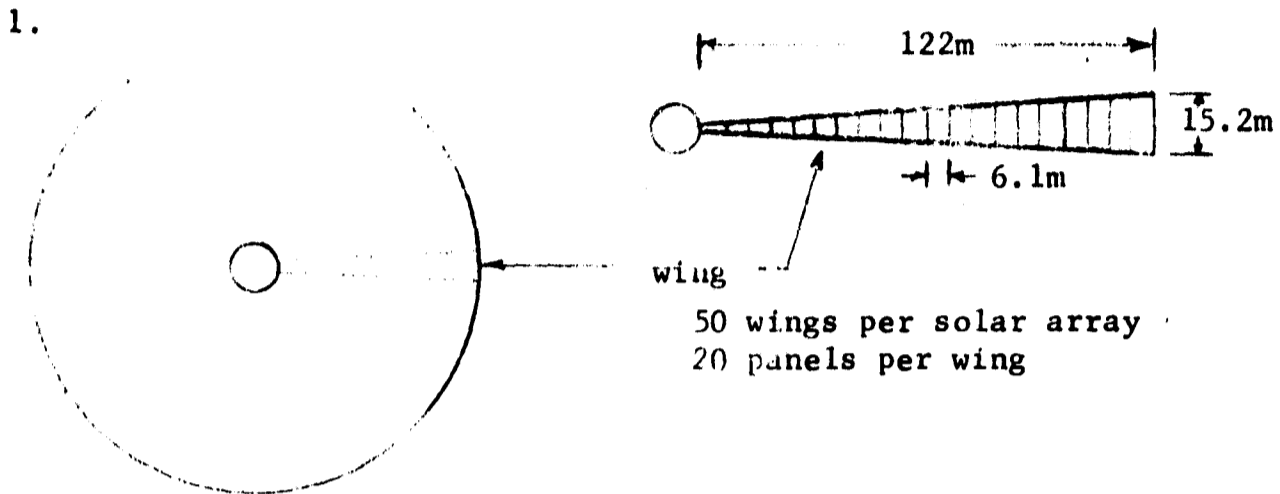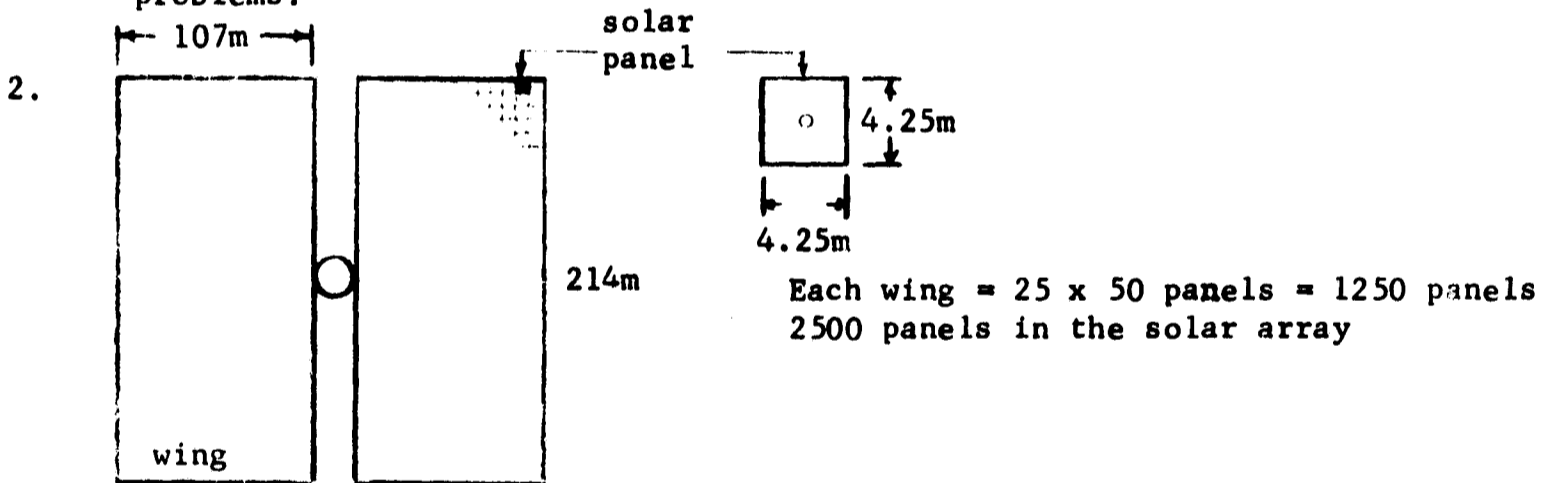
Figure 31. Typical Propulsion Unit Consisting of Solar Panel,
Engine, Power Conditioning and Control

The following are five considerations of formats of 5 MW solar electric propulsion arrays.

1.

122m

15.2m

6.1m

wing

50 wings per solar array
20 panels per wing

The problem with this circular solar array is one of packing it into the launch vehicle. The non-uniform panels are difficult to manufacture. Power distribution and engine placement are not easily solvable problems.

2.

107m

solar
panel

4.25m

4.25m

214m

Each wing = 25 x 50 panels = 1250 panels
2500 panels in the solar array

wing

Here the folding of the array is simplified but there is no need for the two wing format.

3.

4.25m

4.25m

214m

214m

Panel
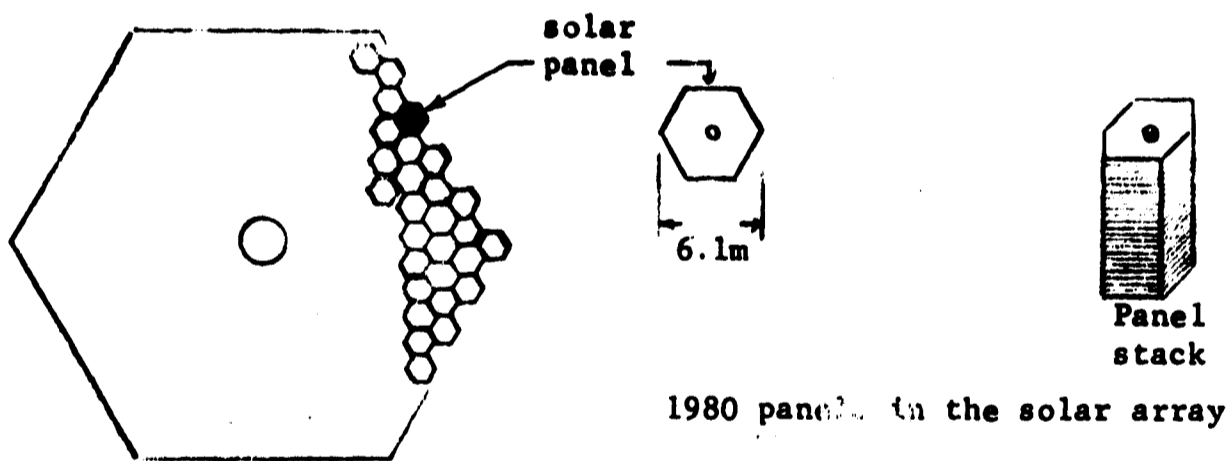stack

wing   array
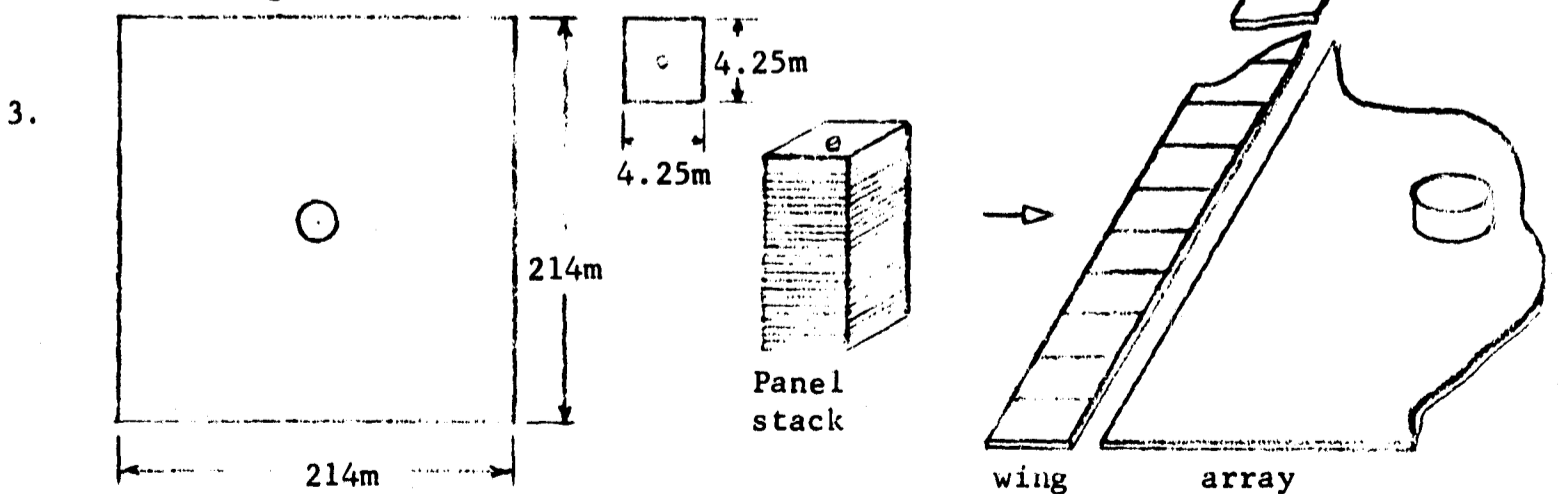
The array could be divided into wings which would unfold in space and be assembled into an array.

4.

4.25m

4.25m

110m
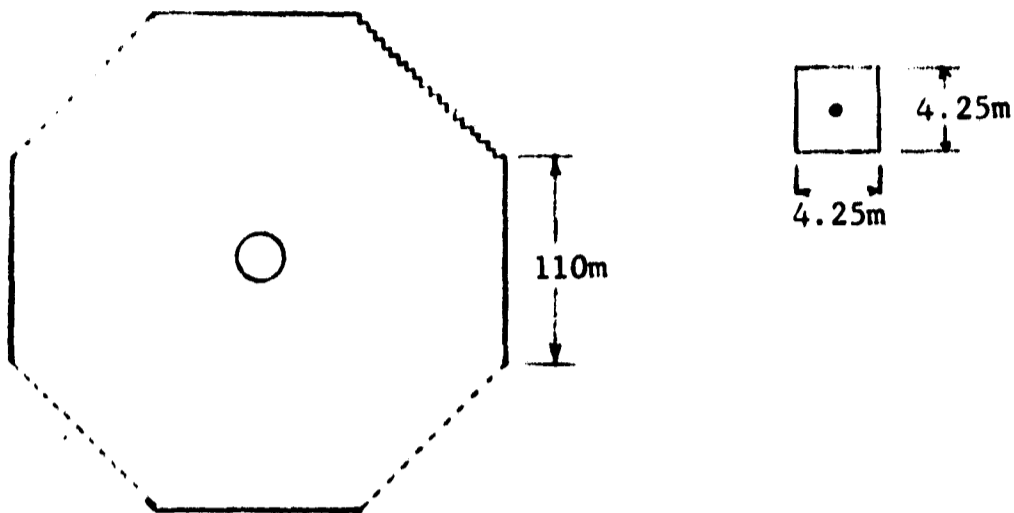
An alternate way of assembling the square solar panels is into an octagon which give smaller total moment of inertia for the spacecraft.

5.

solar
panel

6.1m

Panel
stack

1980 panels in the solar array

This honeycomb design is being considered because the hexagonal shape has a low moment of inertia. The hexagonal panels can be stacked into a cylindrical launch shroud with a higher packing density than a square panel.

To emphasize the problems involved with the packing density of the solar array in the Saturn V shroud, design approaches 3 and 5 will be considered further.

Design Approach		3	5
Total number of square panels	=	2500	1980
Thickness of panel (including engine)	=	20 cm	20 cm
Total height of stack of panels	=	510m	402m
Height of shroud (assumed)	=	15.2m	15.2m
Number of Saturn V launch vehicles required for electric propulsion system	=	34	27

The result of the volume calculations is that with present technology it is not feasible to launch a 5 MW solar array. The minimum number of Saturn V launch vehicles necessary to launch the 5 MW solar electric spacecraft is 27.

SECTION 4

150 kW MANNED SOLAR-ELECTRIC SPACECRAFT

A more sensible approach to a manned Mars spacecraft would be a design
such that the men, equipment, spacecraft and solar array could all be
launched on one Saturn V rocket. The service module could be enlarged
to provide liftoff from the surface of Mars.

The hexagonal array will be used for this model because of its compact-
ness. The hexagonal solar panel thruster-power conditioning modules
in a stack 12.2m high would allow a man and equipment compartment 6.1m
in diameter and 3.1m high.

The optimistic engine performance should be:

Specific Impulse (seconds)	3500	5000	7000
Efficiency (percent)	73	86	90
Thrust-150 kW (Newtons)	6.46	5.25	3.92
Specific Mass (kg/kW)	.5	.5	.5

The starting point 150 kW mass allocations for a 1000 day mission are:

SPECIFIC IMPULSE (seconds)	3500	5000	7000
Mass Solar Array (12 kg/kW)	1,800 kg	1,800 kg	1,800 kg
Mass Engines (.5 kg/kW)	75	75	75
Mass Propellant (700 days)	14,600	7,280	3,630
Mass Tankage (10% propellant)	1,460	728	383
Mass Power Conditioning (4 kg/kW)	600	600	600
Mass Electric Propulsion System	18,535 kg	10,483 kg	6,468 kg

NOTE: This mass is for the electric propulsion system only.

Solar panel with the thruster, PC and C, and propellant is 20 cm thick.

12.2m stack = 1220 cm → $\dfrac{1220}{20 \text{ cm}}$ thick = 60 panels

60 panels at $2.5 \dfrac{kW}{panel}$ = 150 kW

Figure 32 shows a 150 kW manned Mars spacecraft configuration. The array is composed of 60 propulsion units and one manned environmental unit. Figure 5 describes the propulsion unit. A single propulsion unit consists of a 2.5 kW solar array, power conditioning, and a 2.5 kW ion engine. Note that the 2.5 kW power level per solar panel is the result of the size of the launch vehicles shroud.
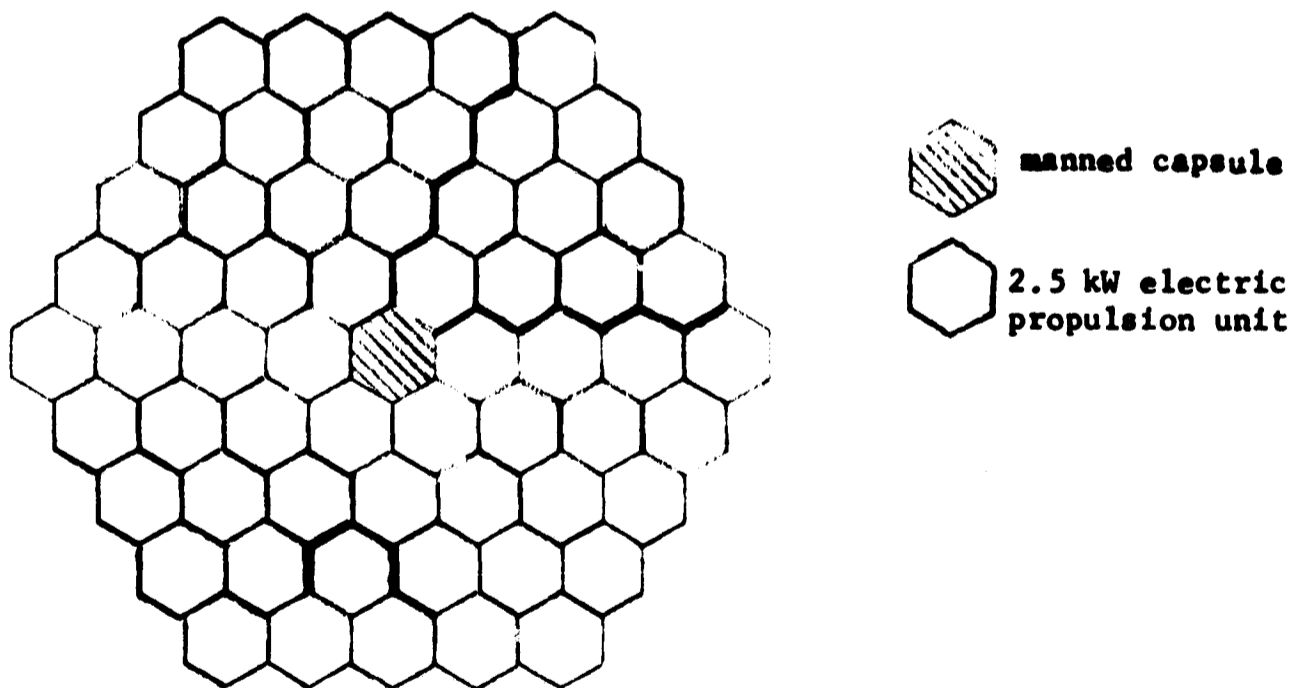

manned capsule

2.5 kW electric propulsion unit

Figure 32. Manned Mars Spacecraft with a 150 kW Solar Array

SECTION 5

PROBLEMS INVOLVING LARGE SOLAR ARRAYS

Present assembly techniques require assemblers to install individual
cells by hand. This requires that the substrate be positioned almost
horizontally. The size of the solar panel is limited by the reach of
the assembler which is about 0.75 meters. This means the present maxi-
mum size of a solar panel is 1.5 meters on a square's side or 1.5 meters
in diameter. Fixtures are used to hold the solar panel horizontally
during the attachment of the cell. Cases are used to transport the
solar cells and the solar panels. Fixtures with wheels are often used
to move the solar panels and/or cases. The frame is fabricated by
stretching and spot welding aluminum. Many jigs and fixtures are
incorporated in this process. During and after assembly of a solar
panel numerous pieces of apparatus are used for test, Checkout, and
qualification of the solar panel.

When choosing the designs for 100 kW-5MW solar array study models,
consideration must be given to the complexity of manufacturing, handling,
and checkout. The larger solar panel will creat many new problems.
Aluminum or berylium will probably be used for the frame. If the
lighter weight berylium is used, new handling and fabrication techniques
will be necessary due to its brittleness. The adhesive presently
used to attach the solar cells to the substrate is RTV-40. It takes
an assembler 15 minutes to completely install one 2 x 2 centimeter
solar cell. The adhesive then requires 3 hours of drying time. If
a 5 MW solar array were to be assembled by this method, the time
for solar cell installation alone would be 5735 man-years. This
assumes that additional factories have been built to manufacture the
required number of thin solar cells. New mechanisms must be developed

to unfold the groups of solar panels into wings in space. Testing
these mechanisms on the actual solar panels will be difficult under
lg conditions. Methods for connecting the wings to form the entire
solar array poses additional problems as will the disconnection of
the part of the array which will land on Mars.

The solution to part of the problem could be the construction of a solar
cell installing machine. The machine would have to pick up a solar cell,
by a slight vacuum, apply the prescribed amount of adhesive, and place
the cell in some exact location. A computer tape could command the
machine. The machine would have to operate on a horizontal plane 6.1
meters in diameter.